

Universidade do Minho
Escola de Ciências

Joana Patrícia Veríssimo Ferreira

**Characterization of dysferlin domain-
containing peroxins in lipid droplet biogenesis**

Tese de Mestrado
em Genética Molecular

Trabalho realizado sob a orientação do
Professor Doutor Pedro Carvalho

Com coorientação da
Professora Doutora Célia Pais

Outubro de 2018

Declaração

Nome:

Joana Patrícia Veríssimo Ferreira

Endereço eletrónico: joanapatriciaf@gmail.com

Telefone: +351 935884099

Número de Bilhete de Identidade: 14788174

Título da tese de mestrado:

Characterization of dysferlin domain-containing peroxins in lipid droplet biogenesis

Orientador:

Professor Doutor Pedro Carvalho

Coorientador:

Professora Doutora Célia Pais

Ano de conclusão: 2018

Designação do Mestrado ou do Ramo de Conhecimento do Doutoramento:

Mestrado em Genética Molecular

É AUTORIZADA A REPRODUÇÃO INTEGRAL DESTA DISSERTAÇÃO APENAS PARA EFEITOS DE INVESTIGAÇÃO, MEDIANTE DECLARAÇÃO ESCRITA DO INTERESSADO, QUE A TAL SE COMPROMETE.

Universidade do Minho, 31 de outubro de 2018

Assinatura: _____

Acknowledgments

First, I would like to thank Professor Pedro Carvalho for the opportunity to join his team and work in his laboratory, his patient guidance, and his confidence in my research, providing me an invaluable environment for personal and professional growth.

Accordingly, I am also very grateful to the members of his team for all their kindness, availability, and suggestions. They created the best environment to develop my research skills. A special thanks to Vitor Teixeira for the first months of endless collaboration, and Sihui “Alexis” Wang, Daniel Fonseca and Logesvaran Krshnan for their constant help and contribution for my research project.

I would also like to acknowledge my co-supervisor Professor Célia Pais for her availability and support before and during this project.

To my good friends in Portugal thank you for being there for me, supporting all my decisions and being excited about my accomplishments. To all my new friends in the United Kingdom, thank you for being there for me and for transforming this new place into another home.

And finally, I am deeply grateful to my parents and my brother for the financial support, continuous encouragement and endless belief in my decisions and skills. They offered me a unique, inestimable opportunity to explore new horizons and grow as a person.

I acknowledge the personal financial support of the Erasmus + programme covered by the European Union.

Characterization of dysferlin domain-containing peroxins in lipid droplet biogenesis

Abstract

Lipid droplets (LDs) are ubiquitous organelles of crucial importance in cell biology, understanding of human diseases and biotechnology because they are cellular reservoirs of neutral lipids for energy production or membrane synthesis and act as hubs for metabolic processes. Despite continued efforts, the molecular mechanisms of LD biogenesis are not completely understood. Recent reports indicated that LD biogenesis and formation of pre-peroxisomal vesicles, which are involved in peroxisomes biogenesis, occur at the same endoplasmic reticulum (ER) sites, suggesting that these sites are specific and distinct from bulk ER. Moreover, the ER budding of both these structurally unrelated organelles involves cooperation between Seipin and Pex30p, since, in absence of these proteins, budding of these organelles is inhibited. However, the molecular mechanisms regarding this cooperation remain elusive. Since no peroxin of pex30p family - dysferlin domain-containing peroxin family - has been described before as involved in LD biogenesis, it is unclear how Pex30p is localised to the LDs in absence of the Seipin complex. It is also unknown what is the central function of Pex30p in LD budding and whether other peroxins of the same family of Pex30p are also involved in LD biogenesis.

In the present work, we show that all dysferlin domain-containing peroxins accumulate at LDs in absence of the Seipin complex. However, Pex28p, Pex29p, Pex31p and Pex32p do not exert the same function as Pex30p in LD budding. Nevertheless, we demonstrate that some of these peroxins seem to regulate and target Pex30p to other organelles in specific metabolic conditions. We also found the novel role of dysferlin domain as essential for Pex30p localisation at the LDs and this propriety is conserved among some of the dysferlin domain-containing peroxins. We propose that the dysferlin domain-containing peroxins associate in a protein complex and act in concert to define their localisation and function in response to the metabolic conditions. Such a complex may then regulate intracellular communication among several organelles in which dysferlin domain-containing peroxins play several functions, contributing to coordinate organelle biogenesis and, consequently, cell homeostasis.

Keywords: LD biogenesis, LD budding, *Saccharomyces cerevisiae*, Seipin, Pex30, Peroxins, Dysferlin domain, Reticulon-homology domain

Caracterização das peroxinas com domínio disferlina na biogénese de partículas lipídicas

Resumo

Partículas lipídicas (PLs) são organelos ubíquos de crucial importância em biologia celular, na compreensão de doenças humanas e em biotecnologia, uma vez que são reservatórios celulares de lípidos neutros para produção de energia e síntese de membranas, assim como atuam como centro dos processos celulares metabólicos. Apesar de esforços contínuos, o mecanismo molecular de biogénese de PLs não é completamente compreendido. Publicações recentes indicaram que a biogénese de PLs e a formação de vesículas pré-peroxissomais, que estão envolvidas na biogénese de peroxissomas, ocorre nos mesmos locais do retículo endoplasmático (RE), sugerindo que estes domínios são específicos e distintos do restante RE. Para além disso, o *budding* destes organelos estruturalmente distintos envolve cooperação entre *Seipin* e Pex30p. Contudo, os mecanismos moleculares relativos a esta cooperação continuam desconhecidos. Visto que nenhuma peroxina da família de Pex30p - peroxinas com domínio disferlina - foi antes descrita como envolvida na biogénese de PLs, não é claro como é que Pex30p se localiza nas PLs na ausência do complexo *Seipin*. A função central de Pex30p também é desconhecida, assim como se outras peroxinas da mesma família também estão envolvidas na biogénese de PLs.

Neste trabalho foi observado que todas as peroxinas com domínio disferlina acumulam-se nas PLs na ausência do complexo *Seipin*. Contudo, Pex28p, Pex29p, Pex31p e Pex32p não exercem a mesma função que Pex30p no *budding* de PLs. Porém, foi demonstrado que algumas destas peroxinas parecem regular e definir a localização de Pex30p em condições metabólicas específicas. Também foi examinado que o domínio disferlina é essencial para a localização de Pex30p nas PLs e esta propriedade é conservada entre algumas das peroxinas da sua família. Deste modo, é proposto que as peroxinas com domínio disferlina associam-se num complexo proteico e atuam em conjunto para definir a sua localização em resposta ao estado metabólico da célula. Este tipo de complexo pode regular a comunicação intracelular entre diversos organelos em que as peroxinas com domínio disferlina realizam diversas funções, contribuindo para coordenar a biogénese de organelos e, conseqüentemente, a homeostasia celular.

Palavras-chave: Biogénese de PLs, *Budding* de PLs, *Saccharomyces cerevisiae*, *Seipin*, Pex30, Peroxinas, Disferlina, Domínio *reticulon-homology*

Table of contents

Declaração	ii
Acknowledgments.....	iii
Abstract.....	v
Resumo.....	vii
Table of contents	ix
Glossary of abbreviations, symbols, and acronyms	xii
List of figures.....	xiv
List of tables.....	xv
1. Introduction	1
1.1. Lipid droplet.....	2
1.1.1. Lipid droplet structure	2
1.1.2. Lipid droplet biogenesis.....	4
1.1.3. Lipid droplet: a well functionally connected organelle	9
1.2. Seipin	11
1.2.1. Seipin function on lipid droplet biogenesis	12
1.2.2. Seipin and Pex30p coordinate organelle biogenesis	14
1.3. Dysferlin domain-containing peroxins family	16
1.3.1. Pex30p domains	17
1.3.2. MCTP2	20
1.4. Work plan and aims.....	21
2. Material and methods.....	23
2.1. Yeast strains and growth.....	24
2.1.1. Yeast transformation using CRISPR-based genome editing	25
2.2. Reagents.....	26

2.3. Structure prediction	27
2.4. Fluorescence microscopy imaging	27
2.5. Yeast growth assays	28
2.6. Whole-cell extracts and western-blot analysis.....	29
2.7. Statistical analysis	29
3. Results	31
3.1. Functional comparison of the dysferlin domain-containing peroxins in lipid droplet biogenesis.....	32
3.1.1. Dysferlin domain-containing peroxins concentrate at lipid droplets in absence of the Seipin complex.....	32
3.1.2. Pex30p has a unique function at the lipid droplets among the dysferlin domain-containing peroxins	34
3.1.3. Pex29p regulates the localisation of Pex30p	38
3.2. Functional characterization of Pex30p in lipid droplet biogenesis	39
3.2.1. Overexpression of Pex30p has no effect on lipid droplet number and size.....	39
3.2.2. The dysferlin and the reticulon-homology domains cooperate on Pex30p localisation in absence of the Seipin complex.....	39
3.2.3. The dysferlin domain is essential for Pex30p function in lipid droplet budding...	42
3.2.4. Endoplasmic reticulum membrane-shaping proprieties of the reticulon-homology domain of Pex30p in lipid droplet budding	44
3.2.5. The function of the dysferlin domain in absence of Seipin is conserved among dysferlin domain-containing peroxins.....	46
3.3. Characterization of MCTP2 as the human homolog of Pex30p.....	48
3.3.1. Function of reticulon-homology domain of MCTP2 in lipid droplet budding.....	48
3.3.2. C2 domains failed to replace the function of dysferlin domain	49
4. Discussion.....	51
4.1. The dysferlin domain-containing peroxins cooperate in lipid storage homeostasis.....	52

4.2. Involvement of Pex30p functional domains in lipid droplet budding.....	55
4.3. Conclusion	59
5. References	61
6. Supplemental material.....	77

Glossary of abbreviations, symbols, and acronyms

µm	Micrometre(s)
ACAT	Acyl-CoA: cholesterol acyltransferase
ACS	Acyl-CoA synthetase
BSDL2	Berardinelli-Seip congenital lipodystrophy type 2
cDNA	Complementary DNA
CGL	Congenital generalised lipodystrophy
CIDEA	Cell death activator CIDE-A
CoA	Coenzyme A
CRISPR	clustered regularly interspaced short palindromic repeats
C-terminal	Carboxyl-terminal
DAG	Diacylglycerol
DGAT	Diacylglycerol acyltransferase
DysF	Dysferlin
eLD(s)	Expanding lipid droplet(s)
ER	Endoplasmic reticulum
FA(s)	Fatty acid(s)
FIT	Fat storage-inducing transmembrane
GFP	Green fluorescent protein
HCV	Hepatitis C virus
HP	Hairpin
HR	Homologous recombination
iLD(s)	Initial lipid droplet (s)
kDa	Kilodalton(s)
LB	Luria-Bertani
LD(s)	Lipid droplet(s)
LPA	Lysophosphatidic acid
MCTP2	Multiple C2 domain and transmembrane region protein 2
MDH	Monodansylpentane
mNG	Monomeric neon green
NL(s)	Neutral lipid(s)
NL(s)	Neutral lipid(s)

nLD(s)Nascent lipid droplet(s)
nmNanometre(s)
NPC2Niemann-Pick type C2 protein
N-terminalAmino-terminal
NVJNuclear membrane-vacuole junction
ODOptical density
PAPhosphatidic acid
PAMProtospacer adjacent motif
PCPhosphatidylcholine
PCR.....Polymerase chain reaction
PEPhosphatidylethanolamine
PEXPeroxin(s)
PL(s)Phospholipid(s)
PPVPre-peroxisomal vesicle
RHDReticulon-homology domain
RTN.....Reticulon
S. cerevisiae*Saccharomyces cerevisiae*
SE(s)Sterol ester(s)
sgRNASingle-guide RNA
sLD(s)Supersized lipid droplet(s)
TAGTriacylglycerol
tdTomato.....tandem dimer Tomato
TMTransmembrane domain
WTWild type
Y. lipolytica*Yarrowia lipolytica*
YPD.....Yeast extract peptone dextrose

List of figures

Figure 1. Current model of lipid droplet biogenesis.....	5
Figure 2. Schematic diagrams of Seipin structure.....	11
Figure 5. Dysferlin domain-containing peroxins concentrate at lipid droplets in absence of the Seipin complex.	33
Figure 6. Pex30p is the only of the dysferlin domain-containing peroxins cooperating with the Seipin complex in lipid droplet budding.	36
Figure 7. Pex29p regulates localisation of Pex30p during stationary phase.....	38
Figure 8. Overexpression of Pex30p does not alter lipid droplet size and number.	40
Figure 9. Both the dysferlin and the reticulon-homology domains are required for Pex30p localisation in absence of the Seipin complex	41
Figure 10. The dysferlin domain is essential for Pex30p function in LD budding.	43
Figure 11. The dysferlin domain of Pex30p is essential for efficient LD budding in absence of the Seipin complex	45
Figure 12. The function of the dysferlin domain of Pex30p in absence of Seipin is conserved in Pex31p and Pex32p.....	48
Figure 13. MCTP2 domains are functional different from Pex30p domains.....	50
Figure S1. Dysferlin domain-containing peroxins concentrate at lipid droplets in absence of the Seipin complex.	78

List of tables

Table S1. Yeast strains used in this study.....	77
--	----

1. Introduction

1.1. Lipid droplet

Lipids are ubiquitous signalling and regulatory molecules involved in the control of cellular physiology and metabolism, which similarly play as structural components of the cell membrane and membranes of organelles, and as an energy source. Since new energy sources are not always available, the ability to store energy in form of lipids within the cell is often crucial for survival. In addition, the ability to buffer and store excess of lipids in an inert form also prevents cells from lipotoxicity and cell death. Therefore, to package lipids efficiently, cells convert them into neutral lipids (NLs) and deposited them into specialized intracellular organelles called lipid droplets (LDs).

Originally viewed as dull organelles that simply store lipids because of lipid overflow, lipid droplets are now recognized as key components in the cell that exert a variety of relevant functions in multiple tissues (Hashemi & Goodman, 2015; Walther & Farese Jr, 2012). Given the diverse functions of the encased lipids, LDs lie at the crossroads of membrane biology and energy metabolism and are important organelles in maintaining cell homeostasis. Specifically, with their role in lipid storage, LDs figure prominently in common pathologies linked to lipid accumulation, including obesity, diabetes, and atherosclerosis (Shimeng Xu, Zhang, & Liu, 2017), and in industrial applications, such as efforts to produce triacylglycerols (TAG) for food, and hydrocarbons more generally, as biofuel (Andrianov et al., 2010).

1.1.1. Lipid droplet structure

Lipid droplets are organelles present virtually in all eukaryotic cells and some prokaryotic cells (Fujimoto & Ohsaki, 2006; Wältermann et al., 2005), which are structurally distinct from most other organelles. These dynamic cytoplasmic organelles consist of a neutral lipid core, mainly of triacylglycerols and steryl esters (SE), encased in a unique phospholipid monolayer instead of the typical bilayer, which segregates their hydrophobic neutral lipid core from the aqueous cytosol (Walther & Farese Jr, 2012). The composition of the hydrophobic core is variable because, depending on the cell type, the relative amounts of TAG and SE varies, and it can also include retinyl esters, waxes, and ether lipids, which are derived from peroxisomes (Bartz et al., 2007). For instances, yeast LDs store a mix of SE and TAG, but the LDs of adipocytes contain primarily TAG (Bartz et al., 2007).

The LD surface comprises polar, amphipathic lipids, mostly phosphatidylcholine (PC), which is important in emulsifying the membranes (Krahmer et al., 2011), followed by

phosphatidylethanolamine (PE) and phosphatidylinositol (Tauchi-Sato, Ozeki, Houjou, Taguchi, & Fujimoto, 2002). Compared with other membranes, the LD monolayer is deficient in phosphatidylserine and phosphatidic acid, but enriched in lysoPC and lysoPE (Bartz et al., 2007).

In addition, the LD membrane exhibits association with numerous proteins which, not surprisingly, exert functions in lipid synthesis and degradation, integration of nutrient signals and contribute to the biogenesis, maturation and stability of LDs (reviewed in Kory, Farese Jr, & Walther, 2016; Yang et al., 2012). The ability to isolate LDs to high purity, together with the modern techniques of proteomics, has allowed the elucidation of the LD proteome under different experimental conditions. Given that the LD proteome varies between cell and tissue type, as well as cell condition, this has yielded maps of the 'housekeeping' proteins of LDs (reviewed in Bersuker & Olzmann, 2017), as well as unexpected insights into their possible interactions with other organelles (Bersuker et al., 2018). However, how proteins target LDs is a major question in the field because unlike proteins targeted to other organelles, there are no targeting consensus sequences in LD-resident proteins. Since the interior of LDs is hydrophobic, it is devoid of proteins and integral proteins are embedded into the monolayer by adopting a monotopic topology, exposing all soluble domains to the cytosol (Thiele & Spandl, 2008). Although the protein structure that LD-resident proteins adopt within the membranes is unknown, these proteins were organized into two different classes (class I and class II), because this generalization provides a conceptual framework for discussing how proteins associate with the LD monolayer (Kory et al., 2016). Proteins with a hydrophobic hairpin (HP) and produced at the endoplasmic reticulum (ER) belong to class I, while proteins with an amphipathic helix synthesized at the cytosol are designed as class II. Several HP proteins exhibit a dual steady-state localisation to LDs and the ER and are first integrated into the cytoplasmic leaflet of the ER membrane before localising to LDs (Klemm, Spooner, & Ploegh, 2011; Olzmann, Richter, & Kopito, 2013; Stevanovic & Thiele, 2013; Wilfling et al., 2013; Zehmer et al., 2009). Even though the HP domains of these proteins are necessary and sufficient for this dual localisation, the molecular machinery by which HP proteins are directed to and inserted into ER or LD membranes is unclear. There are reports that at least some HP proteins require factors involved in peroxisomal membrane protein targeting (Schrul & Kopito, 2016), supporting a link between LD and peroxisome biogenesis (Joshi et al., 2018; S. Wang et al., 2018) (see section 1.2.2.). The class II proteins are characterized by their amphipathic or hydrophobic sequences, which made them bind directly to the LD membrane after translation in the cytoplasm. Some examples include

the perilipin family of proteins (Rowe et al., 2016) and cell death activator CIDE-A (CIDEA) (Barneda et al., 2015).

Lipid droplets can present a wide range of sizes, from tens of nanometres (nm) to several micrometres (μm) in diameter among different cell types, among individual cells of a population or even within a single cell. Moreover, the LD size and abundance varies dynamically and rapidly in response to cellular signals. For instances, oleate loading of *Drosophila* S2 cells increases the LD mean diameter nearly threefold within hours (Krahmer et al., 2011). In contrast, within hours the diameter of LDs decreases in cells with limited nutrients. In *Saccharomyces cerevisiae* (*S. cerevisiae*), LDs are found most prominently during the stationary phase, and catabolism of LDs in the exponential phase is coordinated with an increased need for phospholipids during cell division (Kurat et al., 2009).

1.1.2. Lipid droplet biogenesis

Otherwise other organelles, the major mechanism of LD biogenesis is *de novo* formation from the endoplasmic reticulum. However, fission of LDs has been observed in yeast (Long et al., 2012). Despite recent findings, the molecular mechanisms of LD *de novo* formation are not completely understood. According to the prevailing model (Fig. 1), neutral lipids are synthesized and organized between the bilayer leaflets of ER until the point in which it is thermodynamically favourable to coalesce and nucleate into a lens at specific ER membrane domains, where the lens grow until a threshold diameter, which promotes its budding from the ER membrane. The overall process includes three main steps after neutral lipid synthesis: nucleation, growth and budding, exactly as in phase separation and dewetting phenomena, namely, the process of retraction of a fluid from a non-wettable surface (Thiam & Forêt, 2016).

Neutral lipid synthesis

Neutral lipids are generated by enzymes that localise to the ER, where they encounter their substrates, namely fatty acids (FA) and glycerolipids. Before neutral lipid synthesis reactions occur, FA, which are chemically inert, must be activated by esterification with coenzyme A (CoA). The esterification step occurs in an ATP-dependent two-step reaction catalysed by enzymes of acyl-CoA synthetase (ACS) protein family. Kassan and colleagues (2013) had shown that acyl-CoA synthetase 3 (ACS3), which produces long-chain acyl-CoAs, controls the number and size of LD, likely by activating FA. After FA activation, NL synthesis is catalysed by various enzymes (Buhman,

Chen, & Farese, 2001). In mammalian cells, acyl-coenzyme A (acyl-CoA): diacylglycerol acyltransferase (DGAT) enzymes, DGAT1 and DGAT2, synthesize TAG, and acyl-CoA:cholesterol acyltransferase (ACAT) enzymes, ACAT1 and ACAT2, produce SE (Yen, Stone, Koliwad, Harris, & Farese, 2008). In yeast, the corresponding neutral lipid synthesis enzymes are Dga1p and Lro1p, which synthesize TAG, as well as Are1p and Are2p, which synthesize primarily SE (Zweytick et al., 2000). The sterols biosynthesis occurs in the ER by the mevalonate pathway, whose most enzymes are conserved from yeast to mammals, since synthesis of ergosterol (in yeast) and cholesterol (in mammals) only differs after production of lanosterol (Espenshade & Hughes, 2007). Then, ACAT catalyses the covalent joining of sterols with long chain fatty acyl-CoA moieties to form the SE (Buhman et al., 2001).

The *de novo* TAG synthesis is performed by the glycerol phosphate pathway, also known as the Kennedy pathway, that starts by converting glycerol 3-phosphate into lysophosphatidic acid (LPA) by the covalent linking with a fatty acyl-CoA. Then, LPA is converted to phosphatidic acid (PA), which is next transformed into diacylglycerol (DAG) by lipin (Pah1p, also known as Pet10p, in yeast) (Kennedy, 1956) and DGAT (Dga1p in budding yeast) catalyses the last reaction of the *de novo* TAG synthesis, by joining DAG with a fatty acyl-CoA. Alternatively, *de novo* TAG synthesis can occur

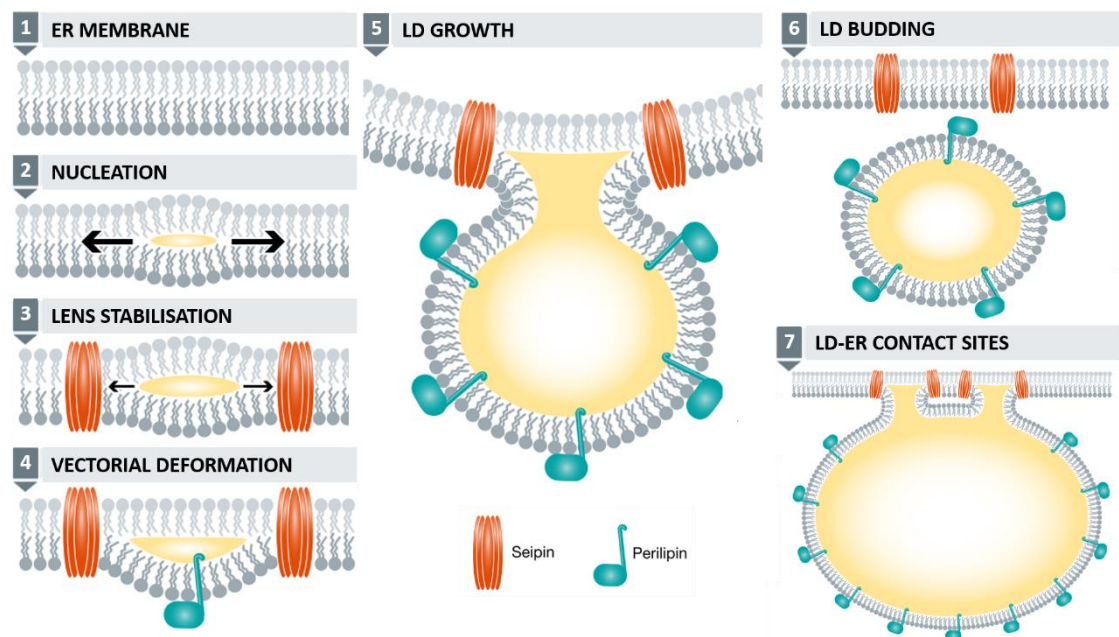


Figure 1. Current model of lipid droplet biogenesis. Lipid droplet formation starts with neutral lipids synthesis and their diffusion within the ER bilayer, leading to their accumulation in specific sites and to the formation of a lens (1,2). The nascent LD (nLD) is stabilized by Seipin (3) and grows asymmetrically towards the cytosol promoting deformation of the ER bilayer (4). During the growth LDs acquire Perilipins on the cytosolic leaflet (5). When a critical size is reached, LD budding is triggered and the initial LD (iLD) is released to the cytosol (6). In yeast, most of the LDs remain attached to the ER membrane due to contact sites between the membranes of the two organelles, stabilised by Seipin, allowing the diffusion of proteins and lipids (7). As a result, the proteome of the iLD changes and it continues growing converting into an expanding LD (eLD) (adapted from Henne, Reese, & Goodman, 2018).

through the monoacylglycerol pathway, where monoacylglycerol is covalently joined with fatty acyl-CoA to produce DAG, and consequently TAG. In yeast, TAG can also be synthesised using an acyl-CoA-independent reaction, where phospholipids (PL) can act as the acyl donor. The reaction is catalysed by phospholipid/diacylglycerol acyltransferase, encoded by *lro1* in yeast (Dahlqvist et al., 2000) and found exclusively in the ER, whereas Dga1p is dually localised to LD and ER (Sorger, 2002).

Yeast lacking all enzymes of NL synthesis (Dga1p, Lro1p, Are1p and Are2p) are viable but lack detectable LDs (Sandager et al., 2002). In mammals, knockout mouse studies show that ACAT1, ACAT2, and DGAT1 are not essential for life (Yen et al., 2008), whereas DGAT2 is, resulting in the lack of energy stores and skin defects related to essential FA deficiency (Stone et al., 2004).

Nucleation

The newly generated neutral lipids are deposited among the leaflets of the ER bilayer, to be sequestered from the polar head groups of phospholipids. As their concentration increases, the NLs laterally diffuse and coalesce to form a lens (Fig. 1), since the energy cost for interaction with each other is less than their interaction with phospholipid acyl chains (Thiam & Forêt, 2016). In model membranes, this transition occurs when TAG concentration is in the range of 5-10mol % (Duelund et al., 2013; Khandelia, Duelund, Pakkanen, & Ipsen, 2010). This process is named nucleation and induces deformation of the membrane since the nascent LD (nLD) is formed (Prévost et al., 2018). For many years, these lenses were maintained as hypothetical, but they have been observed recently in yeast by electron microscopy after triggering lipid droplet formation, consistent with the lenses being early intermediates (Choudhary, Ojha, Golden, & Prinz, 2015). However, this biophysics process was supported by data reported over the years. Localisation studies have found that NL synthesis enzymes are continuously distributed along the ER (Stone et al., 2009), with the exception of DGAT2, which also localises to LDs (Kuerschner, Moessinger, & Thiele, 2008). However, the enzymes not perfectly overlapping (Shockey, 2006), confirming that NL are synthesised throughout the ER and then diffuse through the bilayer to the LD formation sites, where they accumulate. Whether these subdomains form randomly throughout the ER or preferential sites for their formation exist is still unclear. However, there are some reports both in yeast and mammalian cells that indicate the existence of a specialized ER domain for LD biogenesis (Jacquier et al., 2013; Kassin et al., 2013). In addition, recent reports indicated that LD biogenesis

occurs that the same sites where pre-peroxisomal vesicles (PPV), involved in peroxisomes biogenesis, form, suggesting that these sites are specific (Joshi et al., 2018; S. Wang et al., 2018).

Lipid droplet growth

The growth of the nascent LD by addition of more neutral lipids results in significant perturbations in the ER bilayer membrane curvature. Eventually they reach a critical size that triggers budding of the LD, into the cytoplasm, by a mechanism similar to dewetting, basically driven by local thermal fluctuations (Pol, Gross, & Parton, 2014; Thiam, Farese Jr, & Walther, 2013; Thiam & Forêt, 2016). This growth is asymmetry towards the cytosol (Fig. 1). The regulation of this vectorial membrane deformation is not fully understood, but recent progress has been made. According to recent models, slight differences in surface tension between the ER leaflets are sufficient to induce vectorial budding (Chorlay & Thiam, 2018). Specifically, lower bilayer tension favours LD budding. Both phospholipids and proteins can influence the tension in the different leaflets of the membrane. In particular, lipid geometry appears to be a major factor in determining budding efficiency, since conically shaped molecules, such as DAG or PE, disfavour budding and molecules with opposite geometry, such as lysophospholipids, promote budding (Choudhary et al., 2018; M'barek et al., 2017). However, the molecular mechanism regulating the targeting proteins and lipids in the nLD membrane needs to be explored. Recently, based on a new cryo-electron microscopy structure, it was proposed that the protein Seipin controls the diffusion of lipids between ER and LD (Sui et al., 2018).

Lipid droplet budding and ER-LD contact sites

Although the budding of vesicles from the ER requires the involvement of membrane curvature-inducing coat proteins, such as COPII, these are not involved in budding of LDs. Instead, *in vivo*, proper LD budding requires Fat storage-inducing transmembrane (FIT) proteins (Choudhary et al., 2015), an evolutionarily conserved family of ER integral membrane proteins (Kadereit et al., 2008). Two highly related FIT proteins, FIT1 and FIT2, are present in mammals while other metazoan and yeast exclusively express FIT2-related proteins (Kadereit et al., 2008). Depletion of FIT-related proteins in yeast (Scs3p and Yft2p), worm, and mammalian cells inhibit LD budding, resulting in the accumulation of nLD embedded in the ER membrane (Choudhary et al., 2015). However, how FIT proteins promote lipid droplet budding remains unclear.

In yeast, LD budding is also facilitated by Pah1p, a protein related to mammalian perilipins (Gao et al., 2017). In mammals, this class of proteins has a well-established function regulating LD consumption (Sztalryd & Brasaemle, 2017) and may also facilitate LD biogenesis (Bulankina et al., 2009) (Fig. 1). Like other perilipins, Pah1p is recruited from the cytosol to the lipid droplet monolayer, but its LD targeting occurs at very early stages during the biogenesis process. In addition, cells lacking *pah1* show a significant delay in LD budding, suggesting that it facilitates budding. How exactly Pah1p and perhaps other perilipins promote LD budding is unclear. However, by accessing only the nLD from the cytosolic side, it may facilitate budding by changing the balance of tension between the two membrane leaflets.

Seipin, which corresponds to the Fld1p/Ldb16p complex in budding yeast, is another protein also crucial for efficient LD budding since mutations in Seipin lead to aberrant LD biogenesis, morphology, and dynamics in a variety of cells. Consequently, it regulates abundance and size of LDs (Fei et al., 2008; Grippa et al., 2015; Salo, Belevich, Li, Karhinen, Vihinen, Vigouroux, Magré, Thiele, Hölttä-Vuori, et al., 2016; H. Wang et al., 2016) (see section 1.2.).

After budding, the initial lipid droplets (iLD) can remain cytosolic or reconnect with the ER membrane. These ER-LD contact sites allow the diffusion of lipids and proteins between the two organelles and, consequently, it changes LDs proteome. As a result, cells can develop diverse populations of LDs, which respond to cell signals in different ways. Some of these LDs, by acquiring enzymes for local NL synthesis continue growing, resulting in expanded lipid droplets (eLD). In yeast, most of iLD reconnect with the ER (Jacquier et al., 2011; Mishra et al., 2016), but at least in some cells, budded LD are found physically separated from the ER (Wilfling et al., 2013). These cytoplasmic LDs may associate with other organelles in the cell (Gao & Goodman, 2015).

Although not completely explored, the process of LD formation seems evolutionarily conserved. In yeast, LD biogenesis appears to be spatially coordinated with other organelles also related to lipids and the metabolic condition. Not only the sites of LD biogenesis corresponds to the sites of PPV formation, involved in peroxisomes biogenesis (Joshi et al., 2018; S. Wang et al., 2018), but also are associated to ER-vacuole contact sites (nuclear membrane-vacuolar junctions; NVJ), which physically expand in response to metabolic cues and organize membrane tether proteins and fatty acid activating machinery for neutral lipid synthesis and lipid droplet emergence (Hariri et al., 2017). In conclusion, by coordination of several proteins and organelles, LD biogenesis is a well-regulated process to ensure energy homeostasis in the cell.

1.1.3. Lipid droplet: a well functionally connected organelle

Lipid droplets are dynamic organelles acting as metabolic hubs to maintain energy homeostasis within the cell in response to several physiological and environmental cues (Henne, Reese, & Goodman, 2018; Pol et al., 2014; Welte, 2015). Therefore, they have diverse cellular functions, including producing lipids (Kuerschner et al., 2008), sequestering toxic lipids (Bailey et al., 2015; Listenberger et al., 2003) and acting as dynamic lipid storage depots that enable rapid mobilization of fatty acids for energy (Rambold, Cohen, & Lippincott-Schwartz, 2015), membrane biosynthesis (Chauhan, Visram, Cristobal-Sarramian, Sarkleti, & Kohlwein, 2015; Gaspar, Hofbauer, Kohlwein, & Henry, 2011; Kurat et al., 2009), and lipid signaling pathways (Tang et al., 2013).

Much has been explored about the function of LDs as energy storage organelles, their most important function. However, LDs are emerging as intermediaries in other cell functions, such as, protecting against ER stress (Fei, Wang, Fu, Bielby, & Yang, 2009), protein glycosylation (Krahmer, Hilger, et al., 2013), and development of pathogen infection (Herker et al., 2010; Herker & Ott, 2011). For example, LDs are involved in hepatitis C virus (HCV) assembly, since this organelle provides a location for HCV core proteins until viral assembly. Regarding protein storage, increasing evidence has uncovered many examples of LDs recruiting proteins from other cellular compartments, in a cell type-specific and regulated manner. Some proteins targeted to LD are destined for destruction, whereas others are released and reused when conditions change (Fujimoto, Ohsaki, Cheng, Suzuki, & Shinohara, 2008; Hartman et al., 2010; Olzmann et al., 2013). For example, during embryogenesis in *Drosophila*, histones localise to LDs until needed for rapid nuclear division associated with embryo segmentation (Cermelli, Guo, Gross, & Welte, 2006). Therefore, LDs might have a general role in managing the availability of proteins, and they have been proposed to serve as generic sites of protein sequestration. The implications of this emerging role of LDs include regulated inactivation of proteins, prevention of toxic protein aggregates and localised delivery of signalling molecules.

As well as their individual functions, LDs are functionally connected with other cellular compartments through LD membrane contact sites (Barbosa & Siniossoglou, 2017; Fernández-Murray & McMaster, 2016; Welte & Gould, 2017). Besides the ER, LD interact dynamically with mitochondria, peroxisome (Binns et al., 2006; Schrader, 2001), vacuole/lysosome, endosomes (P. Liu et al., 2007) and the plasma membrane, by exchanging lipids and proteins (Gao & Goodman, 2015).

Notably, dysregulation of LD homeostasis has been implicated in the pathogenesis of numerous diseases (Greenberg et al., 2011; Kraemer, Farese Jr, & Walther, 2013; Onal, Kutlu, Gozuacik, & Emre, 2017), including diseases associated with an excess of LDs, namely obesity, diabetes, hepatic steatosis, arteriosclerosis and cardiovascular disease, or with a deficiency of LDs, namely lipodystrophy and cachexia. For instances, mutations in Seipin (see section 1.2.) result in a familial form of lipodystrophy (Fei et al., 2008; Magré et al., 2001; Szymanski et al., 2007), namely Berardinelli-Seip lipodystrophy, the most common form of autosomal recessive lipodystrophy. Moreover, due to the several functional associations with other organelles, malfunction of LDs has also potential relevance to human disorders including cancer and degenerative neurologic diseases (Lodhi & Semenkovich, 2014; H. Wang et al., 2016).

1.2. Seipin

Seipin is a homo-oligomeric integral membrane protein with short N- and C-terminal segments in the cytosol, two transmembrane (TM) helices, and an evolutionarily conserved ER luminal domain (Lundin et al., 2006), that is present at the ER membrane and concentrates at ER-LD contact sites (Fig. 2) (Binns, Lee, Hilton, Jiang, & Goodman, 2010; Cartwright & Goodman, 2012; Sim, Talukder, et al., 2013). Although its function is not completely understood, Seipin is a central player in LD formation, since mutations in Seipin lead to aberrant LD biogenesis, morphology, and dynamics in a variety of cells (Fei et al., 2008; Grippa et al., 2015; Salo, Belevich, Li, Karhinen, Vihinen, Vigouroux, Magré, Thiele, Hölttä-Vuori, et al., 2016; Szymanski et al., 2007; C.-W. Wang, Miao, & Chang, 2014; H. Wang et al., 2016; H. Wolinski, Kolb, Hermann, Koning, & Kohlwein, 2011).

The Seipin protein is encoded by the gene *Berardinelli-Seip congenital lipodystrophy type 2* (BSC2), which was initially identified by missense mutations leading to a rare but severe form of congenital generalised lipodystrophy (CGL) with the same name (Magré et al., 2001) (see section 1.2.1). These mutations occur mainly in the ER luminal region, suggesting that this portion of the protein is crucial for its function. Accordingly, the gene was originally identified in mammals and fruit fly (Magré et al., 2001), then was described in fungi and plants (Fei et al., 2008; Szymanski et al., 2007). The Seipin homologue in *S. cerevisiae* is Fld1p, more recently known as Sei1p (Fei et al., 2008; Fei, Shui, et al., 2011). The orthologs share a central region of about 250 amino acids, conserved in secondary structure, which corresponds to two transmembrane domains and a large ER luminal loop (Fig. 2) (Agarwal & Garg, 2004; Lundin et al., 2006; C.-W. Wang et al., 2014). However, in budding yeast, the Seipin function is only complemented when Fld1p assembles together with Ldb16p, a transmembrane protein in the ER, producing a functional complex (Fei et al., 2008; Szymanski et al., 2007; C.-W. Wang et al., 2014). The stability of Ldb16p

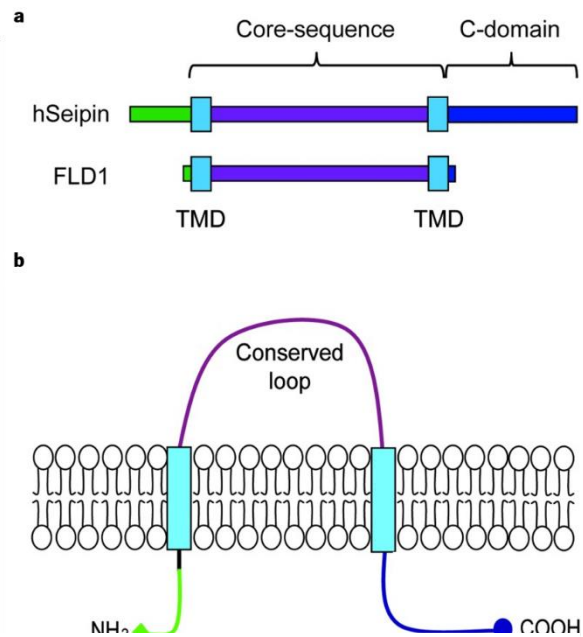


Figure 2. Schematic diagrams of Seipin structure. **a** | Domains structure aligned of human Seipin and yeast orthologue Fld1p. **b** | Protein structure of human Seipin with both N- and C-termini in the cytosol, two transmembrane domains embedded in the ER membrane and a conserved ER luminal loop (adapted from Wee, Yang, Sugii, & Han, 2014).

requires Fld1p since Ldb16p is subjected to ER-associated degradation in absence of Fld1p. In contrast, Fld1p is stable in absence of Ldb16p but not functional (C.-W. Wang et al., 2014).

Recently, using cryo-electron microscopy a structure of the functionally conserved luminal domain of *Drosophila melanogaster* Seipin revealed that Seipin, in this model, forms a dodecamer, with each monomer positioning a hydrophobic helix near the ER bilayer and having a β -sandwich domain with similarity to lipid-binding proteins, as Niemann-Pick type C2 protein (NPC2) (Sui et al., 2018; Sujuan Xu, Benoff, Liou, Lobel, & Stock, 2007). This structure suggests a new model for the molecular mechanisms of Seipin in LD biogenesis.

1.2.1. Seipin function on lipid droplet biogenesis

Seipin is a key regulator of LD cellular dynamics by assisting on their biogenesis and maturation (Cartwright et al., 2015; Grippa et al., 2015; C.-W. Wang et al., 2014; H. Wang et al., 2016). However, the specific molecular mechanism in which Seipin is involved and how is still unclear. In yeast, fly and mammalian cells, Seipin is found at dispersed foci in the ER that are recruited to and stabilized at sites of nascent LD formation, suggesting that Seipin contacts with the small, newly formed LD and enable them to grow as normal (Grippa et al., 2015; Salo, Belevich, Li, Karhinen, Vihinen, Vigouroux, Magré, Thiele, Hölttä-Vuori, et al., 2016; C.-W. Wang et al., 2014; H. Wang et al., 2016).

In absence of Seipin, cells display an aberrant LD morphology phenotype of tiny and clustered LD aggregates, possibly due to failed growth and premature budding (Salo, Belevich, Li, Karhinen, Vihinen, Vigouroux, Magré, Thiele, Hölttä-Vuori, et al., 2016; H. Wang et al., 2016; S. Wang et al., 2018), or a reduce number of supersized LDs (sLD), which likely result of coalescence of smaller LDs (Fei et al., 2008; Grippa et al., 2015; Salo, Belevich, Li, Karhinen, Vihinen, Vigouroux, Magré, Thiele, Hölttä-Vuori, et al., 2016; Szymanski et al., 2007; H. Wang et al., 2016; H Wolinski, Kolb, Hermann, Koning, & Kohlwein, 2011). The aberrant phenotype depends on the presence or absence of the phospholipid precursor inositol in the media, respectively (Fei, Shui, et al., 2011). The growth stage of cells also impacts on the relative distribution of these phenotypes since LD aggregates predominate in dividing cells, and sLDs are found primarily in stationary phase cells. In budding yeast, *fld1Δ*, *ldb16Δ* and *fld1Δldb16Δ* cells exhibit the same two LD phenotypes in the indicated conditions (Fei et al., 2008; Fei, Shui, et al., 2011; Szymanski et al., 2007; C.-W. Wang et al., 2014). Consistent with these results, mutations in Seipin promote an increase of NL content and alterations in phospholipid content, resulting in clustering and formation of supersized LD (Fei

et al., 2008; Fei, Li, et al., 2011; Jiang et al., 2014; L. Liu et al., 2014; Szymanski et al., 2007; Tian et al., 2011). In contrast, in wild-type cells, increased NL often lead to an increase in the number but not the size of LD (Fei et al., 2008). Nevertheless, it is known that Seipin deficiency increases PA levels, which may contribute to LD fusion (Fei, Shui, et al., 2011), explaining the supersized LD in mutated cells.

H. Wang and colleagues (2016) experiments confirmed, using insect and human cells, that cells lacking the Seipin protein, in addition to the supersized LDs, have a big amount of tiny dot-like structures containing TAG, which fail to grow into normal-sized LD and accumulate near the ER. A few of the numerous small iLD have a different proteome on their surface, promoting a different cellular pathway of LD expansion, which turns them into abnormally large LD (H. Wang et al., 2016). In support of this, lipid synthesis enzymes, such as GPAT4, that are normally found only on late-forming eLD are aberrantly targeted to iLD at early time points, in Seipin-deficient cells. This mislocalisation is crucial for the development of the supersized LD phenotype at later time points. Grippa and colleagues (2015) observed the same results in *S. cerevisiae* and showed that the Fld1p/Ldb16p complex is required for the identity of LD. In the absence of this complex, incorporation of PL into the monolayer of growing LD is entirely dependent on the ER phospholipid pools, leading to the generation of membrane defects and abnormal localisation of LD and other lipid-binding proteins, as a consequence of abnormal ER-LD contact sites. The stabilisation of ER-LD contact sites by the Fld1p/Ldb16p complex then establishes a diffusion barrier necessary for normal LD morphology and identity, facilitating the transference of protein and lipid cargo between LD and ER (Salo, Belevich, Li, Karhinen, Vihinen, Vigouroux, Magré, Thiele, Hölttä-Vuori, et al., 2016). Abnormal ER-LD contacts in Seipin mutants also change the type of phospholipids in the monolayer, reduce efficient targeting of LD-specific proteins and increase the packing defects in the LD monolayer, as detected by the unspecific recruitment of amphipathic helix-containing proteins (Grippa et al., 2015; Salo, Belevich, Li, Karhinen, Vihinen, Vigouroux, Magré, Thiele, Hölttä-Vuori, et al., 2016; C.-W. Wang et al., 2014).

In ER-LD contact sites, Seipin also regulates the lipid metabolism (Boutet et al., 2009; Fei et al., 2008; Fei, Li, et al., 2011; Fei, Shui, et al., 2011; Sim et al., 2013; Szymanski et al., 2007; Tian et al., 2011; Wolinski et al., 2015). For instances, the metabolism of PA, acting as a scaffolding protein recruiting PA-metabolism enzymes (Sim, Dennis, et al., 2013; Talukder, Sim, O'Rahilly, Edwardson, & Rochford, 2015) as well as controlling PA levels by inhibiting GPAT (Pagac et al., 2016). This regulation of PA levels is important because PA is a cone-shaped phospholipid

that facilitates LD fusion (Barneda et al., 2015; Fei, Shui, et al., 2011) and could be accommodated in the regions of negative membrane curvature associated with LD budding (Thiam et al., 2013).

Based on the recent Seipin structure, a new more detailed model for LD biogenesis was proposed (see section 1.2.1.). In this model, Seipin forms an oligomeric complex in the ER that moves throughout the reticular network in the absence of LDs. Seipin complexes may recognize the phospholipid packing defects at lipid lenses by binding via their many amphipathic and hydrophobic hairpins located at the cytoplasmic N- terminus and in the ER lumen, respectively. Subsequently, a Seipin oligomer becomes localised to a neutral lipid lens (H. Wang et al., 2016). As nascent LDs grow toward the cytosol, Seipin may anchor the nascent LD to the ER and allow maintenance of the ER–LD connection to enable LD growth and prevent nascent premature severing as found with Seipin deficiency (Grippa et al., 2015; Salo, Belevich, Li, Karhinen, Vihinen, Vigouroux, Magré, Thiele, Hölttä-Vuori, et al., 2016; H. Wang et al., 2016).

In conclusion, Seipin is crucial for proper LD biogenesis because it recognizes, is recruited to, and stabilizes sites of nascent LD formation. During LD growth it regulates the diffusion of proteins and lipids between the two organelles, contributing, also to LD budding.

1.2.2. Seipin and Pex30p coordinate organelle biogenesis

Given that Seipin is a crucial protein for efficient LD biogenesis, but its function remains unclear, Carvalho and collaborators (2018) searched for proteins that would compensate for Seipin loss by being enriched at LDs, in budding yeast. Pex30p, a dysferlin domain-containing peroxin, ER membrane-shaping protein, and involved on peroxisome biogenesis, was identified as a collaborator of the Seipin complex in the biogenesis of LDs since it accumulates at the proximal LD regions in absence of Seipin. Likewise, Pex30p also localises to LDs in situations of high demand for LD production, as upon oleate addition (S. Wang et al., 2018). In yeast, *de novo* peroxisome biogenesis, like LD biogenesis, involves the budding of membrane-bound pre-peroxisomal vesicles from specific ER domains (Joshi et al., 2016; Mast et al., 2016). These PPV-budding sites are enriched in Pex30p but their exact composition and mechanism of formation are unknown (Joshi et al., 2016). Curiously, the ER subdomains where Pex30p is present correspond to sites where most nascent LDs form and where mature LDs usually remain associated with Pex30p subdomains. Therefore, the same Pex30p subdomain can simultaneously associate with

a LD, a PPV or a peroxisome, revealing a coordinated biogenesis of LDs and peroxisomes (Wang et al, 2018; Joshi et al, 2018).

In the absence of Pex30p and the Seipin complex, budding of both LDs and peroxisomes is inhibited, leading to the ER accumulation of their respective constituent molecules, such as triacylglycerols and peroxisomal membrane proteins (S. Wang et al., 2018). Regarding LDs, the accumulation of TAG promotes the formation of aberrant dispersed structures in the ER that corresponds to extra ER membranes enriched in TAG in their intramembrane space. Cells in absence of Pex30p and the Seipin complex also present a strong growth defect that cells with Seipin deletion in conjunction with genes essential for peroxisome biogenesis, such as Pex3p and Pex19p, did not show, indicating that the growth defect was not due to a general loss of peroxisomal function. These double mutants exhibit dramatic lipidome remodelling, with a strong increase in PC and PI, and to a lower extent, DAG levels (S. Wang et al., 2018). Since this phenotype can be reversed by remodelling ER phospholipid composition, Pex30p and Seipin can be involved in LD budding by regulating the lipids and proteins present in the ER membrane. However, neither Seipin nor Pex30p appear to modify lipids directly, considering that individual deletions of Seipin or Pex30p do not result in major global changes in lipid composition (S. Wang et al., 2018). By regulating the lipids and proteins present in the membrane, the ER leaflet tension is regulated and, consequently, the LD budding process. In conclusion, Pex30p and Seipin act in concert to organize membrane domains permissive for organelle budding with a lipid composition distinct from the bulk ER.

1.3. Dysferlin domain-containing peroxins family

Peroxisomes are membrane-enclosed organelles which contain a matrix of enzymes involved in diverse metabolic reactions, such as oxidative reactions involved in energy metabolism. Therefore, they are highly regulated to response the cell needs and external signals (Smith & Aitchison, 2013). However, the molecular mechanism which describes the phenomenon of peroxisomes biogenesis is a big controversial topic. In fungi, the number of peroxisomes increases dramatically in response to distinct carbon and nitrogen sources. This property turned out to be of key importance for the identification of genes required for the formation and maintenance of this organelle. Using several species of fungi, 33 genes of peroxisomal biogenesis factors, also known as peroxins (PEX) were found. The corresponding peroxins are involved in widely distinct aspects of organelle biogenesis, such as matrix protein import, membrane biogenesis, proliferation, and inheritance. Among them, *Yarrowia lipolytica* (*Y. lipolytica*) Pex24p (YIPex24p) was isolated and characterized as a protein required for peroxisome assembly (Tam, Rachubinski, & Gene, 2002). Later, *Saccharomyces cerevisiae* Pex28p (Pex28p) and Pex29p were reported as its orthologs because they share extensive similarity among their protein sequences as well a role in the regulation of peroxisome number, size, and distribution (Vizeacoumar, Torres-guzman, Tam, Aitchison, & Rachubinski, 2003). The same happened between YIPex23p and Pex30p, Pex31p and Pex32p (Vizeacoumar, Torres-Guzman, Bouard, Aitchison, & Rachubinski, 2004). In *Y. lipolytica*, Pex23p and Pex24p, have been shown to be essential for cell growth in the presence of oleic acid, which requires peroxisomes for its metabolism, leading to accumulation of numerous small pre-peroxisomal vesicles or a few enlarged peroxisomes, respectively (Brown, Titorenko, & Rachubinski, 2000; Tam et al., 2002). Their homologues in *S. cerevisiae* are also associated with the number and size of peroxisomes due to cells with single gene deletions of *pex28*, *pex31*, or *pex32* have fewer and slightly enlarged peroxisomes, whereas a single deletion of *pex29* or *pex30* results in increased numbers of smaller peroxisome (Vizeacoumar et al., 2004, 2003).

Pex30p is the founding member of the family dysferlin domain-containing peroxins, also including Pex28p, Pex29p, Pex31p and Pex32p. These five proteins, whose genes are dispersed in different chromosomes, share the same protein domain and domain architecture since all contain a reticulon-homology domain (RHD) and a dysferlin domain (DysF). All five proteins were only identified in yeast and act together in a complex (T. Ito et al., 2001; Mast et al., 2016; Vizeacoumar et al., 2004, 2003), known as the Pex30-anchoring complex. The reticulon-homology

domain-containing proteins, Rtn1p, Rtn2p, and Yop1p, interact with the Pex30-anchoring complex creating a contact site to facilitate ER-peroxisome interactions (David et al., 2013).

Regarding lipid droplet biogenesis, Pex30p cooperates with the seipin complex for efficient LD budding, since *pex30Δfld1Δ* or *pex30Δdbp16Δ* cells exhibited strong growth defect. However, mutants with combined deletion of one of the components of the Seipin complex with *pex28Δ*, *pex29Δ*, *pex31Δ* or *pex32Δ* grow at wild-type rate. In addition, with no dysferlin domain-containing peroxin besides Pex30p was described as involved in lipid droplet biogenesis. However, several experiments have been reported that these proteins interact with important factors of diverse cellular processes, such as chromosome segregation (Logan et al., 2008; Pinsky et al., 2006) or plasma membrane composition (Miller, Zhang, Jiang, Li, & Pugh, 2018). Moreover, their function regulating peroxisome abundance and size is quite explored, allowing to understand that their abundance, stability and function is responsive to different nutrients or metabolic status (M. Yan, Rachubinski, Joshi, Rachubinski, & Subramani, 2008). In *S. cerevisiae* Pex28p and Pex29p are described to interact with Pex25p (Vizeacoumar et al., 2003), a nutrient-responsive transcripts target of the major regulator of stress responses, the complex Ccr4 (Miller et al., 2018).

1.3.1. Pex30p domains

Pex30p contains a reticulon-homology domain with ER membrane-shaping properties (Joshi et al., 2016), which is required for normal peroxisome biogenesis (David et al., 2013; Mast et al., 2016; Vizeacoumar et al., 2004; M. Yan et al., 2008), and a dysferlin domain that may bind DAG (Joshi et al., 2018; Vizeacoumar, Vreden, Aitchison, & Rachubinski, 2006; M. Yan et al., 2008).

Reticulon-homology domain

Proteins containing a reticulon-homology domain are present in all eukaryotic organisms, but they were not described yet in archaea or bacteria (Nziengui et al., 2007; Oertle, Klinger, Stuermer, & Schwab, 2003; Shibata et al., 2010; Voeltz, Prinz, Shibata, Rist, & Rapoport, 2006b). The vertebrate proteins are designed as reticulons (RTNs) and those found in other organisms are known as reticulon-like proteins. In mammals, there are four reticulon genes encoding proteins with RHD, RTN1-4, while yeast contains three conserved reticulon-like proteins, Rtn1p, Rtn2p and Yop1. Recently, Pex30p and Pex31p were described as reticulon-like proteins because a RHD was identified and Pex30p and Pex31p restore the functions of reticulon-like proteins (Joshi et al., 2016).

The RHD corresponds to two hydrophobic regions, which are thought to be membrane-embedded regions, flanking a hydrophilic loop. Although much amino-acid identity has been lost over the course of evolution, the overall structure of this domain has been preserved from yeast to humans. Across phyla, the second hydrophobic region of the RHD is the most highly conserved (R. Yan, Shi, Hu, & Zhou, 2006). However, while in mammals the RHD is conserved at the carboxyl-terminal region of the proteins, in yeast the RHD is found at the amino-terminal region of the proteins. The topology of this domain is only partially defined, but in mammals, the RHD loop region has been detected both on the surface of cells and intracellularly, suggesting that the two hydrophobic regions might span the membrane or form a hairpin. Since Pex30p was described to localized at the LDs, it may indicate that the RHD forms a hairpin in the LD monolayer.

Both in mammalian and yeast cells, the reticulons are largely restricted to the tubular ER and are excluded from the continuous sheets of the nuclear envelope and peripheral ER. They maintain the ER structure by stabilizing high membrane curvature in ER tubules and the edges of ER sheets since overexpression of these proteins results in the formation of tubular membrane structures and their absence in *S. cerevisiae* results in disrupted tubular ER (Voeltz, Prinz, Shibata, Rist, & Rapoport, 2006a). In addition, the elongated hydrophobic domains predicted to form hairpins in the outer leaflet of ER membrane may stabilize the membrane curvature (Shibata et al., 2010; Voeltz et al., 2006a) and these proteins are proposed to form arc-shaped oligomers that scaffold the membrane (Shibata et al., 2008).

Dysferlin domain

The name of the dysferlin domain present in Pex30p is originated from the human protein Dysferlin. The protein has been proposed to play a role in vesicle fusion associated with the Ca²⁺-dependent repair of microlesions of the sarcolemmal membrane in skeletal muscle and cardiomyocytes, since malfunction of this protein is associated with a group of autosomal recessive inherited late onset progressive muscular dystrophies called dysferlinopathies (Bansal et al., 2003; Fuson et al., 2014; Hedrich, Sher, Cox, & Ackert-Bicknell, 2012; McNally, 2012). Dysferlin is a two-anchored membrane protein, which is predicted to include seven C2 domains (C2A to C2G), three Fer domains (FerA, FerB and FerI), two DysF (inner and outer) domains, one nested inside the other, and a C terminal transmembrane domain, but most of the protein is lying in cytoplasm (Sula, Cole, Yeats, Orengo, & Keep, 2014).

Dysferlinopathy causing mutations are dispersed throughout the length of the protein, but the region of the DysF domains deserve attention (Aartsma-Rus, Van Deutekom, Fokkema, Van Ommen, & Den Dunnen, 2006). By gene duplication, one DysF domain is inserted into other DysF domain, producing an inner DysF domain and an two-part outer DysF domain (N terminal and C terminal) (Ponting, Mott, Bork, & Copley, 2008). The human myoferlin, dysferlin paralogue, inner DysF domain structure was solved by nuclear magnetic resonance and shows folding of two long antiparallel beta strands connected by a long loop that caps the sheet edges in certain sections (Patel et al., 2008). The high-resolution structure of human dysferlin inner DysF domain revealed that most of the pathogenic mutations are part of aromatic/arginine stacks that hold the domain in a folded conformation (Sula et al., 2014).

Pex30p contains a dysferlin domain equivalent to the human inner DysF, organized in two motifs one at each terminus of the domain (designed by DysFN and DysFC) and separated by a loop. Based on multiple sequence alignment and supported by structure prediction using PyMol software (Rigsby & Parker, 2016), the dysferlin domain of Pex30p has a similar secondary structure to the human dysferlin inner DysF (Fig. 3), since DysFN and DysFC correspond to the highly conserved β -1 and β -6 strands, respectively, of the human inner DysF (Fig. 4). The major difference between the DysF domains of the two proteins is the linking loop, namely the sequence between the short β strands 4 and 5, that are also conserved.

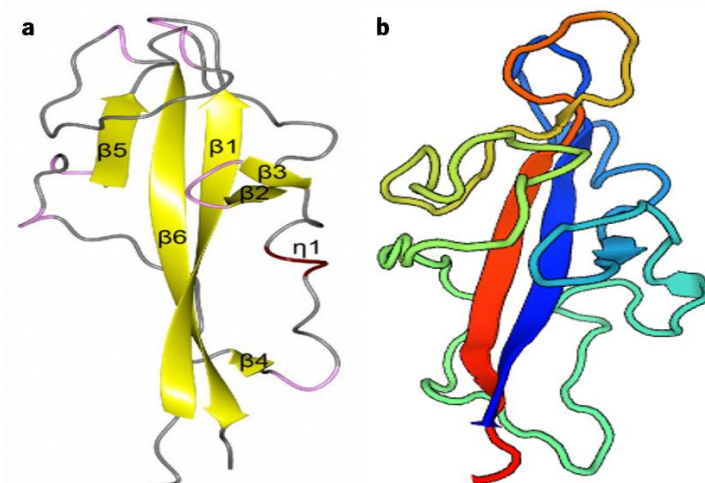


Figure 3. Comparison of DysF domain structures. **a** | Structure of Human Dysferlin inner DysF domain by X-ray crystallography. The amino acid sequence alignment in Figure 4 identifies the six beta strands present in this structure (adapted from Sula et al., 2014). **b** | Homology model of the DysF domain of Pex29p. The model was generated for the amino acid sequence of Pex29p from 353 to 470 and based on the DysF of human Myoferlin, using the automated protein structure homology-modelling server SWISS-MODEL (Waterhouse et al., 2018).

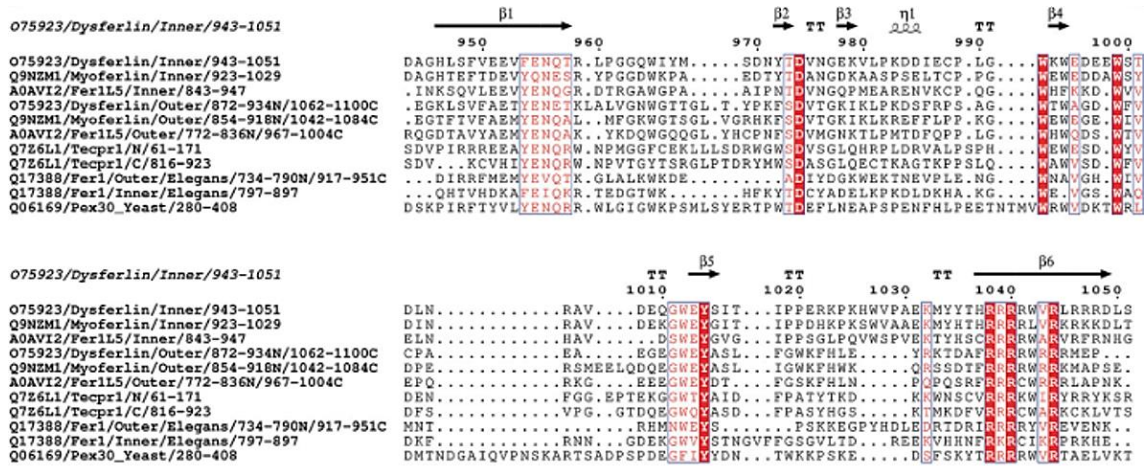


Figure 4. Alignment of DysF domains. Multiple sequence alignment of inner and outer DysF domain of Human Myoferlin, Dysferlin, Fer115; human Tecpr1 DysF domains; inner and outer DysF domain of *C. elegans* Fer1 protein, and Yeast Pex30p DysF domain (adapted from Sula et al., 2014).

1.3.2. MCTP2

The mammalian homolog of Pex30p cannot be identified by protein BLAST. However, when the structural homology prediction program HHpred was used to identify the closest human homolog of Pex30, the Multiple C2 domain and transmembrane region protein 2 (MCTP2), a protein containing a reticulon-homology domain, was identified (Joshi et al., 2018). The full-length 878-amino acid MCTP2 protein has three C2 domains (C2A-C), two transmembrane domains, and a short cytoplasmic C-terminal tail that includes a 12-residue stretch that is identical in all species and isoforms. Alternative splicing produces proteins with variable size of the linker between the C2A and C2B domains and/or that lack the first transmembrane domain. The three C2 domains share several residues among their amino acid sequences and the same predicted secondary structure. However, while the C2B domain of MCTP2 lacks two of the five residues required to bind calcium, C2C showed saturable calcium binding *in vitro* (Shin, Hau, Wang, & Südhof, 2005). Therefore, only C2A and C2C function as calcium binding module, but only in absence of phospholipids.

The same observations of Pex30p in lipid droplet and peroxisomes biogenesis were made for MCTP2 (see section 1.2.2.), proposing that sites where MCTP2 resides are relatively stable and exist before LD biogenesis being induced. They define the sites where proteins that mediate LD biogenesis assemble (Joshi et al., 2018). Although Pex30p/MCTP2 sites seem to facilitate LD growth, they are not required since some LDs mature outside of these sites and elimination or depletion of Pex30p or MCTP2 does not block LD biogenesis (Joshi et al., 2018).

1.4. Work plan and aims

The present work was developed in the scope of my second year of the Master Course in Molecular Genetics at the Department of Biology, School of Sciences, University of Minho, Braga. The experimental work was performed at the Sir William Dunn School of Pathology, University of Oxford, United Kingdom, under the supervision of the EP Abraham Professor of Cell Biology Pedro Carvalho.

The work comprised the following tasks:

- a) Determine the localisation of the dysferlin domain-containing peroxins in absence of the Seipin complex.
- b) Examine the function of dysferlin domain-containing peroxins in lipid droplet biogenesis.
- c) Assess the involvement of others dysferlin domain-containing peroxins in localisation and function of Pex30p.
- d) Determine the domain of Pex30p involved on its localisation at the lipid droplets;
- e) Explore, using genetic editing tools, the role of the reticulon-homology domain and the dysferlin domain of Pex30p in its function at lipid droplets.
- f) Examine the potential of MCTP2 as human homolog of Pex30p.
- g) Interpret and discuss the results and evaluate the involvement of the dysferlin domain-containing peroxins in lipid droplet biogenesis.

The main aims of this project are the determination of factors involved in the functional difference in lipid droplet biogenesis among the dysferlin domain-containing peroxins and the elucidation of the molecular and genetic mechanisms involved in localisation and function of Pex30p in efficient lipid droplet budding, in budding yeast.

This should validate the involvement of dysferlin domain-containing peroxins in lipid droplet biogenesis and contribute to the understanding of how Pex30p is localised at the lipid droplets in absence of the Seipin complex and cooperates in lipid droplet budding. Consequently, it should enhance the knowledge about the regulation of lipid droplet biogenesis in *Saccharomyces cerevisiae* and, consequently, in humans.

2. Material and methods

2.1. Yeast strains and growth

Standard procedures were used to maintain and generate *Saccharomyces cerevisiae* strains (Dymond, 2013). All strains used in the experiments present in this document are isogenic to the BY4741 (*MAT a his3Δ1 leu2Δ0 met15Δ0 ura3Δ0*) strain background, derived from the S288C strain of *S. cerevisiae*, and are listed in table S1. Cells were grown at 30 °C and assessed in exponential growth phase at an optical density at $\lambda = 600$ nm (OD_{600}) between 0.8–1.2 or in early stationary phase at 3-4, except when indicated. Unless otherwise stated, all data present in this document was collect from yeast grown at least overnight in the described conditions after being thawed from frozen stocks (-80 °C) to verify the phenotype and health of the cells prior to the experiments.

In most of the procedures, including preparation of competent cells for transformation, prior to freezing or sporulation, and for general nonselective growth, the strains were cultured in rich yeast extract peptone dextrose (YPD) medium, but the carbon source, dextrose, was substituted by glucose (1% yeast extract, 2% bactopectone, and 2% glucose). After yeast transformation, YPD media was supplemented with geneticin (G418) (200 μ g/ml), nourseothricin (clonNAT) (100 μ g/ml) and/or hygromycin (200 μ g/ml) to select the transformed cells. Following the same approach, synthetic complete (0.17% yeast nitrogen base, 5 g/liter ammonium sulfate, 2% glucose, and amino acids) medium customized with a 'drop-out' mix, namely leaving out amino acids and/or other supplements for which selective growth is required, was used to select the transformed cells. The mentioned media were used as liquid or solid, when prepared with agar.

Endogenous protein tagging, promoter replacements, and individual gene deletions were performed using standard polymerase chain reaction (PCR)-based homologous recombination (HR) (Janke, Magiera, Rathfelder, Taxis, & Reber, 2004; Longtine, Iii, Demarini, & Shah, 1998) and lithium acetate transformation. Strains with multiple gene deletions or multiple genetic modifications were generated either by PCR-based homologous recombination or by crossing haploid cells of opposite mating types followed by sporulation and tetrad dissection using standard protocols. In all these strains generated directly or indirectly by PCR-based homologous recombination coding sequences for drug resistance or synthesis of an amino acid, for which cells were previous auxotrophic, were introduced in the edited genome to select the transformed cells. To avoid the introduction of these sequences during genome editing, a protocol using a clustered regularly interspaced short palindromic repeats (CRISPR)-based tool was developed (see section

2.2.1.). Using this genome editing tool, full gene and gene fragment deletions, gene fragment replacements (designed posteriorly as chimeras) and nucleotide substitutions were performed.

2.1.1. Yeast transformation using CRISPR-based genome editing

CRISPR-Cas9 technology is an important tool for genome editing since the Cas9 endonuclease can induce targeted DNA double-strand breaks. Targeting of the DNA break is typically controlled by a single-guide RNA (sgRNA) – a small nucleotide guide sequence that hybridizes to the genomic DNA target. Previous studies used CRISPR-Cas9 technology for efficient, marker-free genome editing in *S. cerevisiae*, but the protocols were extensive and complex. Laughery and colleagues (2016) developed a vector for easy and rapid cloning and utilization during yeast transformation. In the experiments present in this document, the plasmid pML107 (Laughery et al., 2016) was used but their methods were adapted, as described below. In general, this genome editing system is based in the standard yeast transformation protocol with lithium acetate with homologous recombination (H. Ito, Fukuda, Murata, & Kimura, 1983). However, the cells were transformed simultaneously with a vector (100 µg), expressing the Cas9 machinery and specific sgRNAs, and a homologous recombination template (5 µg). Therefore, the sgRNA indicates the *locus* where Cas9 should induce DNA double-strand breaks, which induces DNA repair by homologous recombination. Considering that this genome editing approach does not introduce selection markers in the genome, the transformed cells were selected through the selection marker in the vector, that cells could lose when they were not in selection medium.

The plasmid

Initially, the plasmid pML107 was transformed into *dam*⁻/*dcm*⁻ competent *Escherichia coli* bacteria cells to avoid methylation at *BclI* digestion restriction site, and single colonies were selected in Luria-Bertani (LB) medium supplemented with ampicillin (100 µg/mL). After DNA extraction, the plasmid was digested with *BclI* and *SmiI*, following by a standard restriction digestion protocol.

To design the guide RNA sequence, which is inserted into the vector, a 20-base par sequence with higher off-target at the *locus* of interest was selected by using the online software Benchling (“Benchling (Biology Software),” 2018). Considering that the Cas9 encoded in the vector is from *Streptococcus pyogenes*, it requires a 5'-NGG-3' protospacer adjacent motif (PAM) sequence for efficient cleavage, although 5'-NAG-3' PAM sites can be cleaved with less efficiency (Hsu et al.,

2013; Hsu, Lander, & Zhang, 2014; Wenyan Jiang, David Bikard, David Cox, Feng Zhang, 2013). After defining the sequence for the guide RNA, the software developed by Laughery et al., (2016) was used to design the sgRNA fragment, since it corresponds to a chimeric RNA sequence containing a structural segment important for Cas9 binding and the 20-base par nucleotide guide sequence. Posteriorly, the nucleotide fragment was synthesized as double-strand and inserted into the digested plasmid by standard DNA ligation. The resulting vector was transformed into NEB stable competent *E. coli* and the single colonies were selected in LB medium supplemented with ampicillin (100 µg/mL). Positive colonies were selected, and the insertion of the sgRNA into the extracted plasmid was confirmed by sequencing.

The homologous recombination template

When used for full gene or partial gene deletion, a 200-base par nucleotide, correspondent to 100-base par nucleotide sequence before and after the sequence to be deleted, was synthesized. For single nucleotide substitution, the HR template was designed by including about 200-base par of the *locus* of interest, making sure that the mutated nucleotide was in the centre of the template. For gene fragment replacement, the HR template was obtained by amplification of the sequence to be inserted into the genome with primers containing at least 65-base par of recombination with the flanked regions of the *locus* being editing. The amplified sequence was previously obtained from total yeast genomic DNA or complementary DNA (cDNA) obtained from other organism of interest. Instead, this HR template can also be synthesized. When designing the HR template, it also included a nucleotide substitution in the PAM sequence to assure that Cas9 do not continue breaking the genomic DNA because that is lethal. For all experiments, the HR template was amplified by PCR to increase the DNA concentration before transformation.

2.2. Reagents

The plasmid pML107 (Laughery et al., 2016), used for CRISPR genome editing, was purchased from Addgene. The total cDNA library of U250 glioma cell line was a kind gift from Adam Grieve (Sir William Dunn School of Pathology, University of Oxford, United Kingdom).

The bacteria cells NEB Stable Competent *E. coli* and dam-/dcm- Competent *E. coli* were purchased from New England Biolabs Inc.

The fluorescent lipid droplet dye 4,4-difluoro-1,3,5,7,8-pentamethyl-4-bora-3a,4a-diaza-s-indacene, known as Bodipy^{493/503}, was purchased from Invitrogen and used at a final concentration of 1 µg/ml, while monodansyl pentane (MDH) was purchased from Abgent and used at 0,1 mM.

The anti-Pex30 antibody (rabbit) was a kind gift from William Prinz (National Institute of Diabetes and Digestive and Kidney Diseases, NIH, Bethesda, United States of America), the anti-Pgk1 antibody (mouse monoclonal clone) was purchased from Life Technologies and the anti-HA antibody (rat monoclonal clone; 3F10) was purchased from Roche. The anti-rabbit or anti-mouse secondary antibodies peroxidase conjugated were purchased from Jackson ImmunoResearch.

2.3. Structure prediction

HHpred is a software used for automated protein homology detection and structure prediction. When a homologous protein can be identified with known structure, this can be used as a template to model the 3D structure of the protein of interest, since even remotely homologous proteins generally have quite similar 3D structure (Kinch & Grishin, 2002). Using Pex30p protein sequence as single query sequence, the reticulon-homology domain and the dysferlin domain were predicted, based on the homology with the reticulons (Rtn1p and Rtn2p) and the human Dysferlin protein, respectively. Posteriorly, the RHD and DysF of the remaining dysferlin domain-containing peroxins (Pex28p, Pex29p, Pex31p and Pex32p) were predicted, based on the same proteins in addition to Pex30p. To confirm the domains limits, the domain architecture of Pex30p was also analysed by SMART (Letunic & Bork, 2018) and Pfam (Finn et al., 2016), two domain family resources.

2.4. Fluorescence microscopy imaging

Images from all experiments were captured using a Zeiss Cell Observer HS equipped with a CMOS camera (Hamamatsu ORCA-Flash4.0), fitted with a Plan-APOCHROMAT 100x 1.4 objective and controlled by 3i Slidebook 6.0 software (Intelligent Imaging Innovations, UK). BODIPY^{493/503} and green fluorescent protein (GFP), MDH and tandem dimer Tomato (tdTomato) signals were detected using GFP, DAPI and RFP filters, respectively, with standard settings. All imaging was performed at room temperature with live non-fixed cells. Moreover, for each image 11 z-planes were obtained, but only one representative z-slide was exhibited in this document.

Before analysis of the microscopy data, the intensity signal from GFP, DAPI and RFP channels were deconvoluted using the No Neighbours algorithm. Deconvolution is a quantitative method to

improve the information content of a 3D image because it uses an algorithm to determine and correct the systematic error of blur - the loss of contrast in smaller features - in optical systems such as fluorescence microscope. By determining the expected out-of-focus light for the used system, it redistributes the light to its points of origin in the specimen. The characterization of out-of-focus light is based on the 3D image of a point source of light, the so-called point-spread function (PSF) (Abraham, Allan, & Levings, 2010). No Neighbours deconvolution is a deblurring algorithm characterized by its computing speed. It works by boosting only the higher spatial frequencies in the specimen. After deconvolution, each channel range levels were renormalized in all images, to allow qualitative and quantitative relative analysis. All the microscopy images treatment and analysis were performed using 3i Slidebook 6.0 software.

The colocalization analysis of the lipid droplet signal, Bodipy, and the signal of the protein of interest, tdTomato, was performed by manually create a signal mask defined by intensity levels which recognize only lipid droplets of both wild-type and Seipin mutant cells in most of the z planes. Then, by using the Mask Statistics tool of 3i Slidebook 6.0 software, the Pearson's correlation coefficient was calculated. This coefficient calculates the correlation of intensity between the channels of interest and varies between -1 and 1, where 1 means complete correlation, -1 implies anti-correlation and 0.0 signifies no matching trend in intensities (Manders, Verbeek, & Aten, 1993). In each microscopy field, the mask identified several objects and the objects correspondent to lipid droplets were selected based on the ratio between the major and minor axis length. Only objects with a ration between 0.8 and 1.2 were considered lipid droplets due to their spherical form. For statistical analysis, 50 objects (one per cell) were scored per condition and genotype from multiple microscopy fields and analysed by GraphPad Prism 7 (La Jolla, United States of America). To confirm the Pearson's correlation result, line intensity graph was drawn in ten cells of each condition and genotype, but only one example was shown.

2.5. Yeast growth assays

For comparison of cell growth, after a preculture overnight, cells were grown to exponential phase ($OD_{600} = 0.5-0.8$) in YPD, diluted to OD_{600} of 0.1 followed by 10-fold serial dilutions. Diluted cells were spotted on YPD plates and incubated at 25 °C, 30 °C and 37 °C for two days.

2.6. Whole-cell extracts and western-blot analysis

For whole-cell extracts, cells were grown to exponential phase in YPD ($OD_{600}=0.8-1.2$) and 1 OD_{600} units of cells were pelleted. These cells were washed with phosphate-buffered saline solution (PBS), and the extracts were prepared by alkaline extraction (250 μ L of 0.015M NaOH) on ice for 10 minutes. After centrifugation at maximum speed for 2 min at 4 °C, the pellet was resuspended in 1x Laemmli sample buffer and heated at 65 °C for 10 minutes. Proteins were separated by SDS-PAGE Criterion TGX™ pre-casted gels (BioRad), transferred to polyvinylidene difluoride (PVDF) membrane and analysed with the indicated antibodies. Anti-rabbit or anti-mouse secondary antibodies peroxidase conjugated (1:10000) were used and visualized with the Western Lightning™ Chemiluminescence Reagent Plus (PerkinElmer).

2.7. Statistical analysis

Data for all microscopy experiments were generated from at least three independent experiments and cells were randomly selected. For colocalization analysis, the Pearson's coefficient between green and red intensity was measured using the 3iSlidebook 6.0 software. For each experiment, 50 cells were scored per condition and genotype from multiple microscopy fields. Distributions were present in box and whisker plot, where the box covers the 25th and 75th percentiles, the whiskers mark the highest and lowest values and the median is also indicated. Statistical significance and P-value were calculated in GraphPad Prism 7 using One-way ANOVA and the multiple comparison procedure Dunnett's test. Previously, all samples were tested for normality, using D'Agostino-Pearson and Shapiro-Wilk test, and homogeneity of variances, using Bartlett's test.

Growth assay data resulted from at least two independent replicates.

Protein levels data resulted from at least two independent replicates of whole cell extracts and western-blot analysis.

3. Results

3.1. Functional comparison of the dysferlin domain-containing peroxins in lipid droplet biogenesis

In budding yeast, during lipid droplet (LD) biogenesis, Pex30p, a dysferlin domain-containing peroxin with endoplasmic reticulum (ER) membrane-shaping function, cooperates with the Seipin complex, constituted by Fld1p and Ldb16p (Joshi et al., 2018; S. Wang et al., 2018). The Seipin complex is crucial for proper LD biogenesis, since its absence results LD aggregates or supersized LD. Therefore, mutant cells with combined deletion of one of the Seipin complex members and Pex30p exhibit an aberrant LD phenotype, as a result of defected LD budding (Fei et al., 2008; Grippa et al., 2015; Salo, Belevich, Li, Karhinen, Vihinen, Vigouroux, Magré, Thiele, Hölttä-Vuori, et al., 2016; H. Wang et al., 2016). This phenotype corresponds to a reduced number of LDs surrounded by highly convoluted ER membranes enriched of neutral lipids in their intramembrane space (S. Wang et al., 2018). In addition to the LD phenotype, the combined deletion of one of the Seipin complex members and Pex30p resulted in a cell growth defect. However, mutants with combined deletion of Fld1p/Ldb16p and another member of the dysferlin domain-containing peroxin family (Pex28p, Pex29p, Pex31p or Pex32p) grow at normal rate, meaning that efficient LD budding occurs independently of these proteins (S. Wang et al., 2018).

3.1.1. Dysferlin domain-containing peroxins concentrate at lipid droplets in absence of the Seipin complex

The findings described above had motivated us to study the functional difference between Pex30p and the remaining members of its protein family, since the five proteins share the same functional domains and domain architecture (Fig. 5a). First, we hypothesized that Pex28p, Pex29p, Pex31p and Pex32p could cooperate with the function of the Seipin complex and localise to the LDs in absence of the Seipin complex, similarly to Pex30p (S. Wang et al., 2018). To test this possibility, we performed fluorescence microscopy experiments to investigate the localisation of endogenously expressed Pex28p, Pex29p, Pex30p, Pex31p and Pex32p fused to the tandem dimer Tomato (tdTomato) fluorescent protein in wild-type (WT) and Seipin mutant cells (*fld1Δ* and *ldb16Δ*). In these experiments, LDs were detected by staining with the neutral lipid-specific dye Bodipy. In WT cells, the five proteins localised non-uniformly throughout the ER (Fig. 5b), as previously reported for Pex30p (S. Wang et al., 2018). In contrast, *fld1Δ* and *ldb16Δ* cells showed the typical supersized LD phenotype with a dramatic enrichment of all tdTomato-fused peroxin

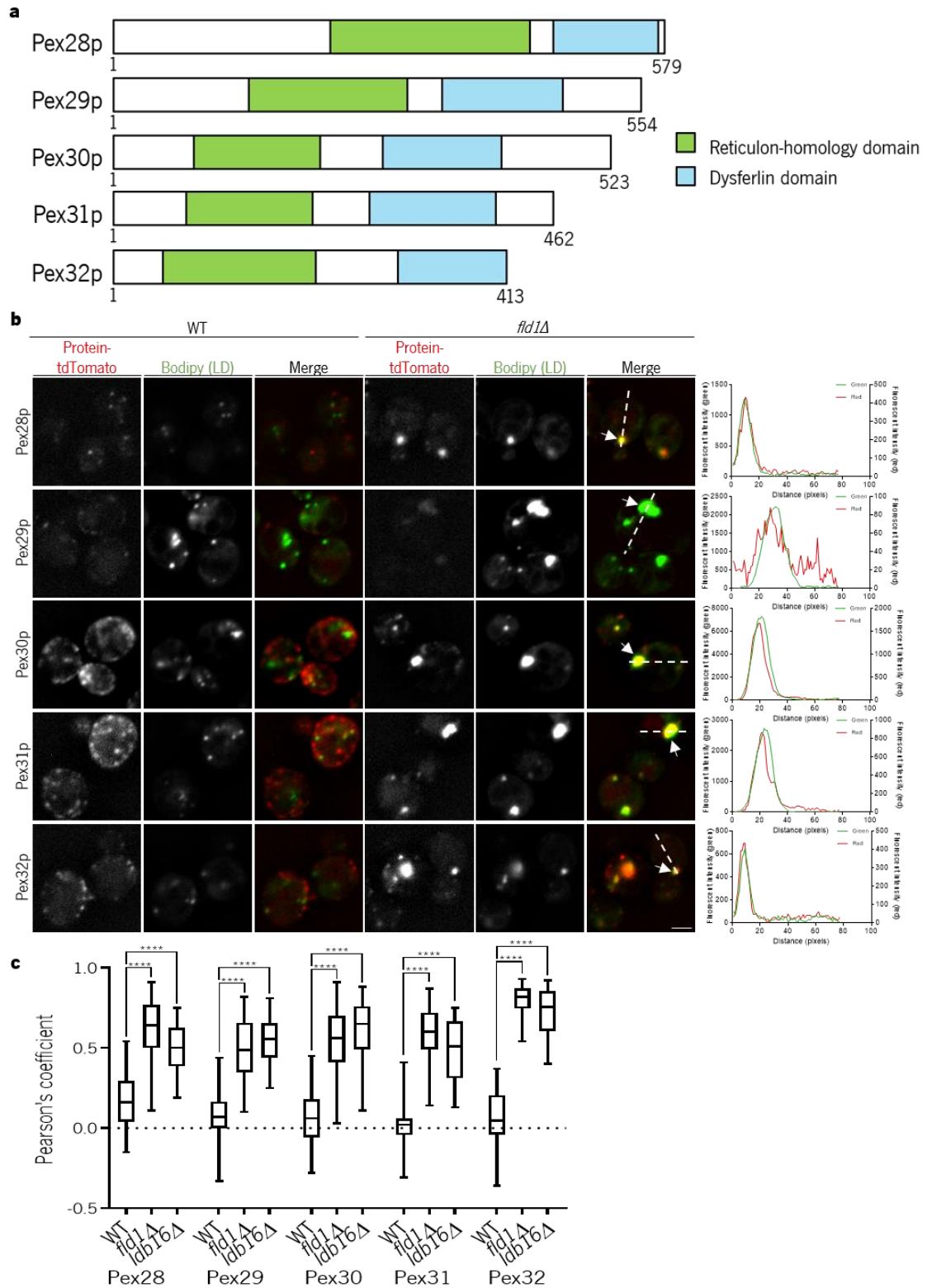


Figure 3. Dysferlin domain-containing peroxins concentrate at lipid droplets in absence of the Seipin complex. **a** | The proteins of the dysferlin domain-containing peroxin family share the same domain architecture, by containing a reticulon-homology domain (RHD) and a dysferlin domain (DysF). **b** | Localisation of endogenous Pex28p, Pex29p, Pex30p, Pex31p and Pex32p tagged with tdTomato (Protein-tdTomato) in WT and *fld1Δ* cells. Graphs to right of *fld1Δ* cells show signal intensity of green and red fluorescence on white line. LDs were stained with the neutral lipid dye Bodipy. White arrows show where the peroxin-tdTomato is located proximal to lipid droplets (LD). Bar 2μm. **c** | Pearson's coefficient for colocalisation of peroxin-tdTomato punctae associated with LD. $n \geq 50$ cells/ genotype/ condition. The box covers the 25th and 75th percentiles, the whiskers mark the highest and the lowest values and the median is indicated ($p=0.05$).

proteins in LD-proximal regions, as demonstrated by the overlap of the intensity graphs between Bodipy and tdTomato signals and the increase in the coefficient of Pearson's correlation (Fig. 5b, c, and Supplementary Fig. S1). The localisation of these peroxins at the LD-proximal regions was observed during all growth stages. Thus, in the absence of the Seipin complex, all the dysferlin domain-containing peroxins specifically accumulates at ER-LD contacts.

3.1.2. Pex30p has a unique function at the lipid droplets among the dysferlin domain-containing peroxins

Although the other dysferlin domain-containing peroxins showed a similar pattern of localisation to Pex30p in the absence of the Seipin complex, they had no effect on LD budding since double mutants of *fld1/lbd16* and *pex28/pex29/pex31/pex32* had no defect in their growth rate (S. Wang et al., 2018). Therefore, we speculated that this functional difference may arise from their lower endogenous protein levels compared to the protein level of Pex30p, which is markedly higher in cells in exponential phase (Fig. 6a). Thus, we hypothesized that these five proteins could share the same function at the LDs, which as observed for Pex30p, in cooperating with the Seipin complex. However, only the absence of Pex30p, but not the other peroxins, was sufficiently strong to influence the growth rate and the LD phenotype due to its higher homeostatic protein levels. To this end, we decided to analyse whether overexpression of Pex28p, Pex29p, Pex31p or Pex32p would compensate for the absence of Pex30p and rescue the cell growth defect phenotype, as well as the aberrant dispersed Bodipy structures, in *pex30Δ fld1Δ* and *pex30Δ lbd16Δ* cells. Thus, we analysed the growth rate, by spotting assay, and the LD phenotype, by fluorescent microscopy, in cells expressing Pex28p, Pex29p, Pex31p and Pex32p under the strong glyceraldehyde-3-phosphate dehydrogenase promoter (GPDpr), amino-terminal (N-terminal) fused to the protein HA (GPDpr-3HA-Pex28/Pex29/Pex31/Pex32).

In cells overexpressing Pex28p, "WT" cells and all the single mutants (*fld1Δ*, *lbd16Δ* and *pex30Δ*) strains exhibited similar growth rate as the WT cells (Fig. 6b), and the expected LD phenotypes for the corresponding genotypes (Fig. 6d). Intriguingly, overexpression of Pex28p in double mutant (*pex30Δ fld1Δ* and *pex30Δ lbd16Δ*) cells exhibited an intermediate phenotype, whereby these cells grew slower than the WT cells, but faster than a double mutant strain with WT levels of Pex28p (Fig. 6b). The cell growth defect was observed at 30 °C and 25 °C and was much exacerbated at 37 °C. However, in this case, this experimental method revealed to be inadequate to analyse effects on growth rate, given that the spotting assay is not extremely sensitive for small

differences in growth rate. Nevertheless, since these strains were obtained by haploids crossing, we observed the existence of three different sizes of spores after the dissection (Fig. 6c), which are associated to the three different growth rates we observed: the WT size (phenotype 1), which correspond to the wild-type and single mutant cells; the cell growth defect size (phenotype 3) correspondent to the double mutant cells with normal levels of Pex28; and the intermediate size (phenotype 2), which correspond to the double mutant cells overexpressing Pex28. While we observed slight improvement in growth rate, double mutant cells overexpressing Pex28 exhibited the aberrant Bodipy staining, typical of the double mutants (*pex30Δ fld1Δ* and *pex30Δ ldb16Δ*) cells (Fig. 6d), indicating that the function of Pex30p during LD budding cannot be compensated by Pex28p. We observed the same phenotypes in the strains overexpressing Pex29p (Fig. 6d). Nonetheless, unexpectedly the single mutants *fld1Δ* and *ldb16Δ* overexpressing Pex29 also showed a cell growth defect and the highly convoluted ER membranes stained by Bodipy, which is the distinctive phenotype of a double mutant (*pex30Δ fld1Δ* and *pex30Δ ldb16Δ*). Based on this observation, we asked whether overexpression of Pex29p was affecting normal accumulation of Pex30p at the LDs in the absence of the Seipin complex or if overexpression of Pex29p was promoting localisation of Pex30p to another specific cell subdomain. To this end, we fused the functional endogenously expressed Pex30p to the tdTomato fluorescent protein (Pex30-tdTomato) in strains overexpressing Pex29p. When compared to the WT cells in exponential phase, we observed that in cells with deletion of one of the components of the Seipin complex Pex30p was not localised throughout the ER. In contrast, Pex30p was concentrated in a specific cell subdomain that is not colocalised with LDs. Preliminary data (not shown) indicated that Pex30p signal may concentrate at the nuclear membrane-vacuole junction. Therefore, overexpression of Pex29p prevents Pex30p of localise to the LDs in Seipin mutant cells, explaining the inefficient LD budding observed even in presence of Pex30p.

Yeast strains overexpressing Pex31p and Pex32p also exhibited similar phenotypes to the observed in *pex30Δ* and double mutant strains of GPDpr-3HA-Pex28/Pex29 (Fig. 6b, d). However, we were not able to obtain single mutant (*pex30Δ*, *fld1Δ* and *ldb16Δ*) strains overexpressing Pex31p and Pex32p by haploids crossing nor genomic yeast transformation, suggesting that overexpression of Pex31p and Pex32p in presence of Pex30p may be lethal. These phenotypes should to be further confirmed with the statistical analysis of the proportions of each spore genotype obtained after the haploids crossing because the small number of spores dissected was not

enough. In conclusion, Pex30p has a specific and unique function cooperating with the Seipin complex during LD budding that is not shared among the remaining proteins of its family.

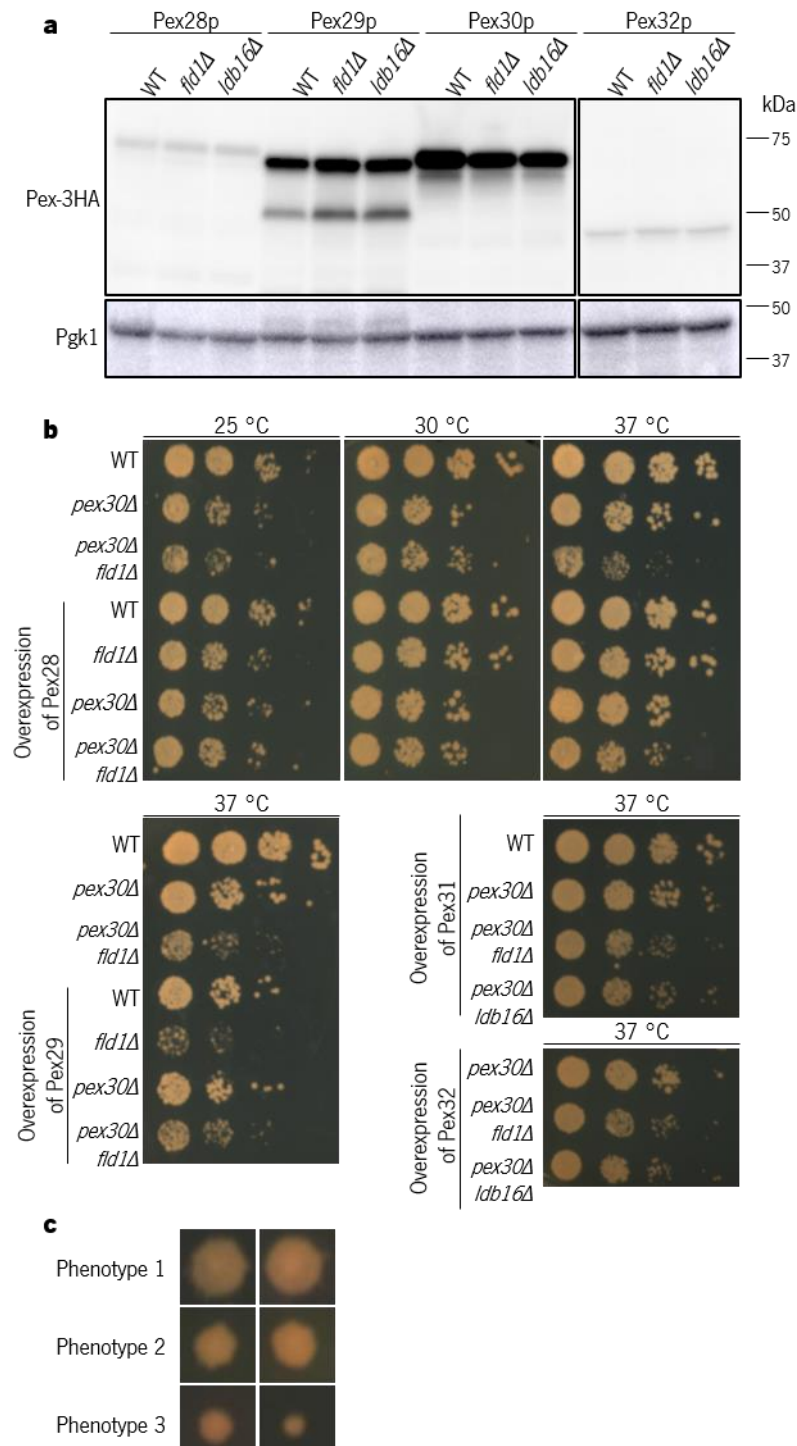


Figure 4. Pex30p is the only of the dysferlin domain-containing peroxins cooperating with the Seipin complex in lipid droplet budding. **a** | Levels of endogenous 3HA-tagged Pex28p, Pex29p, Pex30p and Pex32p, during exponential phase ($OD_{600}=1$), in WT, *fid1Δ* and *ldb16Δ* cells. Whole-cell extracts were separated by SDS-PAGE and analysed by western blotting. Peroxin-3HA and Pgk1p, used as loading control, were detected with anti-HA and anti-Pgk1 antibodies, respectively. **b** | Tenfold serial dilutions of cells with the indicated genotype were spotted on YPD media and incubated at 25 °C, 30 °C or 37 °C for 2 days. **c** | Possible three sizes of dissected spores, after growth for 2 days at 30 °C on YPD media, were obtained from the haploids crossing to generate the all the strains overexpressing one of the peroxins. Figure 6. Continued on next page.

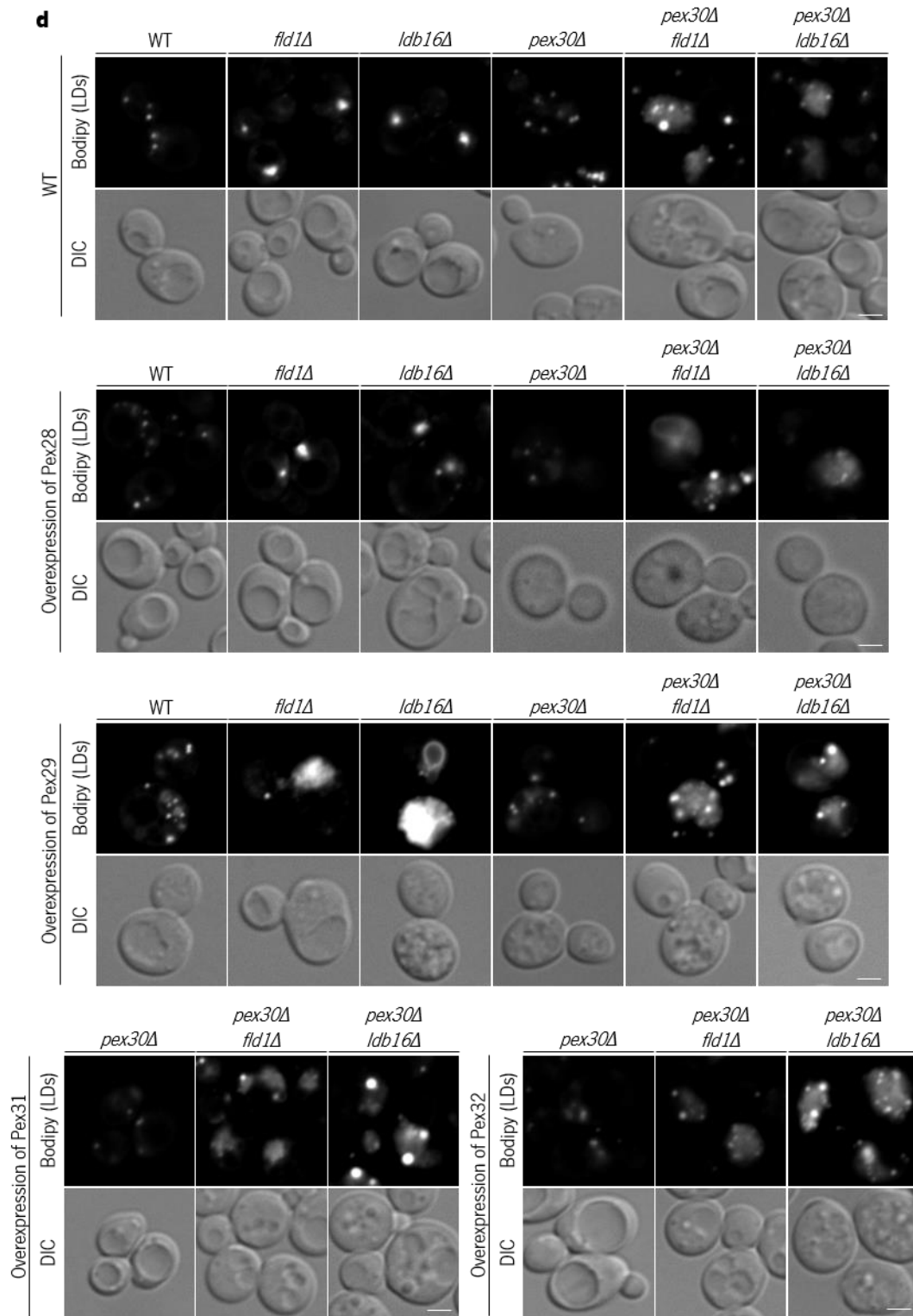


Figure 6. Continued.

d | Analysis of LDs in cells with the indicated genotype after staining with the neutral lipid dye Bodipy. Bar 2 μ m.

3.1.3. Pex29p regulates the localisation of Pex30p

Although the other dysferlin domain-containing peroxins showed the same localisation comparatively to Pex30p in absence of the Seipin complex, we showed that they do not share the same function of Pex30p. Since previous studies have proposed that these five peroxins are associated in a complex (David et al., 2013; Mast et al., 2016; Vizeacoumar et al., 2003), we hypothesized that their individual localisation to the LDs was defined by Pex30p presence, and that other peroxins rather than having an function at the LDs could regulate Pex30p localisation in specific nutritional states, as well as the cooperation with the Seipin complex or with other organelles in which Pex30p has also a function. To assess this idea, we explored the localisation of endogenously expressed Pex30p fused to the monomeric Neon Green fluorescent protein (Pex30p-mNG) in single mutant cells (*pex28Δ/pex29Δ/pex31Δ/pex32Δ*) and in the same mutants with combined deletion of the proteins members of the Seipin complex. For these imaging experiments, LDs were detected by fluorescence microscopy in cells stained with the blue fluorescent lipid-droplet marker MDH. In cells where individual peroxins has been deleted, Pex30p-mNG localised non-uniformly throughout the ER (Fig. 7a), which is consistent with a previous report (S. Wang et al., 2018). When combined with Seipin deletions, the absence of these peroxins did not affect localisation of Pex30p-mNG to the LD and there was no alteration of the characteristic

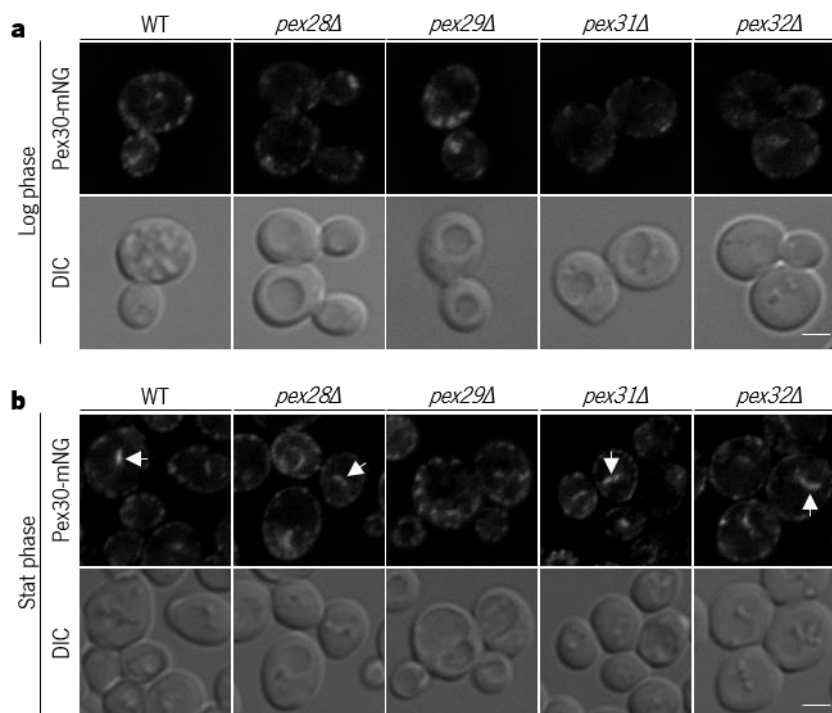


Figure 5. Pex29p regulates localisation of Pex30p during stationery phase. **a** | Localisation of endogenous Pex30p tagged with monomeric Neon Green (Pex30-mNG) in WT, *pex28Δ*, *pex29Δ*, *pex31Δ* and *pex32Δ* cells in exponential and **b** | stationary phase. White arrows show where Pex30-mNG is located proximal to NVJ. Bar 2 μm.

supersized LD phenotype of *fld1Δ* and *ldb16Δ* cells during the exponential phase (data not shown). However, when the same strains were analysed in stationary phase, Pex30p-mNG, which in WT cells partially localises to the nuclear membrane-vacuole junction, exhibited a different phenotype in *pex29Δ* cells. Only in absence of Pex29p, Pex30p-mNG was no more capable of localising and accumulating at the NVJ in the stationary phase (Fig. 7b). This data revealed that Pex29p contributes to the regulation of Pex30p localisation in this specific cellular metabolic status.

3.2. Functional characterization of Pex30p in lipid droplet biogenesis

3.2.1. Overexpression of Pex30p has no effect on lipid droplet number and size

Although the function of Pex30p is not completely revealed, it was recently shown to be involved in the budding of PPVs (Joshi et al., 2016; H. Wang et al., 2016) and LDs (S. Wang et al., 2018) from the ER, as well as in regulating the size and number of peroxisomes (Vizeacoumar et al., 2004). Therefore, we hypothesised that Pex30p could regulate abundance and size of LDs, particularly in the absence of the Seipin complex, since it is known that this complex regulates LD phenotype and Pex30p cooperates with it during LD budding. To test this, we sought to analyse the LD phenotype of cells expressing Pex30p under the strong GPD promoter, N-terminal fused to the protein HA (GPDpr-3HA-Pex30), by Bodipy staining conjugated with fluorescent microscopy. In both WT and *fld1Δ/ldb16Δ* cells, the LD number and size were not affected by increasing amount of Pex30p (Fig. 8), as described in WT cells in absence of Pex30p (S. Wang et al., 2018). In addition, the growth rate was not changed by the overexpression of Pex30p (Fig. 8c).

3.2.2. The dysferlin and the reticulon-homology domains cooperate on Pex30p localisation in absence of the Seipin complex

Previous studies have shown that in the absence of the Seipin complex, Pex30p localises to the LDs (S. Wang et al., 2018). Based on this information, we hypothesized that discrete domains of Pex30p would be required for its targeting to LDs. To study this, endogenously expressed C-terminal truncations of Pex30p were produced, by carboxy-terminal (C-terminal) fusion with the monomeric

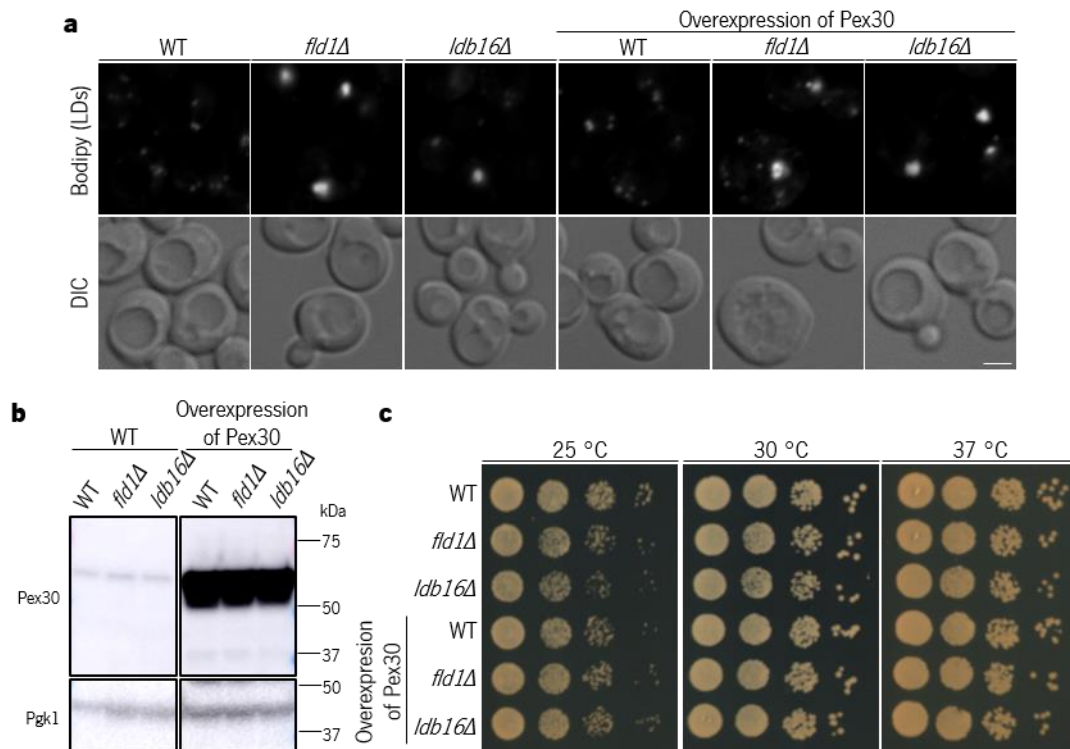


Figure 6. Overexpression of Pex30p does not alter lipid droplet size and number. **a** | Analysis of LDs in cells with the indicated genotype after staining with the neutral lipid dye Bodipy. Bar 2 μ m. **b** | Levels of endogenous 3HA-tagged Pex30p during exponential phase ($OD_{600}=1$), in WT, *fld1Δ* and *ldb16Δ* cells. Whole-cell extracts were separated by SDS-PAGE and analysed by western blotting. 3HA-Pex30 and Pgk1p, used as loading control, were detected with anti-Pex30 and anti-Pgk1 antibodies, respectively. **c** | Tenfold serial dilutions of cells with the indicated genotype were spotted on YPD media and incubated at 25 °C, 30 °C or 37 °C for 2 days.

Neon-Green (mNG) fluorescent protein, in WT and Seipin mutant (*fld1Δ/ldb16Δ*) cells. Four truncations were produced to study the possible contribution of several portions of the protein (Fig. 9a). For studying the involvement of the reticulon-homology domain for Pex30p targeting to the LDs, we deleted all amino acids from the residue 60 (Pex30 Δ 60-523) and produced another truncated protein in which the ER membrane-shaping function of the reticulon-homology domain is unaffected (Pex30 Δ 235-523) (Joshi et al., 2016). The protein truncations Pex30 Δ 284-523 and Pex30 Δ 410-523 were used to study the participation of the dysferlin domain and the C-terminal portion of Pex30p, respectively, in Pex30p targeting to the LDs. The amino acids corresponding to each domain were identified by comparison with other proteins and domain prediction using HHpred (Fidler et al., 2016). The reticulon-homology domain was compared with other yeast reticulons, namely Rtn1p and Rtn2p. In addition, the dysferlin domain of Pex30p was analysed together with the human dysferlin protein. The localisation of the proteins and the resultant LD phenotype was monitored by fluorescent microscopy and staining with MDH.

In WT cells, all truncated proteins showed similar ER localisation as the full-length Pex30p, expected for Pex30 Δ 60-523, which showed cytosolic localisation (Fig. 9b). This is consistent with the fact that this truncated protein lacks an integral protein domain to be anchored at the ER membrane. Similarly, in Seipin deletion background, this truncation protein also exhibited a soluble distribution. In contrast, the two truncated proteins in which the dysferlin domain was deleted (Pex30 Δ 235-523 and Pex30 Δ 284-523) did not localise to the LDs (Fig. 9b, c). Consistently, the truncated Pex30 Δ 410-523, which still contains the dysferlin domain, was localised to the LDs (Fig. 9a, b), confirming that the dysferlin domain is involved in the localisation process of Pex30p to the LDs in absence of the Seipin complex.

In addition, these strains were analysed in stationary phase and none of them was able to diffuse to the NVJ, as full Pex30p normally does, indicating that some residues in the carboxy-

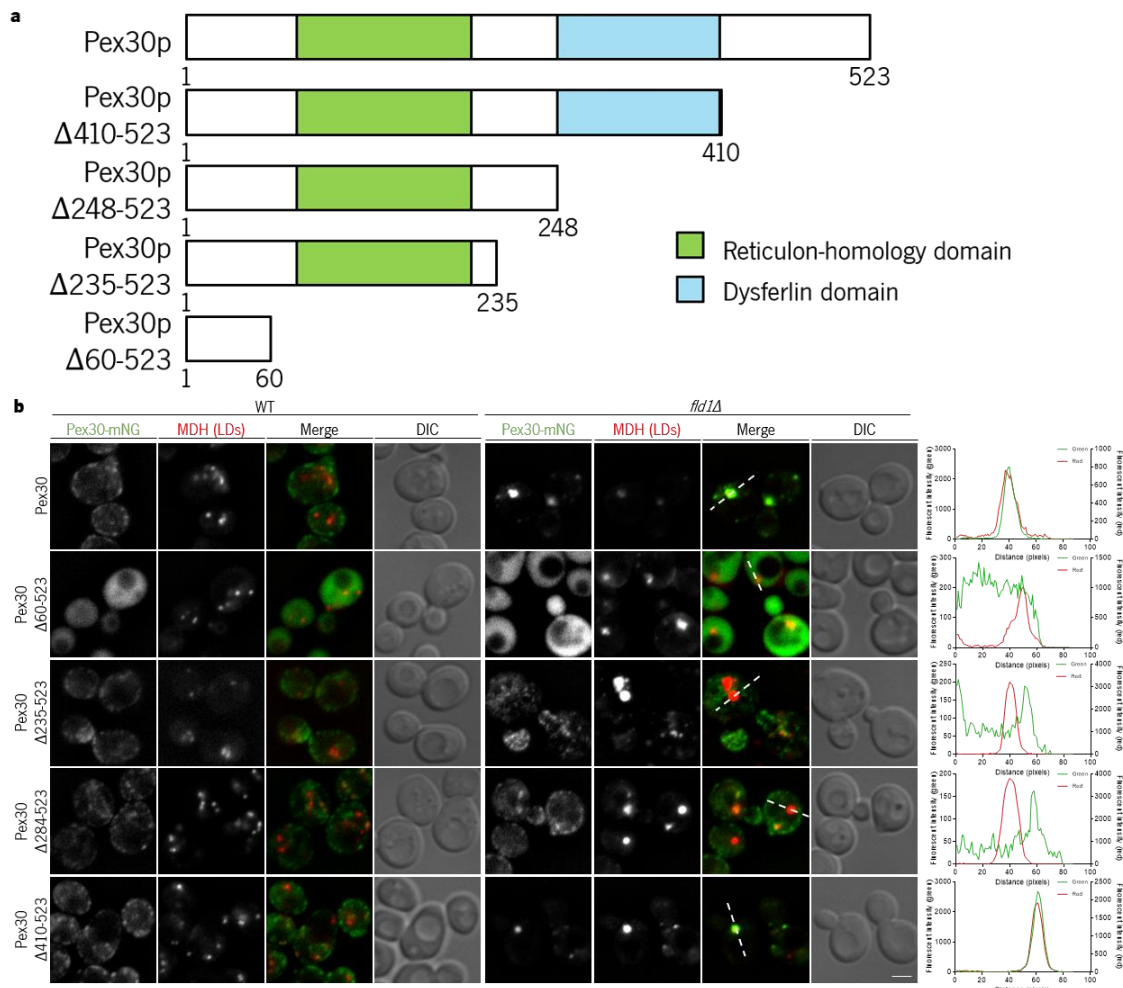


Figure 7. Both the dysferlin and the reticulon-homology domains are required for Pex30p localisation in absence of the Seipin complex **a** | C-terminal truncated variants of Pex30p to explore the involvement of the reticulon-homology domain (RHD) and the dysferlin domain (DysF) in the localisation of Pex30p in absence of the Seipin complex. **b** | Localisation of endogenous Pex30p full length and its truncated variants tagged with the monomeric Neon-Green (Pex30p-mNG) in WT and *fld1* Δ cells. LDs were stained with the neutral lipid dye MDH. Bar 2 μ m. **c** | Graphs to right of *fld1* Δ cells show signal intensity on white line.

terminal sequence of Pex30p, between amino acids 410 and 523 are in some way involved in the process of Pex30p diffusion to the NVJ (data not shown).

In conclusion, both the reticulon-homology and the dysferlin domains of Pex30p were required for its localisation to the LDs in absence of the Seipin complex. The RHD is required for Pex30p to be anchored into the ER and LD membranes, while the dysferlin domain is required to target Pex30p localisation to the LDs.

3.2.3. The dysferlin domain is essential for Pex30p function in lipid droplet budding

From the previous experiments, we determined that the dysferlin domain is involved in the localisation of Pex30p to the LDs. However, these experiments were inadequate to conclude whether the reticulon-homology domain also participates in targeting Pex30 to the LDs because the truncation experiment only suggested that the reticulon-homology domain was fundamental for the protein to be anchored in the membrane. To clarify whether both dysferlin and reticulon-homology domains would be required for Pex30p targeting to LDs, the reticulon-homology domain and the dysferlin domain were deleted in the endogenously expressed Pex30p (Pex30-*retΔ* and Pex30-*dysΔ*, respectively) in WT and Seipin mutant background (Fig. 10a). We utilised a CRISPR gene editing technique to enable deletion of only the amino acids corresponding to the domains of interest, ensuring that the remaining protein sequence persisted as the wild-type sequence. Additionally, the localisation of these modified Pex30p was monitored by fluorescent microscopy due to carboxy-terminal fusion with the tandem dimer Tomato fluorescent protein (Pex30-tdTomato). In this experiment, LDs were detected by fluorescence microscopy by staining with the neutral lipid-specific dye Bodipy. In WT cells, full-length Pex30-tdTomato and Pex30-*dysΔ*-tdTomato localised non-uniformly throughout the ER (Fig. 10b), as previously reported (Joshi et al., 2016; Mast et al., 2016). In contrast, Pex30-*retΔ*-tdTomato was not enriched in ER tubules and the edges of ER sheets anymore; instead, it was soluble, what confirms that the reticulon-homology domain is the only integral domain in Pex30p (Fig. 10b). However, while *fld1Δ* and *ldb16Δ* cells showed a dramatic enrichment of Pex30-tdTomato in ER-LD contact sites (S. Wang et al., 2018), Pex30-*dysΔ*-tdTomato and Pex30-*retΔ*-tdTomato were not targeted to the LDs (Fig. 10b). Pex30-*dysΔ*-tdTomato continued to be distributed non-uniformly throughout the ER and Pex30-*retΔ*-tdTomato remains soluble. As a result of the failed localisation of Pex30p to the LDs, in *fld1Δ* and *ldb16Δ* cells, Pex30-*dysΔ*-

tdTomato and Pex30-*ret4*-tdTomato strains showed the highly convoluted ER membranes phenotype (Fig. 10b). These localisation results were observed during all growth stages. Thus, the reticulon-homology domain is required for the insertion of Pex30p in the ER membrane and, consequently, for its localisation. In addition, in absence of Seipin, the dysferlin domain is essential for Pex30p specific accumulation at ER-LD contact sites.

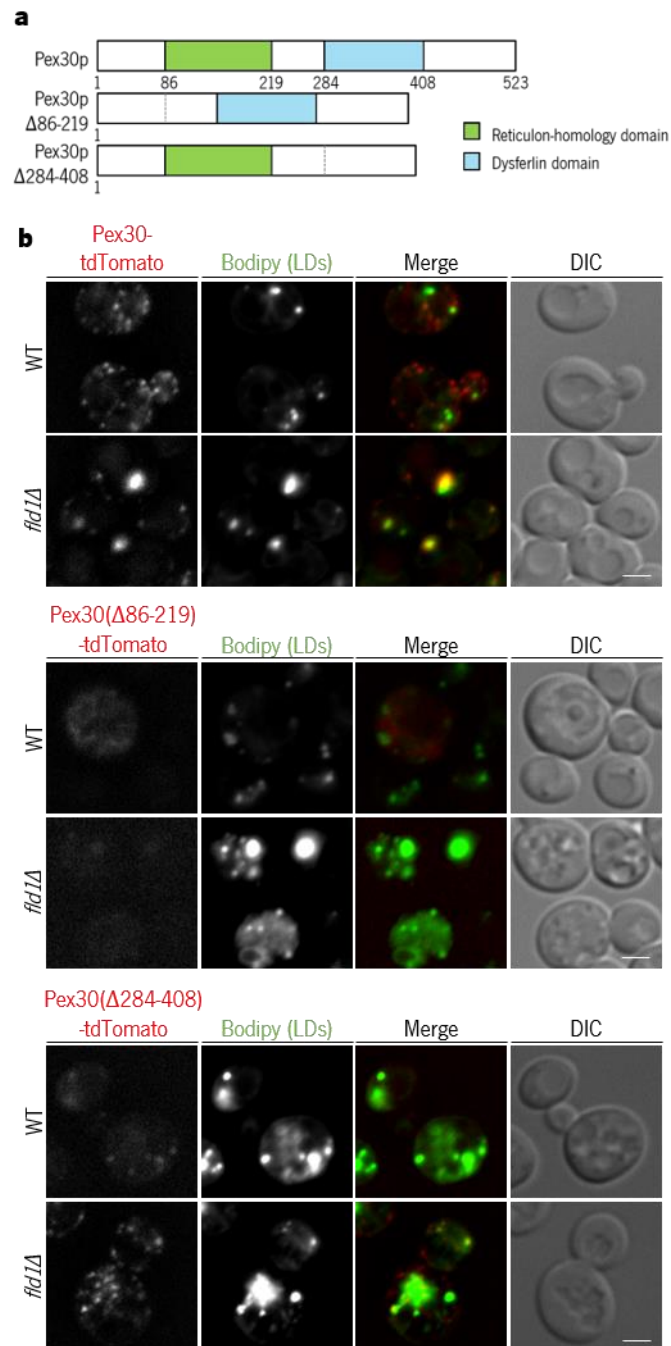


Figure 8. The dysferlin domain is essential for Pex30p function in LD budding. **a** | Pex30p variants without the reticulon-homology domain (RHD) or the dysferlin domain (DysF). **b** | Localisation of endogenous Pex30p full length and its variants tagged with tdTomato (Pex30-tdTomato) in WT and *fid1Δ* cells. LDs were stained with the neutral lipid dye Bodipy. Bar 2 μ m.

3.2.4. Endoplasmic reticulum membrane-shaping proprieties of the reticulon-homology domain of Pex30p in lipid droplet budding

Given that the reticulon-homology domain has ER membrane-shaping proprieties, we decided to investigate whether this function could be associated with the localisation of Pex30p at the LDs. To study this, we mutated a conserved residue that was reported as required for the ER-shape function of any protein with a reticulon-homology domain (Joshi et al., 2016). In Pex30p, this residue corresponds to a tryptophan in position 94, and it was mutated to cysteine in endogenously expressed Pex30p fused to the tdTomato fluorescent protein (Pex30W94C-tdTomato). In WT cells, Pex30W94C-tdTomato localised non-uniformly throughout the ER (Fig. 11a), as previously reported to the full-length Pex30-tdTomato (Joshi et al., 2016; Mast et al., 2016). In Seipin mutants, the mutated protein was able to diffuse to the LDs, as supported by the overlap of the intensity graphs (Fig. 11a). The localised Pex30p ensured the normal supersized phenotype of LDs in a Seipin deletion background, avoiding the formation of highly convoluted ER membranes (Fig. 11a). In conclusion, even when the ER-shape function of this domain was comprised, Pex30p localised to the LDs to compensate for the absence of the Seipin complex in the LD budding.

To further clarify the possible contribution of the reticulon-domain of Pex30p in its cellular distribution in the absence of the Seipin complex, we decided to focus in the fact that Pex30p is the only reticulon-like protein that is strongly localised to the LDs in absence of the Seipin complex (S. Wang et al., 2018). We generated cells endogenously expressing a chimera protein in which the reticulon-homology domain of Pex30p was substituted by the reticulon domain of Rtn1p, by using CRISPR gene editing tool. The chimeric Pex30p variant was also fused at the C-terminal with the tdTomato fluorescent protein for fluorescence microscopy. We hypothesised that if the reticulon-homology domain of Pex30p was involved in the localisation at the LDs and was functionally different from the domains of other reticulons, this chimera protein would not be targeted to the LDs anymore. In WT cells, the chimera protein was distributed non-uniformly throughout the ER (Fig. 11b) similarly to the full-length Pex30p. However, in *fld1Δ* and *ldb16Δ* the chimera protein remained in the ER tubules and the edges of ER sheets, suggesting that the localisation of this chimera protein was affected. Consequently, the LD supersized phenotype was substituted by the aberrant Bodipy structures, characteristic of double mutant *pex30Δfld1Δ/ldb16Δ* (Fig. 11b). Nevertheless, this result does not allow us to conclude the reason for the mislocalisation. On the one hand, it could indicate that the RHD of Pex30p is different from the RHD of the remaining reticulons-like and cooperate in the localisation. On the other hand, the

swapping of the reticulon domains between Pex30p and Rtn1p could result in a defect in folding of the protein, which could affect its normal behaviour.

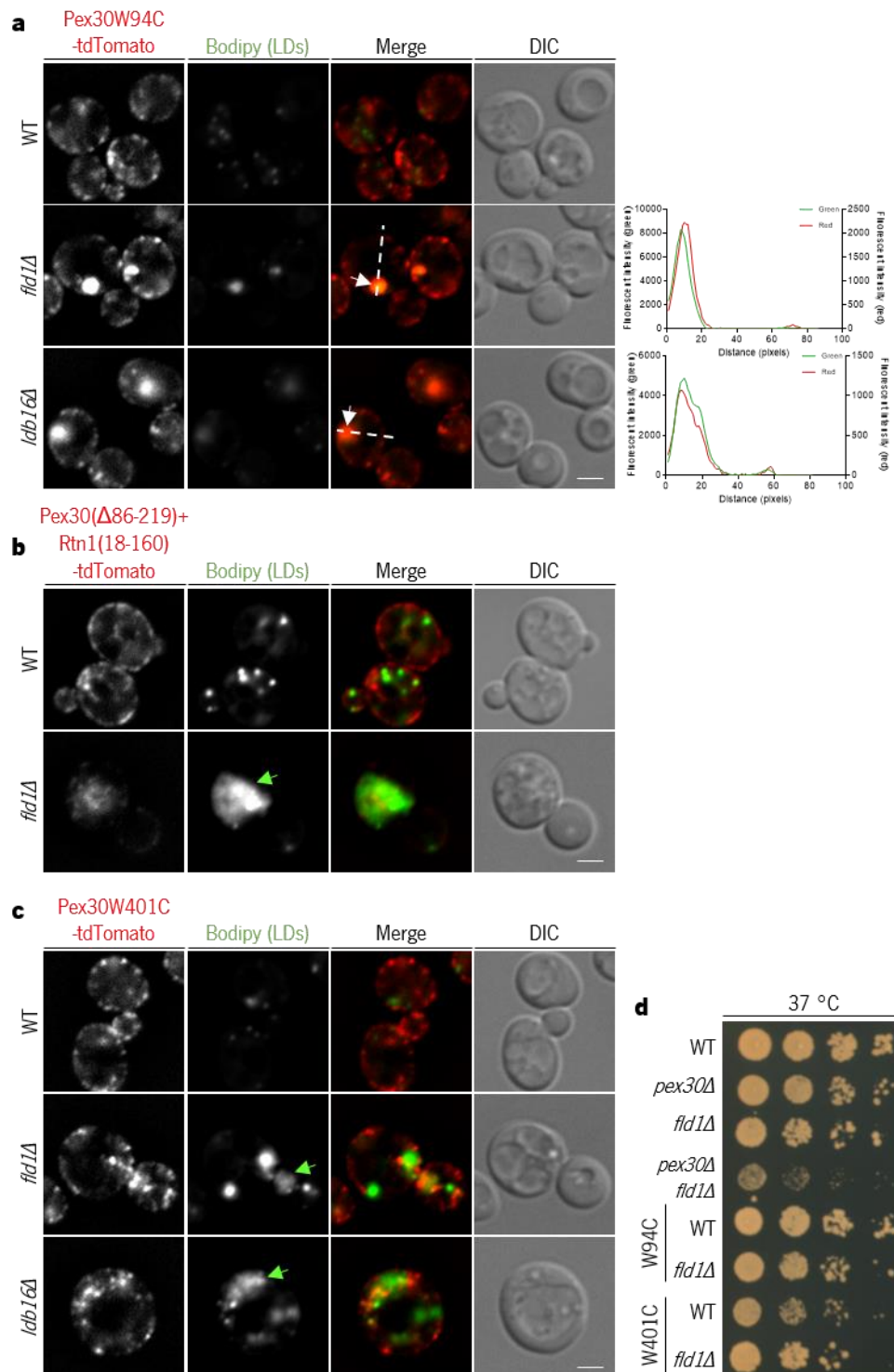


Figure 9. The dysferlin domain of Pex30p is essential for efficient LD budding in absence of the Seipin complex. **a** | Localisation of endogenous Pex30p with a point mutation on the RHD tagged with tdTomato (Pex30-tdTomato) in WT, *fld1Δ* and *ldb16Δ* cells. LDs were stained with the neutral lipid dye Bodipy. White arrows show where Pex30W401C-tdTomato is located proximal to lipid droplets. LDs were stained with the neutral lipid dye Bodipy. Graphs to right of *fld1Δ* cells show signal intensity on white line. Bar 2μm. **b** | Localisation of endogenous Pex30p chimera in which the RHD was swapped with the RHD of Rtn1p. The chimeric protein was tagged with tdTomato (Pex30-tdTomato) in WT and *fld1Δ* cells. The green arrows show the aberrant dispersed Bodipy structures. LDs were stained with the neutral lipid dye Bodipy. Bar 2μm. Figure 11. Continued on next page.

Figure 11. Continued.

c| Localisation of endogenous Pex30p with a point mutation on the DysF tagged with tdTomato (Pex30-tdTomato) in WT, *fld1Δ* and *ldb16Δ* cells. The green arrows show the aberrant dispersed Bodipy structures. LDs were stained with the neutral lipid dye Bodipy. Bar 2μm. **d|** Tenfold serial dilutions of cells with the indicated genotype were spotted on YPD media and incubated at 37 °C for 2 days.

3.2.5. The function of the dysferlin domain in absence of Seipin is conserved among dysferlin domain-containing peroxins

To further study the involvement of the dysferlin domain in the localisation of Pex30p in absence of the Seipin complex, we analysed an alignment of protein sequences of several dysferlin-like domains from yeast to human and selected an evolutionarily conserved residue for mutagenesis study (Sula et al., 2014). Our rationale was that a conserved residue could be involved in its unknown function and by mutating it we could analyse the involvement of the dysferlin domain in the localisation of Pex30p to the LDs without deleting the entire domain.

The selected residue W401 (in yeast, W1042 in human inner dysferlin) was surrounded by evolutionarily conserved residues, which belong to the list of pathogenic missense mutations in the inner dysferlin domain. In addition, this residue was described as crucial for the correct folding of the domain (Sula et al., 2014). Therefore, this tryptophan was mutated to cysteine in endogenously expressed Pex30p fused to the tdTomato fluorescent protein (Pex30W401C-tdTomato). In WT cells, Pex30W401C-tdTomato localised non-uniformly throughout the ER tubules and edges of ER sheets, but in *fld1Δ* and *ldb16Δ* cells, there was no enrichment of Pex30p at the LD-proximal regions (Fig. 11c). Consequently, the Seipin deletion mutants exhibited the highly convoluted ER membranes phenotype instead of the supersized LDs. As a result, these cells grew slower than WT and single deletions of *Fld1* and *Ldb16* with functional dysferlin domain (Fig. 11d). The cell growth defect was observed at 30 °C and much exacerbated at 25 °C and 37 °C. These results indicate not only that this residue participates in the unknown function of the dysferlin domain, but also confirms the contribution of this domain in the Pex30p function in LD budding because the non-functional domain resulted in the same phenotype of Pex30p deletion.

From earlier experiments, we have established that all the dysferlin domain-containing peroxins were targeted to the LDs in the absence of the Seipin complex, and the dysferlin domain of Pex30p was revealed to be essential for localisation of Pex30p to LDs and, consequently, for its function on LD budding. These findings have let us hypothesize whether the dysferlin domain could also affect the localisation and/or function of the other peroxins of this family. To test this, we examined the localisation of endogenously expressed dysferlin-domain truncated variants of Pex28p, Pex29p,

Pex30p, Pex31p and Pex32p fused to the tdTomato fluorescent protein in WT and Seipin deletion background, by using fluorescence microscopy. The truncations were limited before the first amino acid of each dysferlin domain. The amino acids sequences corresponded to dysferlin domain of each peroxin were identified by comparing protein sequences of Pex30p and human dysferlin, followed by domain prediction using HHpred (Fidler et al., 2016). In this experiment, LDs were imaged after staining with the neutral lipid-specific dye Bodipy. Consistently, the five truncated proteins localised non-uniformly throughout the ER in WT cells (data not shown), similarly to the full-length proteins (Fig. 5). In *fld1Δ* and *ldb16Δ* cells, the truncated versions of Pex31p and Pex32p failed to enrich in the LD-proximal regions, consistent with our previous observations in Pex30p with deleted dysferlin domain. Intriguingly, we observed that the truncated proteins of Pex28p and Pex29p were able to concentrate at the LD-proximal region. Thus, this suggested that the dysferlin domains are not required for localisation of all dysferlin domain-containing peroxins at ER-LD contact sites in absence of the Seipin complex.

While the dysferlin domains of these peroxins may have differential requirement for LD targeting, we thought that the dysferlin domain might be important for a conserved function among the five proteins of this family. To test this, we analysed wild-type and *fld1Δ/ldb16Δ* cells endogenously-expressing protein chimeras of Pex30p in which the Pex30p dysferlin domain has been swapped with the dysferlin domain from another peroxin of this family (Pex28p, Pex29p, Pex31p or Pex32p). These chimeras were fused to the tdTomato fluorescent protein to allow fluorescence imaging. In the WT cells, the four chimera proteins localised non-uniformly throughout the ER, similarly to the canonical Pex30p (Fig. 12). In contrast, in *fld1Δ* and *ldb16Δ*, while the chimera proteins with Pex31p and Pex32p dysferlin domains exhibited typical accumulation at the LDs proximal region (Fig. 12), Pex30p chimeras with the dysferlin domain of Pex28p and Pex29p continued distributed throughout the ER, resulting in the highly convoluted ER membranes phenotype (data not shown). The Pex30p chimeras with dysferlin domain of Pex31p and Pex32p exhibited only supersized LDs and no cell growth defect (Fig. 12). This finding suggested that, the function of the dysferlin domain is not conserved among the proteins of dysferlin domain-containing peroxins family. Nevertheless, the dysferlin domain of Pex31p and Pex32p may have functional similarity to the dysferlin domain of Pex30p due to their ability to rescue the characteristic phenotype of Pex30p in absence of the Seipin complex.

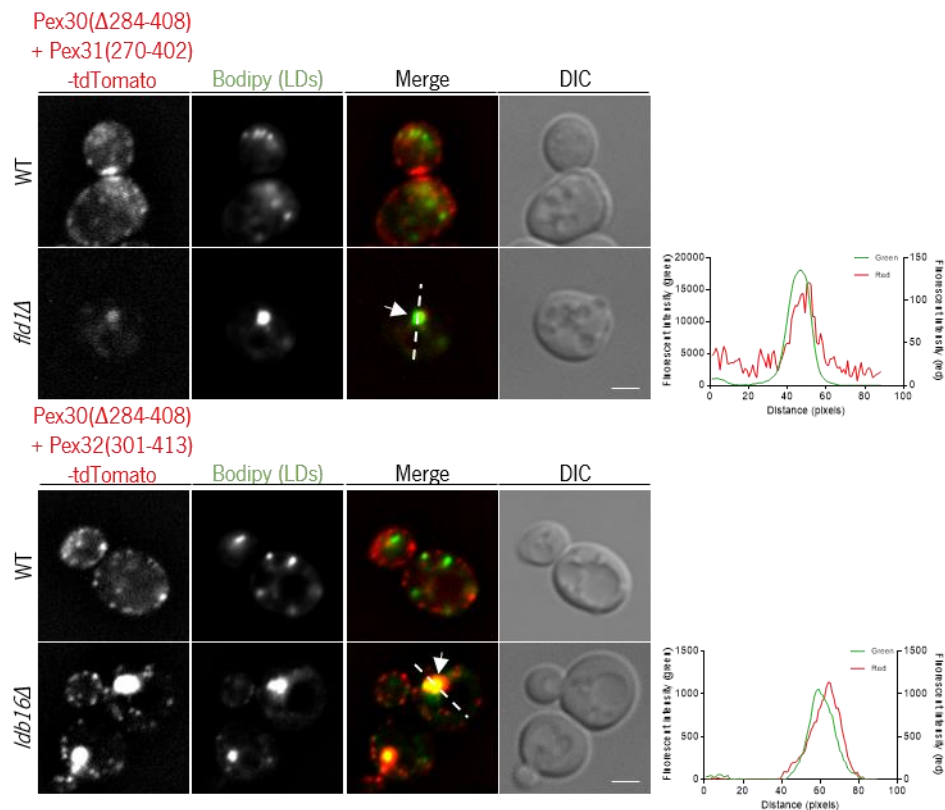


Figure 10. The function of the dysferlin domain of Pex30p in absence of Seipin is conserved in Pex31p and Pex32p. **a** Localisation of endogenous Pex30p chimeras in which the dysferlin domain was swapped with the dysferlin domain of Pex31p and Pex32p tagged with tdTomato (Chimera-tdTomato) in WT and *fld1 Δ* /*ldb16 Δ* cells. LDs were stained with the neutral lipid dye Bodipy. White arrows show where the Chimera-tdTomato is located proximal to lipid droplets. Graphs to right of *fld1 Δ* /*ldb16 Δ* cells show signal intensity on white line. Bar 2 μ m.

3.3. Characterization of MCTP2 as the human homolog of Pex30p

Previous studies have shown that the mammalian homolog of Pex30p cannot be identified by protein BLAST. Therefore, the structural homology prediction program HHpred was used to identify the closest human homolog of Pex30 and MCTP2, a protein with also a reticulon-homology domain, was the selected one (Joshi et al., 2018).

3.3.1. Function of reticulon-homology domain of MCTP2 in lipid droplet budding

Overexpression of only the protein region containing the reticulon-homology domain of MCTP2 was sufficient to rescue the cell growth defect observed in *pex30 Δ fld1 Δ* cells (Joshi et al., 2018).

This data is inconsistent with the findings in this document since the dysferlin domain revealed to be the essential domain for the function of Pex30p at the LDs.

To further explore whether MCTP2 is the true mammalian functional homolog of Pex30p, we produced an endogenously expressed chimera protein in which the reticulon-homology domain of Pex30p was substituted with the reticulon-homology domain of MCTP2, using a CRISPR genome editing tool, in WT and Seipin single mutant cells (Fig. 13a). The RHD sequence of MCTP2 was obtained from a total cDNA library of U250 glioma cell line. The localisation of this chimera protein was analysed by C-terminal fusion with the tdTomato fluorescent protein and LDs were visualized by staining with the neutral lipid-specific dye Bodipy. In WT cells, the chimeric Pex30p was distributed throughout the ER and the phenotype of the LDs were the expected, suggesting that reticulon domain of MCTP2 was properly folded and inserted in the ER membrane (Fig. 13b). However, in *fld1Δ* cells instead of the supersized LDs where canonical Pex30p tend to accumulate, we observed Bodipy staining all over the cell, suggesting that the LD budding was not effective, producing several extra membranes, because Pex30p did not diffuse to the LDs (Fig. 13a). Intriguingly, we observed this aberrant phenotype despite the presence of functional dysferlin domain of Pex30p. However, we cannot conclude about the function of this domain of MCTP2, because the chimera protein folding is unknown. Indeed, we do not know whether the entire protein was unfunctional (including the dysferlin domain) due to unsuccessful protein folding.

3.3.2. C2 domains failed to replace the function of dysferlin domain

The specific molecular mechanism in which the dysferlin domain is involved remains unknown. However, some data suggest that this domain may bind to lipids, as DAG. The human Dysferlin protein contains two DysF domain and several C2 domains, which are known to bind to phospholipids or proteins, often in a calcium-dependent manner (Lek et al., 2012). In this specific protein, the seven C2 domains are involved in calcium-mediated membrane fusion events (Davis, Doherty, Delmonte, & McNally, 2002; Therrien, Fulvio, Pickles, & Sinnreich, 2009). In addition, MCTP2 also contains three C2 domains. Thus, we hypothesize that the function of the dysferlin domain of Pex30 could be related to the function of C2 domains. To test this, we produced two chimera proteins of the endogenously expressed Pex30p in which its dysferlin domain was substituted with the sequence of amino acids which includes the three C2 domains or by the sequence of amino acids corresponded to the first C2 domain alone, C2A, in WT and Seipin mutant cells (Fig. 13a) (Shin et al., 2005). The protein localisation was analysed by fluorescent microscopy

since the protein was C-terminal fused to the tdTomato fluorescent protein, and the LDs were visualized by staining with Bodipy. In WT cells, the chimera proteins displayed distribution throughout the ER, as expected for canonical Pex30p. However, similar continuous distribution throughout the ER was also observed in *fld1Δ* cells, instead of typical accumulation in LD-proximal regions (Fig. 13c). Consistently, the LD phenotype was also compromised, and highly convoluted ER membranes stained by Bodipy were observed. This data revealed that the function of the dysferlin domain cannot be replaced by C2 domains.

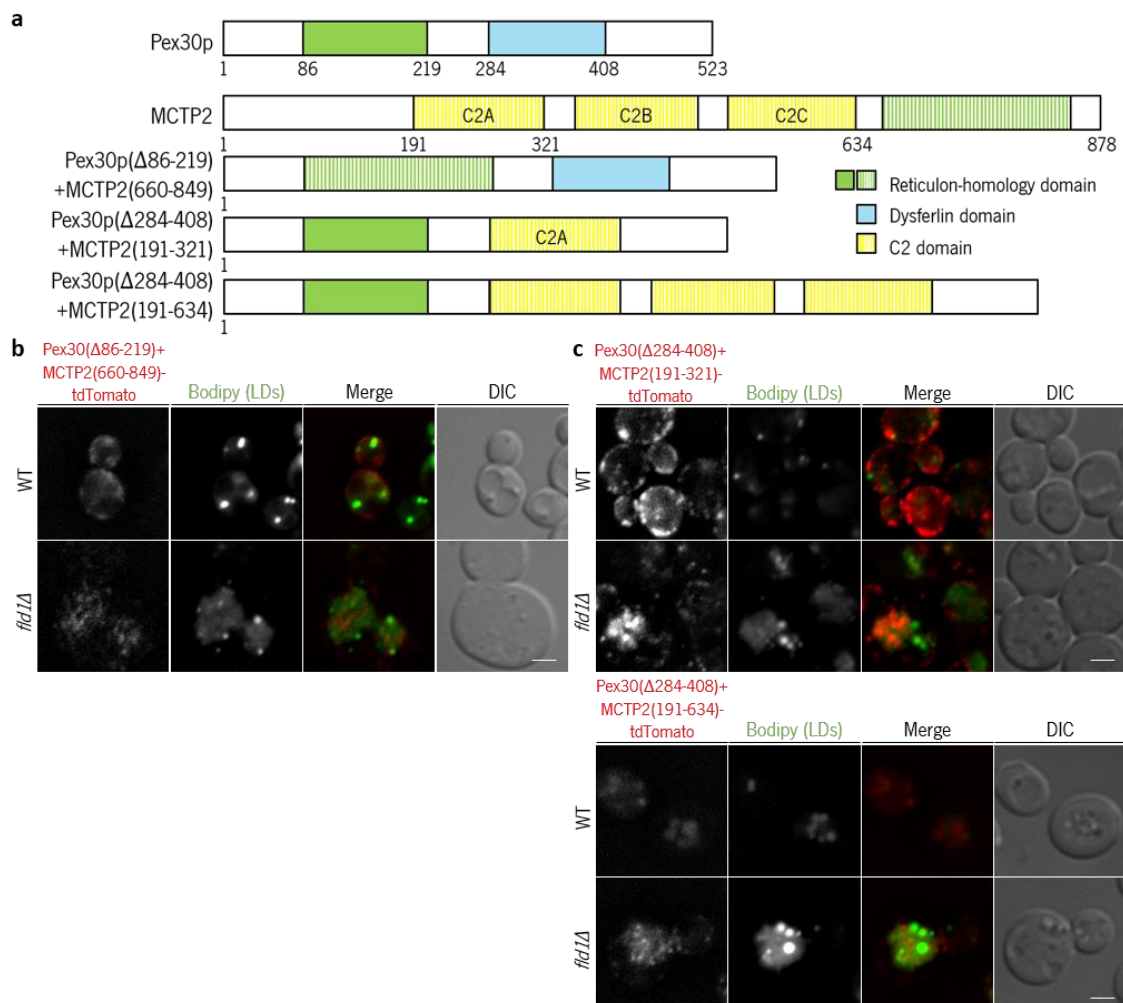


Figure 11. MCTP2 domains are functional different from Pex30p domains. **a** | The dysferlin domain-containing peroxin Pex30p and its human homolog MCTP2 contain a reticulon-homology domain (RHD). Pex30p also contains a dysferlin domain (DysF) and MCTP2 contains three C2 domains. We generated three chimeric proteins of Pex30p in which its domains were swapped with MCTP2 domains. **b** | Localisation of endogenous Pex30p, in which its RHD was swapped with the RHD of MCTP2, with tdTomato (Protein-tdTomato) in WT and *fld1Δ* cells. LDs were stained with the neutral lipid dye Bodipy. Bar 2μm. **c** | Localisation of endogenous Pex30p, in which its dysferlin domain was swapped with the C2A domain or the protein portion containing the three C2 domains of MCTP2, with tdTomato (Protein-tdTomato) in WT and *fld1Δ* cells. LDs were stained with the neutral lipid dye Bodipy. Bar 2μm.

4. Discussion

Lipid droplets are ubiquitous organelles that lie at the crossroads of membrane biology and energy metabolism, being important in the maintenance of cell homeostasis. However, the mechanism for LD biogenesis at the endoplasmic reticulum remain elusive. In addition, this organelle is often in close proximity to other central organelles in cellular metabolism, as the nucleus, peroxisomes, vacuole, and mitochondria. How LDs coordinate their functions remain unclear. Recently, in budding yeast, it was shown that LDs and pre-peroxisomal vesicles bud from similar ER domains through a process requiring cooperation between the Seipin complex and Pex30p (Joshi et al., 2018; S. Wang et al., 2018).

Seipin is a transmembrane protein that concentrates at ER-LD contact sites and corresponds to the protein complex Fld1p/Ldb16p in budding yeast. Although the molecular mechanism behind it is unclear, Seipin is a crucial protein for effective lipid droplet biogenesis because its deficiency alters LDs phenotype, producing LD aggregates or supersized LDs. Recently it was proposed that Seipin may recognize sites of disrupted phospholipid bilayer packing, due to the formation of neutral lipids lens at the ER membrane. Therefore, Seipin may anchor the nascent LD to the ER and allow maintenance of the ER-LD connection to enable LD growth. Furthermore, it is also hypothesized that Seipin may bind lipids and, consequently, regulate the leaflet tension which contributes to the LD budding.

In budding yeast, Pex30p is the founding member of the dysferlin domain-containing peroxins family, that also includes Pex28p, Pex29p, Pex31p and Pex32p. All these proteins share the same functional domains and domain architecture and since they are peroxins, they are involved in peroxisome biogenesis (Joshi et al., 2016; H. Wang et al., 2016), regulating abundance and size of these organelles (Vizeacoumar et al., 2004). Surprisingly, Pex30p was reported as intervenient in LD biogenesis.

4.1. The dysferlin domain-containing peroxins cooperate in lipid storage homeostasis

The involvement of peroxins, namely the dysferlin domain-containing peroxins in LD biogenesis started to be explored recently when Pex30p was described as a collaborator of the Seipin complex (Fld1p/Ldb16p) in lipid droplet budding (Joshi et al., 2018; S. Wang et al., 2018). Cells with combined deletion of the Fld1p/Ldb16p and Pex30p exhibited a cell growth defect, but mutants with combined deletions of Fld1p/Ldb16p and another of the dysferlin domain-containing peroxins (Pex28p, Pex29p, Pex31p or Pex32p) grew at wild-type rate (S. Wang et al., 2018). Since the cell

growth defect phenotype was associated with an aberrant LD budding in *pex30Δ fld1Δ/ldb16Δ* cells, we expected that cells with wild-type growth rate would exhibit effective LD budding. Therefore, we hypothesise that Pex30p-mediated organelle budding could be independent of Pex28p, Pex29p, Pex31p and Pex32p since budding still occurred in combined deletions of Seipin and the other dysferlin domain-containing peroxins. However, we observed that in absence of the Seipin complex, Pex28p, Pex29p, Pex31p and Pex32p are localised to the LDs, which is similar to the way the localization of Pex30p changes from dispersed throughout the ER to concentrated at the proximal LD regions. The observation is compatible with the involvement of these proteins in organelle budding and could happen due to shared functional domains and domain architecture within this family. Therefore, they could be regulated to concentrate at the LDs while their function at the organelle could differ from the function of Pex30p. The concentration of all these proteins at the proximal LD regions in absence of the Seipin complex could also result from the association of these proteins in a protein complex (David et al., 2013; Mast et al., 2016), whose stoichiometry and regulation are unknown. Based on the whole cell levels of these proteins, Pex30p would be probably the protein in higher amounts in such complex, which means that it would define the complex localisation to the LDs in situations of highly lipid droplet biogenesis or absence of the Seipin complex. In the future, the same assays should be performed in the absence of Pex30p to confirm its role in the localisation of the other peroxins.

Another hypothesis to explain the localisation of all dysferlin domain-containing peroxins at the LDs in absence of the Seipin complex is that all of them have the same function. The absence of aberrant LD budding with the loss of Pex28p, Pex29p, Pex31p and Pex32p would still be compatible with this hypothesis if one considers that their levels are lower than Pex30p. Therefore, we decided to analyse whether the overexpression of Pex28p, Pex29p, Pex31p or Pex32p would compensate for the absence of Pex30p and rescue the aberrant LD budding. We observed that none of these proteins can fully compensate Pex30p function since we continued to observe the aberrant dispersed Bodipy structures instead of LD aggregates or supersized LDs. Nevertheless, the cell growth defect was slightly smaller than in *pex30Δ fld1Δ/ldb16Δ*. The improvement of the growth defect could be associated with other functions of Pex30p in other organelles that may be rescued/compensated by overexpression of these peroxins. For instances, all five proteins have been described as to be involved in regulation of size and number of peroxisomes and all the five proteins have a reticulon-homology domain, which is involved in ER membrane-shaping. Therefore, they may reduce cell stress and the cell growth defect by contributing to these processes. This will

be addressed in future experiments by exploring the effects of overexpression of these peroxins in other organelles.

Following the idea of a Pex30p-anchoring complex, we hypothesize that the other dysferlin domain-containing peroxins, which protein levels are lower, could be important to regulate Pex30p localisation and function at the LDs. Nevertheless, this was not observed when the deletion of *pex28*, *pex29*, *pex31* and *pex32* did not alter Pex30p localisation during the exponential growth phase. However, in stationary phase Pex29p regulates Pex30p localisation. During this metabolic condition a portion of Pex30p concentrates at the nuclear membrane-vacuole junction, but in absence of Pex29p, Pex30p remains only dispersed throughout the ER. In addition, overexpression of Pex29p in single mutants of the Seipin complex (*fld1Δ/dbp16Δ*) revealed a cell growth defect and aberrant LD budding as a trait of combine Pex30p and Seipin complex double mutants. Although it needs further confirmation, this phenotype revealed that overexpression of Pex29p alters the localisation of Pex30p probably to the nuclear membrane-vacuole junction, producing an artificial double mutant at the LDs. It was recently reported that yeast ER–vacuole contact sites physically expand in response to metabolic stress and serve as sites for LD production (Hariri et al., 2017). Thus, Pex29p may recognise these signals and regulate Pex30p localisation, contributing to the spatial coordination of the LD biogenesis at ER–vacuole contacts under nutritional stress. Pex29p and Pex30p interact together with reticulon proteins (Rtn1p and Yop1p) to form focal points at the ER from which new peroxisomes arise (David et al., 2013; Mast et al., 2016). In addition, ER containing Pex29 and Pex30p dynamically associate with peroxisomes and are more stably associated when cells are grown in the presence of oleic acid, instead of glucose. Since upon addition of oleic acid LD biogenesis is induced, the interaction of Pex29p and Pex30p should also be more stable and may interfere in the regulation of several organelles.

Surprisingly, our preliminary results revealed that overexpression of *pex31* and *pex32* in single mutants of the Seipin complex components (*fld1Δ/dbp16Δ*) or *pex30Δ* may be lethal. Pex31p is unstable in absence of Pex30p, but Pex30p levels show no change in *pex31Δ* (M. Yan et al., 2008). Therefore, overexpression of *pex31* can turn Pex31p unstable and induce cell stress. Since the number of LDs increases up to several fold in yeast with cellular stress (Fei et al., 2009), the absence of the Seipin complex may not be compensated by Pex30p resulting in more cell stress and, consequently, in cell death. A similar molecular mechanism may happen with overexpression of Pex32p.

These observations suggest that the levels of the diverse dysferlin domain-containing peroxins may regulate Pex30p localisation by increasing or decreasing its recruitment for different organelles. In conclusion, here we present insight evidence that Pex30p is not the only peroxin of this family being involved in lipid droplet biogenesis. We show that although these proteins have no direct function in LD budding, they may be involved in the regulation of the cellular metabolic status since they regulate the localisation of Pex30p, which influences the process of LD and peroxisomes production.

4.2. Involvement of Pex30p functional domains in lipid droplet budding

It is well-established that the dysferlin domain-containing peroxins form a complex with reticulon homology domain-containing proteins and define peroxisome contact sites at ER subdomains (David et al., 2013; Mast et al., 2016). Consequently, they regulate peroxisome size and proliferation. In contrast, their association with LD biogenesis have only recently been shown, since in the absence of the Seipin complex, Pex30p localises to the LDs (S. Wang et al., 2018). Pex30p contains a RHD with ER membrane-shaping properties (Joshi et al., 2016), which is required for normal peroxisome biogenesis (David et al., 2013; Mast et al., 2016; Vizeacoumar et al., 2004; M. Yan et al., 2008), and a dysferlin domain that may bind diacylglycerol DAG (Joshi et al., 2018; Vizeacoumar et al., 2006; M. Yan et al., 2008). However, whether both ER membrane-shaping and DAG-binding proprieties were involved in promoting organelle budding in Seipin mutants was unclear. To uncover the signalling mechanisms behind Pex30p localisation to the LDs, we tried to define the protein portion which would be required for its targeting to LDs. We explored the role of the RHD, the dysferlin domain and, complementarily, the C-terminal portion in the localisation and function of Pex30p and other dysferlin domain-containing peroxins. Overall, in the present work we showed the dysferlin domain is crucial for the concentration of Pex30p at the LD-proximal regions in absence of the Seipin complex.

Reticulon-homology domain

As stated above, the RHD has been shown to have membrane-shaping proprieties. Here, by analysis of the localisation of the C-terminal truncated variants of Pex30p in absence of the Seipin complex, we determined that the truncation of RHD in the Pex30 Δ 60-523 variant generated a soluble protein. In contrast, the Pex30 Δ 235-523 variant, in which the RHD was not deleted, was still anchored in the membrane. This observation allowed us to associate this domain with insertion

of Pex30p in the ER and LD membrane. We further validated this association by testing another variant of Pex30p in which only the amino acids corresponding to the domain were deleted, ensuring that the remaining protein was unaltered, and observed similar localisation. This is consistent with previous reports whereas Pex30(1–170)p, which contains only the first half of the hairpin of this domain, showed an almost exclusive cytosolic localisation (Vizeacoumar et al., 2006). In addition, these results revealed that the RHD is not essential for the localisation of Pex30p to proximal LD regions in absence of the Seipin complex, since Pex30 Δ 235-523, which contains the entire domain, was anchored in the membrane, but it was not localised to the LDs in *fld1 Δ /ldb16 Δ* cells. The Pex30 Δ 235-523 truncated variant of Pex30p was previously shown to retain the ER membrane-shaping function of the RHD of Pex30p (Joshi et al., 2016), which suggests that this feature of the domain is not associated to the localisation of Pex30p in absence of the Seipin complex. To confirm this hypothesis, we mutated the conserved residue reported as required for the ER membrane-shape function of any reticulon-homology domain-containing protein (Pex30W94C) (Joshi et al., 2016). The presence of Pex30W94C at the LDs in *fld1 Δ /ldb16 Δ* cells suggests that the ER membrane-shape function of Pex30p is not related to its localisation at the LDs, nor associated with the role of Pex30p in LD budding, since *fld1 Δ /ldb16 Δ* cells with Pex30W94C presented typical supersized LD-phenotype.

Whereas the ER membrane-shaping properties were not involved in the localisation of Pex30p and LD budding in absence of the Seipin complex, we questioned whether the RHD of Pex30p was functionally different of other RHD. To study this, we created a chimeric variant of Pex30p in which its RHD was swapped with RHD from Rtn1p, a reticulon protein which does not localise at LDs in absence of the Seipin complex (S. Wang et al., 2018). We observed that this chimeric Pex30p was distributed throughout the ER even in *fld1 Δ /ldb16 Δ* cells, leading to disrupted LD budding. This result can be interpreted in several ways. One hypothesis is that the RHD of Pex30p could have different properties of the RHD of Rtn1p, since even in presence of the dysferlin domain, the protein was not localised to the LDs. Therefore, the RHD of Pex30p may be also required for its localisation in absence of the Seipin complex. Such requirement could mean that the RHD is responsible for the insertion of the protein on the membrane, and that the selection of anchoring ER membrane sites could be different between the RHD of Pex30p. Moreover, in different ER regions the signal to alter Pex30p localisation in absence of the Seipin complex could not be recognized. In contrast, since the folding of the chimeric protein is unknown, another hypothesis is that the protein is not functional. For this reason, the folding of the Pex30p could be affected,

preventing its association with the dysferlin domain-containing peroxins, or the dysferlin domain could be affected, preventing its role in the definition of protein localisation.

MCTP2 was reported as the human homolog of Pex30p, based on their structural homology. In addition, it was reported that overexpression of only the RHD of MCTP2 was sufficient to rescue the defects in LD budding observed in *pex30Δfld1Δ/ldb16Δ* cells (Joshi et al., 2018). This observation contracts with our observations in yeast. Therefore, we decided to confirm whether the RHD of MCTP2 could substitute RHD of Pex30p, by using the same approach used previously for Rtn1p. We observed that this chimeric Pex30p failed to localise at the LD-proximal regions in absence of the Seipin complex, promoting defected LD budding. This result contradicts our observation because the dysferlin domain was also present in the chimeric variant of Pex30p. However, likewise for the chimeric protein with RHD of Rtn1p, the protein folding is unknown. Therefore, we cannot exclude the possibility that the RHD of MCTP2 is functionally different from the RHD of Pex30p.

Dysferlin domain

We also analysed the localisation of C-terminal truncated variants of Pex30p in absence of the Seipin complex. All the truncated variants of Pex30p, in which the dysferlin domain was deleted, showed distribution throughout the ER, instead Pex30p accumulation at the LDs. Therefore, we suggest that the dysferlin domain is involved in the targeting of this protein. The result was confirmed by generation of a Pex30p mutant with the deletion of only the amino acids correspondents to the dysferlin domain (Pex30 Δ 284-408), to ensure that the rest of the protein was unaltered and functional. In this strain, the protein exhibited the typical ER distribution both in WT and *fld1Δ/ldb16Δ* cells. For further confirmation that the dysferlin domain is essential for Pex30p localisation at the LDs in absence of the Seipin complex, we mutated an evolutionarily conserved residue which is critical for the folding of the dysferlin domain (Pex30W401C). The conserved residue is included in the aromatic/arginine stocks which hold the domain in a folded conformation. As expected, Pex30W401C was not localised at the LDs in *fld1Δ/ldb16Δ* cells, confirming that the dysferlin domain is crucial for targeting of Pex30p to LDs. Moreover, the folding of this domain was shown to be essential for its function, since deletions of only the N- or C-terminal motifs of the domain were sufficient to prevent LD localisation of Pex30p (data not shown).

After confirming the essential role of the dysferlin domain on Pex30p localisation and given that all the dysferlin domain-containing peroxins accumulate at LDs in absence of the Seipin complex,

we decided to explore if this role of the dysferlin domain was a conserved feature. We observed that C-terminal truncated variants of Pex31p and Pex32p remained at the ER in *fld1Δ/dbp16Δ* cells, indicating that the dysferlin domain is also essential for the localisation of these two proteins at the LDs. However, the truncated variants of Pex28p and Pex29p were localised at the LDs in absence of the Seipin complex. This observation indicates that the dysferlin domain is not essential for the targeting of all the peroxins of this family to LDs. Therefore, Pex28p and Pex29p might depend on their association with other peroxins in the complex to be localised to the LDs. One can also infer that the dysferlin domain is not involved in the interaction of dysferlin domain-containing peroxins and that interactions between Pex28p and Pex29p and the complex occur through other mechanisms. Then, we further explored if the role of the dysferlin domain in the function of Pex30p was conserved. By analyzing the localisation of chimeric variants of Pex30p and correspond LD phenotype in which its dysferlin domain was swapped with the dysferlin domains of Pex31p and Pex32p, we confirmed the conserved role of the dysferlin domain in the localisation of Pex30p in absence of the Seipin complex. Additionally, these two Pex30p variants exhibit effective LD budding, suggesting that the features of localization at the LDs in absence of the Seipin complex and cooperation on LD budding of the dysferlin domain is conserved in Pex31p and Pex32p. Overall, these results suggest that some dysferlin domain-containing peroxins require the dysferlin domain for proper localization and function, while others may rely on other mechanisms to localize at the lipid droplets.

Although we discover the involvement of the dysferlin domain in this crucial step for Pex30p role in LD budding, the molecular mechanism behind its localization and cooperation with the Seipin complex is still unknown. However, some recent reports hypothesized that the dysferlin domain may bind DAG. Since MCTP2, the human homolog of Pex30p, contains C2 domains which bind to lipids, we hypothesize that the function of the dysferlin domain of Pex30 could be related to the function of the C2 domains. To test this, we generated two chimera proteins of Pex30p in which its dysferlin domain was substituted by the sequence of amino acids which includes the three C2 domains of MCTP2 or by the sequence of amino acids corresponded to only the first C2 domain of MCTP2, C2A. The proteins were not localised at the LDs in absence of the Seipin complex and, consequently, the LD budding was disrupted. In conclusion, although both domains may bind to lipids, the lipids which may induce Pex30p targeting by interacting with the dysferlin domain may not interact with C2 domains. Another explanation for the observed result is that the

unknown protein folding of the chimeric proteins affected the interaction with the targeting signal, preventing the proper localisation of the proteins.

C-terminal portion

Following up on data produced during this work, we also observed that the most C-terminal portion of Pex30p is required for its localisation at the nuclear membrane-vacuole junction in stationary phase, namely the amino acids 430-523. In this region, protein phosphorylation is described to happen in some of these amino acids residues (Albuquerque et al., 2008; Holt et al., 2010), which may be involved in the induction of the targeting. Since we observed that Pex29p is involved in the targeting of Pex30p to the NVJ in stationary phase, Pex29p may interact with Pex30p through these residues when phosphorylated as a response to the cellular metabolic status.

Besides the distribution throughout the ER and the accumulation at LDs and NVJ, all in different metabolic conditions, Pex30p also targets the peroxisomes, and a small sequence of this protein (amino acids 230-250) was found to function as peroxisomal targeting signal (Vizeacoumar et al., 2006). Therefore, since its cellular localisation is regulated among several organelles in which plays different roles, Pex30p reveals to an important protein to coordinate organelle function and, consequently, maintains cell homeostasis.

4.3. Conclusion

In the present document, we determined that all the dysferlin domain-containing peroxins localize at the LDs in absence of the Seipin complex. However, only Pex30p seems to be involved in LD budding by cooperating with the Seipin complex since neither absence or overexpression of the remaining dysferlin domain-containing peroxins affected LD budding. Although they do not have the same function of Pex30p at LDs, Pex29p revealed to regulate Pex30p localisation, consequently, the success of LD budding, during exponential phase.

Regarding the localisation of Pex30p at the LDs, the dysferlin domain is essential, which is a conserved feature for Pex31p and Pex32p, but not for Pex28p and Pex29p. In contrast, the RHD is fundamental for the protein be anchored in the membrane, but no essential requirement of this domain for Pex30p localisation was observed. The same way, the ER-membrane shape properties are not involved in the localisation of Pex30p nor in the LD budding.

Based on all our observations, we propose that the dysferlin domain-containing peroxins associate in a protein complex and act in concert to define their localisation and function in

response to the metabolic conditions. Such a complex may regulate intracellular communication among several organelles in which dysferlin domain-containing peroxins play several functions, contributing to coordinate organelle biogenesis and, consequently, cell homeostasis.

5. References

- Aartsma-Rus, A., Van Deutekom, J. C. T., Fokkema, I. F., Van Ommen, G. J. B., & Den Dunnen, J. T. (2006). Entries in the Leiden Duchenne muscular dystrophy mutation database: An overview of mutation types and paradoxical cases that confirm the reading-frame rule. *Muscle and Nerve*, *34*(2), 135–144. doi:10.1002/mus.20586
- Abraham, T., Allan, S. E., & Levings, M. K. (2010). Deconvolution and chromatic aberration corrections in quantifying colocalization of a transcription factor in three-dimensional cellular space. *Micron*, *41*(6), 633–640. doi:10.1016/j.micron.2010.03.005
- Agarwal, A. K., & Garg, A. (2004). Seipin: A mysterious protein. *Trends in Molecular Medicine*, *10*(9), 440–444. doi:10.1016/j.molmed.2004.07.009
- Albuquerque, C. P., Smolka, M. B., Payne, S. H., Bafna, V., Eng, J., & Zhou, H. (2008). A Multidimensional Chromatography Technology for In-depth Phosphoproteome Analysis. *Molecular & Cellular Proteomics*, *7*(7), 1389–1396. doi:10.1074/mcp.M700468-MCP200
- Andrianov, V., Borisjuk, N., Pogrebnyak, N., Brinker, A., Dixon, J., Spitsin, S., ... Koprowski, H. (2010). Tobacco as a production platform for biofuel: Overexpression of Arabidopsis DGAT and LEC2 genes increases accumulation and shifts the composition of lipids in green biomass. *Plant Biotechnology Journal*, *8*(3), 277–287. doi:10.1111/j.1467-7652.2009.00458.x
- Bailey, A. P., Koster, G., Guillermier, C., Hirst, E. M. A., MacRae, J. I., Lechene, C. P., ... Gould, A. P. (2015). Antioxidant Role for Lipid Droplets in a Stem Cell Niche of *Drosophila*. *Cell*, *163*(2), 340–353. doi:10.1016/j.cell.2015.09.020
- Bansal, D., Miyake, K., Vogel, S. S., Groh, S., Chen, C.-C., Williamson, R., ... Campbell, K. P. (2003). Defective membrane repair in dysferlin-deficient muscular dystrophy. *Nature*, *423*(May), 1–5. doi:10.1038/nature01604.1.
- Barbosa, A. D., & Siniosoglou, S. (2017). Function of lipid droplet-organelle interactions in lipid homeostasis. *Biochimica et Biophysica Acta - Molecular Cell Research*, *1864*(9), 1459–1468. doi:10.1016/j.bbamcr.2017.04.001
- Barneda, D., Planas-Iglesias, J., Gaspar, M. L., Mohammadyani, D., Prasannan, S., Dormann, D., ... Christian, M. (2015). The brown adipocyte protein CIDEA promotes lipid droplet fusion via a phosphatidic acid-binding amphipathic helix. *eLife*, *4*, e07485. doi:10.7554/eLife.07485
- Bartz, R., Li, W.-H., Venables, B., Zehmer, J. K., Roth, M. R., Welti, R., ... Chapman, K. D. (2007). Lipidomics reveals that adiposomes store ether lipids and mediate phospholipid traffic .

- Journal of Lipid Research*, 48(4), 837–847. doi:10.1194/jlr.M600413-JLR200
- Benchling (Biology Software). (2018). Retrieved from <https://benchling.com>
- Bersuker, K., & Olzmann, J. A. (2017). Establishing the lipid droplet proteome: Mechanisms of lipid droplet protein targeting and degradation. *BBA - Molecular and Cell Biology of Lipids*, 1862(10), 1166–1177. doi:10.1016/j.bbalip.2017.06.006
- Bersuker, K., Peterson, C. W. H., To, M., Sahl, S. J., Savikhin, V., Grossman, E. A., ... Olzmann, J. A. (2018). A Proximity Labeling Strategy Provides Insights into the Composition and Dynamics of Lipid Droplet Proteomes. *Developmental Cell*, 44(1), 97–112.e7. doi:10.1016/j.devcel.2017.11.020
- Binns, D., Januszewski, T., Chen, Y., Hill, J., Markin, V. S., Zhao, Y., ... Goodman, J. M. (2006). An intimate collaboration between peroxisomes and lipid bodies. *Journal of Cell Biology*, 173(5), 719–731. doi:10.1083/jcb.200511125
- Binns, D., Lee, S., Hilton, C. L., Jiang, Q. X., & Goodman, J. M. (2010). Seipin is a discrete homooligomer. *Biochemistry*, 49(50), 10747–10755. doi:10.1021/bi1013003
- Boutet, E., El Mourabit, H., Prot, M., Nemani, M., Khallouf, E., Colard, O., ... Magré, J. (2009). Seipin deficiency alters fatty acid D9 desaturation and lipid droplet formation in Berardinelli-Seip congenital lipodystrophy. *Biochimie*, 91(6), 796–803. doi:10.1016/j.biochi.2009.01.011
- Brown, T. W., Titorenko, V. I., & Rachubinski, R. A. (2000). Mutants of the *Yarrowia lipolytica* PEX23 gene encoding an integral peroxisomal membrane peroxin mislocalize matrix proteins and accumulate vesicles containing peroxisomal matrix and membrane proteins. *Mol Biol Cell*, 11(1), 141–152. doi:10.1091/mbc.11.1.141
- Buhman, K. K., Chen, H. C., & Farese, R. V. (2001). The enzymes of neutral lipid synthesis. *The Journal of Biological Chemistry*, 276(44), 40369–40372. doi:10.1074/jbc.R100050200
- Bulankina, A. V., Deggerich, A., Wenzel, D., Mutenda, K., Wittmann, J. G., Rudolph, M. G., ... Höning, S. (2009). TIP47 functions in the biogenesis of lipid droplets. *Journal of Cell Biology*, 185(4), 641–655. doi:10.1083/jcb.200812042
- Cartwright, B. R., Binns, D. D., Hilton, C. L., Han, S., Gao, Q., & Goodman, J. M. (2015). Seipin performs dissectible functions in promoting lipid droplet biogenesis and regulating droplet morphology. *Molecular Biology of the Cell*, 26(4), 726–739. doi:10.1091/mbc.E14-08-1303
- Cartwright, B. R., & Goodman, J. M. (2012). Seipin: From human disease to molecular mechanism. *Journal of Lipid Research*, 53(6), 1042–1055. doi:10.1194/jlr.R023754

- Cermelli, S., Guo, Y., Gross, S. P., & Welte, M. A. (2006). The Lipid-Droplet Proteome Reveals that Droplets Are a Protein-Storage Depot. *Current Biology*, *16*(18), 1783–1795. doi:10.1016/j.cub.2006.07.062
- Chauhan, N., Visram, M., Cristobal-Sarramian, A., Sarkleti, F., & Kohlwein, S. D. (2015). Morphogenesis checkpoint kinase Swe1 is the executor of lipolysis-dependent cell-cycle progression. *Proceedings of the National Academy of Sciences*, *112*(10), E1077–E1085. doi:10.1073/pnas.1423175112
- Chorlay, A., & Thiam, A. R. (2018). An Asymmetry in Monolayer Tension Regulates Lipid Droplet Budding Direction. *Biophysical Journal*, *114*(3), 631–640. doi:10.1016/j.bpj.2017.12.014
- Choudhary, V., Golani, G., Joshi, A. S., Cottier, S., Schneider, R., Prinz, W. A., & Kozlov, M. M. (2018). Architecture of Lipid Droplets in Endoplasmic Reticulum Is Determined by Phospholipid Intrinsic Curvature. *Current Biology*, *28*. doi:10.1016/j.cub.2018.02.020
- Choudhary, V., Ojha, N., Golden, A., & Prinz, W. A. (2015). A conserved family of proteins facilitates nascent lipid droplet budding from the ER. *The Journal of Cell Biology*, *211*(2), 261–271. doi:10.1083/jcb.201505067
- Dahlqvist, A., Ståhl, U., Lenman, M., Banas, A., Lee, M., Sandager, L., ... Stymne, S. (2000). Phospholipid:diacylglycerol acyltransferase: An enzyme that catalyzes the acyl-CoA-independent formation of triacylglycerol in yeast and plants. *Proceedings of the National Academy of Sciences of the United States of America*, *97*(12), 6487–6492. doi:10.1073/pnas.120067297
- David, C., Koch, J., Oeljeklaus, S., Laernsack, A., Melchior, S., Wiese, S., ... Brocard, C. (2013). A Combined Approach of Quantitative Interaction Proteomics and Live-cell Imaging Reveals a Regulatory Role for Endoplasmic Reticulum (ER) Reticulon Homology Proteins in Peroxisome Biogenesis. *Molecular & Cellular Proteomics*, *12*(9), 2408–2425. doi:10.1074/mcp.M112.017830
- Davis, D. B., Doherty, K. R., Delmonte, A. J., & McNally, E. M. (2002). Calcium-sensitive phospholipid binding properties of normal and mutant ferlin C2 domains. *Journal of Biological Chemistry*, *277*(25), 22883–22888. doi:10.1074/jbc.M201858200
- Duelund, L., Jensen, G. V., Hannibal-Bach, H. K., Ejsing, C. S., Pedersen, J. S., Pakkanen, K. I., & Ipsen, J. H. (2013). Composition, structure and properties of POPC-triolein mixtures. Evidence of triglyceride domains in phospholipid bilayers. *Biochimica et Biophysica Acta - Biomembranes*, *1828*(8), 1909–1917. doi:10.1016/j.bbamem.2013.03.020

- Dymond, J. S. (2013). *Saccharomyces Cerevisiae Growth Media*. *Methods in Enzymology*, *533*, 191–204. doi:10.1016/B978-0-12-420067-8.00012-X
- Espenshade, P. J., & Hughes, A. L. (2007). Regulation of sterol synthesis in eukaryotes. *Annual Review of Genetics*, *41*, 401–427. doi:10.1146/annurev.genet.41.110306.130315
- Fei, W., Li, H., Shui, G., Kapterian, T. S., Bielby, C., Du, X., ... Yang, H. (2011). Molecular characterization of seipin and its mutants: implications for seipin in triacylglycerol synthesis. *Journal of Lipid Research*, *52*(12), 2136–2147. doi:10.1194/jlr.M017566
- Fei, W., Shui, G., Gaeta, B., Du, X., Kuerschner, L., Li, P., ... Yang, H. (2008). Fld1p, a functional homologue of human seipin, regulates the size of lipid droplets in yeast. *Journal of Cell Biology*, *180*(3), 473–482. doi:10.1083/jcb.200711136
- Fei, W., Shui, G., Zhang, Y., Krahmer, N., Ferguson, C., Kapterian, T. S., ... Yang, H. (2011). A role for phosphatidic acid in the formation of “supersized” Lipid droplets. *PLoS Genetics*, *7*(7), e1002201. doi:10.1371/journal.pgen.1002201
- Fei, W., Wang, H., Fu, X., Bielby, C., & Yang, H. (2009). Conditions of endoplasmic reticulum stress stimulate lipid droplet formation in *Saccharomyces cerevisiae*. *The Biochemical Journal*, *424*(1), 61–67. doi:10.1042/BJ20090785
- Fernández-Murray, J. P., & McMaster, C. (2016). Lipid synthesis and membrane contact sites: A crossroads for cellular physiology. *Journal of Lipid Research*, *58*(12), 7250–7257. doi:10.1194/jlr.R070920
- Fidler, D. R., Murphy, S. E., Curtis, K., Antonoudiou, P., El-Tohamy, R., Ient, J., & Levine, T. P. (2016). Using HHsearch to tackle proteins of unknown function: A pilot study with PH domains. *Traffic*, *17*(11), 1214–1226. doi:10.1111/tra.12432
- Finn, R. D., Coggill, P., Eberhardt, R. Y., Eddy, S. R., Mistry, J., Mitchell, A. L., ... Bateman, A. (2016). The Pfam protein families database: Towards a more sustainable future. *Nucleic Acids Research*, *44*(D1), D279–D285. doi:10.1093/nar/gkv1344
- Fujimoto, T., & Ohsaki, Y. (2006). Cytoplasmic lipid droplets: Rediscovery of an old structure as a unique platform. *Annals of the New York Academy of Sciences*, *1086*(2006), 104–115. doi:10.1196/annals.1377.010
- Fujimoto, T., Ohsaki, Y., Cheng, J., Suzuki, M., & Shinohara, Y. (2008). Lipid droplets: A classic organelle with new outfits. *Histochemistry and Cell Biology*, *130*(2), 263–279. doi:10.1007/s00418-008-0449-0
- Fuson, K., Rice, A., Mahling, R., Snow, A., Nayak, K., Shanbhogue, P., ... Sutton, R. B. (2014).

- Alternate splicing of dysferlin C2A confers Ca²⁺-dependent and Ca²⁺-independent binding for membrane repair. *Structure*, *22*(1), 104–115. doi:10.1016/j.str.2013.10.001
- Gao, Q., Binns, D. D., Kinch, L. N., Grishin, N. V, Ortiz, N., Chen, X., & Goodman, J. M. (2017). Pet10p is a yeast perilipin that stabilizes lipid droplets and promotes their assembly. *Journal of Cell Biology*, 1–19.
- Gao, Q., & Goodman, J. M. (2015). The lipid droplet - A well-connected organelle. *Frontiers in Cell and Developmental Biology*, *3*(49), 1–12. doi:10.3389/fcell.2015.00049
- Gaspar, M. L., Hofbauer, H. F., Kohlwein, S. D., & Henry, S. A. (2011). Coordination of storage lipid synthesis and membrane biogenesis: Evidence for cross-talk between triacylglycerol metabolism and phosphatidylinositol synthesis. *Journal of Biological Chemistry*, *286*(3), 1696–1708. doi:10.1074/jbc.M110.172296
- Greenberg, A. S., Coleman, R. A., Kraemer, F. B., Mcmanaman, J. L., Obin, M. S., Puri, V., ... Mashek, D. G. (2011). Review series The role of lipid droplets in metabolic disease in rodents and humans. *The Journal of Clinical Investigation*, *121*(6), 2102–2110. doi:10.1172/JCI46069.2102
- Grippa, A., Buxó, L., Mora, G., Funaya, C., Idrissi, F. Z., Mancuso, F., ... Carvalho, P. (2015). The seipin complex Fld1/Ldb16 stabilizes ER-lipid droplet contact sites. *Journal of Cell Biology*, *211*(4), 829–844. doi:10.1083/jcb.201502070
- Hariri, H., Rogers, S., Ugrankar, R., Liu, Y. L., Feathers, J. R., & Henne, W. M. (2017). Lipid droplet biogenesis is spatially coordinated at ER–vacuole contacts under nutritional stress. *EMBO Reports*, e201744815. doi:10.15252/embr.201744815
- Hartman, I. Z., Liu, P., Zehmer, J. K., Luby-Phelps, K., Jo, Y., Anderson, R. G. W., & DeBose-Boyd, R. A. (2010). Sterol-induced dislocation of 3-Hydroxy-3-methylglutaryl coenzyme a reductase from endoplasmic reticulum membranes into the cytosol through a subcellular compartment resembling lipid droplets. *Journal of Biological Chemistry*, *285*(25), 19288–19298. doi:10.1074/jbc.M110.134213
- Hashemi, H. F., & Goodman, J. M. (2015). The life cycle of lipid droplets. *Current Opinion in Cell Biology*, *33*, 119–124. doi:10.1016/j.ceb.2015.02.002
- Hedrich, H. J., Sher, R. B., Cox, G. A., & Ackert-Bicknell, C. (2012). Development and Disease of Mouse Muscular and Skeletal Systems. *The Laboratory Mouse*, 209–239. doi:10.1016/B978-0-12-382008-2.00010-6
- Henne, W. M., Reese, M. L., & Goodman, J. M. (2018). The assembly of lipid droplets and their

- roles in challenged cells. *The EMBO Journal*, e98947. doi:10.15252/emj.201898947
- Herker, E., Harris, C., Hernandez, C., Carpentier, A., Kaehlcke, K., Rosenberg, A. R., ... Ott, M. (2010). Efficient hepatitis C virus particle formation requires diacylglycerol acyltransferase-1. *Nature Medicine*, *16*(11), 1295–1298. doi:10.1038/nm.2238
- Herker, E., & Ott, M. (2011). Unique ties between Hepatitis C Virus replication and intracellular lipids. *Trends in Endocrinology and Metabolism*, *22*(6), 241–248. doi:10.1016/j.immuni.2010.12.017.Two-stage
- Holt, L. J., Tuch, B. B., Villén, J., Johnson, A. D., Gygi, S. P., & Morgan, D. O. (2010). Insights into evolution. *Science*, *325*(5948), 1–11. doi:10.1126/science.1172867.Global
- Hsu, P. D., Lander, E. S., & Zhang, F. (2014). Development and Applications of CRISPR-Cas9 for Genome Engineering. *Cell*, *157*(6), 1262–1278. doi:10.1016/j.cell.2014.05.010.Development
- Hsu, P. D., Scott, D. A., Weinstein, J. A., Ran, F. A., Konermann, S., Agarwala, V., ... Zhang, F. (2013). DNA targeting specificity of RNA-guided Cas9 nucleases. *Nat Biotechnol*, *31*(9), 827–832. doi:10.1038/nbt.2647.DNA
- Ito, H., Fukuda, Y., Murata, K., & Kimura, A. (1983). Transformation of Intact Yeast Cells Treated with Alkali Cations. *Journal of Bacteriology*, *153*(1), 163–168.
- Ito, T., Chiba, T., Ozawa, R., Yoshida, M., Hattori, M., & Sakaki, Y. (2001). A comprehensive two-hybrid analysis to explore the yeast protein interactome. *Proceedings of the National Academy of Sciences*, *98*(8), 4569–4574. doi:10.1073/pnas.061034498
- Jacquier, N., Choudhary, V., Mari, M., Toulmay, A., Reggiori, F., & Schneider, R. (2011). Lipid droplets are functionally connected to the endoplasmic reticulum in *Saccharomyces cerevisiae*. *Journal of Cell Science*, *124*(14), 2424–2437. doi:10.1242/jcs.076836
- Jacquier, N., Mishra, S., Choudhary, V., Schneider, R., Adeyo, O., Horn, P. J., ... Londos, C. (2013). Expression of oleosin and perilipins in yeast promotes formation of lipid droplets from the endoplasmic reticulum. *Journal of Cell Science*, *126*(22), 5198–5209. doi:10.1242/jcs.131896
- Janke, C., Magiera, M. M., Rathfelder, N., Taxis, C., & Reber, S. (2004). A versatile toolbox for PCR-based tagging of yeast genes : new fluorescent proteins , more. *Yeast*, *21*, 947–962. doi:10.1002/yea.1142
- Jiang, M., Gao, M., Wu, C., He, H., Guo, X., Zhou, Z., ... Sha, J. (2014). Lack of testicular seipin causes teratozoospermia syndrome in men. *Proceedings of the National Academy of*

- Sciences of the United States of America*, 111(19), 7054–7059.
doi:10.1073/pnas.1324025111
- Joshi, A. S., Huang, X., Choudhary, V., Levine, T. P., Hu, J., & Prinz, W. A. (2016). A family of membrane-shaping proteins at ER subdomains regulates pre-peroxisomal vesicle biogenesis. *Journal of Cell Biology*, 215(4), 515–529. doi:10.1083/jcb.201602064
- Joshi, A. S., Nebenfuehr, B., Choudhary, V., Satpute-Krishnan, P., Levine, T. P., Golden, A., & Prinz, W. A. (2018). Lipid droplet and peroxisome biogenesis occur at the same ER subdomains. *Nature Communications*, 9(1), 2940. doi:10.1038/s41467-018-05277-3
- Kadereit, B., Kumar, P., Wang, W.-J., Miranda, D., Snapp, E. L., Severina, N., ... Silver, D. L. (2008). Evolutionarily conserved gene family important for fat storage. *Proceedings of the National Academy of Sciences*, 105(1), 94–99. doi:10.1073/pnas.0708579105
- Kassan, A., Herms, A., Fernández-Vidal, A., Bosch, M., Schieber, N. L., Reddy, B. J. N., ... Pol, A. (2013). Acyl-CoA synthetase 3 promotes lipid droplet biogenesis in ER microdomains. *The Journal of Cell Biology*, 203(6), 985–1001. doi:10.1083/jcb.201305142
- Kennedy, E. P. (1956). Metabolism of lipides. *Annual Review of Biochemistry*, 26, 119–148.
- Khandelia, H., Duelund, L., Pakkanen, K. I., & Ipsen, J. H. (2010). Triglyceride blisters in lipid bilayers: Implications for lipid droplet biogenesis and the mobile lipid signal in cancer cell membranes. *PLoS ONE*, 5(9), 1–8. doi:10.1371/journal.pone.0012811
- Kinch, L. N., & Grishin, N. V. (2002). Evolution of protein structures and functions. *Current Opinion in Structural Biology*, 12(3), 400–408. doi:10.1016/S0959-440X(02)00338-X
- Klemm, E. J., Spooner, E., & Ploegh, H. L. (2011). Dual role of Ancient Ubiquitous Protein 1 (AUP1) in lipid droplet accumulation and Endoplasmic Reticulum (ER) protein quality control. *Journal of Biological Chemistry*, 286(43), 37602–37614. doi:10.1074/jbc.M111.284794
- Kory, N., Farese Jr, R. V., & Walther, T. C. (2016). Targeting fat: Mechanisms of protein localization to lipid droplets. *Trends in Cell Biology*, 26(7), 535–546. doi:10.1016/j.tcb.2016.02.007
- Krahmer, N., Farese Jr, R. V., & Walther, T. C. (2013). Balancing the fat: Lipid droplets and human disease. *EMBO Molecular Medicine*, 5(7), 905–915. doi:10.1002/emmm.201100671
- Krahmer, N., Guo, Y., Wilfling, F., Hilger, M., Lingrell, S., Heger, K., ... Walther, T. C. (2011). Phosphatidylcholine synthesis for lipid droplet expansion is mediated by localized activation of CTP:phosphocholine cytidylyltransferase. *Cell Metabolism*, 14(4), 504–515. doi:10.1016/j.cmet.2011.07.013
- Krahmer, N., Hilger, M., Kory, N., Wilfling, F., Stoehr, G., Mann, M., ... Walther, T. C. (2013).

- Protein correlation profiles identify lipid droplet proteins with high confidence. *Molecular & Cellular Proteomics*, *12*(5), 1115–1126. doi:10.1074/mcp.M112.020230
- Kuerschner, L., Moessinger, C., & Thiele, C. (2008). Imaging of lipid biosynthesis: How a neutral lipid enters lipid droplets. *Traffic*, *9*(3), 338–352. doi:10.1111/j.1600-0854.2007.00689.x
- Kurat, C. F., Wolinski, H., Petschnigg, J., Kaluarachchi, S., Andrews, B., Natter, K., & Kohlwein, S. D. (2009). Cdk1/Cdc28-Dependent Activation of the Major Triacylglycerol Lipase Tgl4 in Yeast Links Lipolysis to Cell-Cycle Progression. *Molecular Cell*, *33*(1), 53–63. doi:10.1016/j.molcel.2008.12.019
- Laughery, M. F., Hunter, T., Brown, A., Hoopes, J., Ostbye, T., Shumaker, T., & Wyrick, J. J. (2016). New Vectors for Simple and Streamlined CRISPR-Cas9 Genome Editing in *Saccharomyces cerevisiae*. *Yeast*, *32*(12), 711–720. doi:10.1002/yea.3098
- Lek, A., Evesson, F. J., Sutton, R. B., North, K. N., Cooper, S. T., & Cooper, S. T. (2012). Ferlins : Regulators of Vesicle Fusion for Auditory Neurotransmission , Receptor Trafficking and Membrane Repair, 185–194. doi:10.1111/j.1600-0854.2011.01267.x
- Letunic, I., & Bork, P. (2018). 20 years of the SMART protein domain annotation resource. *Nucleic Acids Research*, *46*(October 2017), 493–496. doi:10.1093/nar/gkx922
- Listenberger, L. L., Han, X., Lewis, S. E., Cases, S., Farese, R. V., Ory, D. S., & Schaffer, J. E. (2003). Triglyceride accumulation protects against fatty acid-induced lipotoxicity. *Proceedings of the National Academy of Sciences*, *100*(6), 3077–3082. doi:10.1073/pnas.0630588100
- Liu, L., Jiang, Q., Wang, X., Zhang, Y., Lin, R. C. Y., Lam, S. M., ... Yang, H. (2014). Adipose-specific knockout of Seipin/Bscl2 results in progressive lipodystrophy. *Diabetes*, *63*(7), 2320–2331. doi:10.2337/db13-0729
- Liu, P., Bartz, R., Zehmer, J. K., Ying, Y., Zhu, M., Serrero, G., & Anderson, R. G. W. (2007). Rab-regulated interaction of early endosomes with lipid droplets. *Biochimica et Biophysica Acta - Molecular Cell Research*, *1773*(6), 784–793. doi:10.1016/j.bbamcr.2007.02.004
- Lodhi, I. J., & Semenkovich, C. F. (2014). Peroxisomes: A Nexus for Lipid Metabolism and Cellular Signaling. *Cell Metabolism*, *19*(3), 380–392. doi:10.1016/j.cmet.2014.01.002
- Logan, M. R., Nguyen, T., Szapiel, N., Knockleby, J., Por, H., Zadworny, M., ... Lesage, G. (2008). Genetic interaction network of the *Saccharomyces cerevisiae* type 1 phosphatase Glc7. *BMC Genomics*, *9*, 1–18. doi:10.1186/1471-2164-9-327
- Long, A. P., Mannes Schmidt, A. K., Verbrugge, B., Dortch, M. R., Minkin, S. C., Prater, K. E., ... Dalhaimer, P. (2012). Lipid droplet de novo formation and fission are linked to the cell cycle

- in fission yeast. *Traffic*, *13*(5), 705–714. doi:10.1111/j.1600-0854.2012.01339.x
- Longtine, M. S., Iijima, A. M. K., Demarini, D. J., & Shah, N. G. (1998). Additional Modules for Versatile and Economical PCR-based Gene Deletion and Modification in *Saccharomyces cerevisiae*. *Yeast*, *96*(1), 953–961.
- Lundin, C., Nordström, R., Wagner, K., Windpassinger, C., Andersson, H., von Heijne, G., & Nilsson, I. (2006). Membrane topology of the human seipin protein. *FEBS Letters*, *580*(9), 2281–2284. doi:10.1016/j.febslet.2006.03.040
- M'barek, K. Ben, Ajjaji, D., Chorlay, A., Vanni, S., Fore, L., & Thiam, A. R. (2017). ER membrane phospholipids and surface tension control cellular lipid droplet formation. *Developmental Cell*, *41*(6), 591–604. doi:10.1016/j.devcel.2017.05.012
- Magré, J., Delépine, M., Khallouf, E., Gedde-Dahl, T., Van Maldergem, L., Sobel, E., ... Capeau, J. (2001). Identification of the gene altered in Berardinelli-Seip congenital lipodystrophy on chromosome 11q13. *Nature Genetics*, *28*(4), 365–370. doi:10.1038/ng585
- Manders, E. M. M., Verbeek, F. J., & Aten, J. A. (1993). Measurement of co-localization of objects in dual-colour confocal images. *Journal of Microscopy*. doi:10.1111/j.1365-2818.1993.tb03313.x
- Mast, F. D., Jamakhandi, A., Saleem, R. A., Dilworth, D. J., Rogers, R. S., Rachubinski, R. A., & Aitchison, J. D. (2016). Peroxis Pex30 and Pex29 Dynamically Associate with Reticulons to Regulate Peroxisome Biogenesis from the. *The Journal of Biological Chemistry*, *291*(30), 15408–15427. doi:10.1074/jbc.M116.728154
- McNally, E. (2012). Novel Targets and Approaches to Treating Skeletal Muscle Disease. *Muscle*, 1095–1103. doi:10.1016/B978-0-12-381510-1.00081-8
- Miller, J. E., Zhang, L., Jiang, H., Li, Y., & Pugh, B. F. (2018). Genome-Wide Mapping of Decay Factor – mRNA Interactions in Yeast Identifies Nutrient-Responsive Transcripts as Targets of the Deadenylase Ccr4. *G3: Genes - Genomes - Genetics*, *8*(January), 315–330. doi:10.1534/g3.117.300415
- Mishra, S., Khaddaj, R., Cottier, S., Stradalova, V., Jacob, C., & Schneiter, R. (2016). Mature lipid droplets are accessible to ER luminal proteins. *Journal of Cell Science*, *129*(20), 3803–3815. doi:10.1242/jcs.189191
- Nziengui, H., Bouhidel, K., Pillon, D., Der, C., Marty, F., & Schoefs, B. (2007). Reticulon-like proteins in *Arabidopsis thaliana*: Structural organization and ER localization. *FEBS Letters*, *581*(18), 3356–3362. doi:10.1016/j.febslet.2007.06.032

- Oertle, T., Klinger, M., Stuermer, C. A. O., & Schwab, M. E. (2003). A reticular rhapsody: phylogenetic evolution and nomenclature of the RTN/Nogo gene family. *The FASEB Journal*, *17*(10), 1238–1247. doi:10.1096/fj.02-1166hyp
- Olzmann, J. A., Richter, C. M., & Kopito, R. R. (2013). Spatial regulation of UBXD8 and p97/VCP controls ATGL-mediated lipid droplet turnover. *Proceedings of the National Academy of Sciences of the United States of America*, *110*(4), 1345–1350. doi:10.1073/pnas.1213738110
- Onal, G., Kutlu, O., Gozuacik, D., & Emre, S. D. (2017). Lipid Droplets in Health and Disease. *Lipids in Health and Disease*, *16*(128), 1–15. doi:10.1186/s12944-017-0521-7
- Pagac, M., Cooper, D. E., Qi, Y., Lukmantara, I. E., Mak, H. Y., Wu, Z., ... Yang, H. (2016). SEIPIN regulates lipid droplet expansion and adipocyte development by modulating the activity of glycerol-3-phosphate acyltransferase. *Cell Reports*, *17*(6), 1546–1559. doi:10.1016/j.celrep.2016.10.037
- Patel, P., Harris, R., Geddes, S. M., Strehle, E. M., Watson, J. D., Bashir, R., ... Keep, N. H. (2008). Solution Structure of the Inner DysF Domain of Myoferlin and Implications for Limb Girdle Muscular Dystrophy Type 2B. *Journal of Molecular Biology*, *379*(5), 981–990. doi:10.1016/j.jmb.2008.04.046
- Pinsky, B. a., Kotwaliwale, C. V., Sean, Y., Tatsutani, S. Y., Breed, C. a., & Biggins, S. (2006). Glc7 / Protein Phosphatase 1 Regulatory Subunits Can Oppose the Ipl1 / Aurora Protein Kinase by Redistributing Glc7. *Molecular and Cellular Biology*, *26*(7), 2648–2660. doi:10.1128/MCB.26.7.2648
- Pol, A., Gross, S. P., & Parton, R. G. (2014). Biogenesis of the multifunctional lipid droplet: Lipids, proteins, and sites. *Journal of Cell Biology*, *204*(5), 635–646. doi:10.1083/jcb.201311051
- Ponting, C. P., Mott, R., Bork, P., & Copley, R. R. (2008). Novel protein domains and repeats in *Drosophila melanogaster* : Insights into structure, function, and evolution. *Genome Research*, *11*, 1996–2008. doi:10.1101/gr.198701.single
- Prévost, C., Sharp, M. E., Kory, N., Lin, Q., Voth, G. A., Farese, R. V., & Walther, T. C. (2018). Mechanism and Determinants of Amphipathic Helix-Containing Protein Targeting to Lipid Droplets. *Developmental Cell*, *44*(1), 73–86.e4. doi:10.1016/j.devcel.2017.12.011
- Rambold, A. S., Cohen, S., & Lippincott-Schwartz, J. (2015). Fatty acid trafficking in starved cells: Regulation by lipid droplet lipolysis, autophagy, and mitochondrial fusion dynamics. *Developmental Cell*, *32*(6), 678–692. doi:10.1016/j.devcel.2015.01.029

- Rigsby, R. E., & Parker, A. B. (2016). Using the PyMOL application to reinforce visual understanding of protein structure. *Biochemistry and Molecular Biology Education*, *44*(5), 433–437. doi:10.1002/bmb.20966
- Rowe, E. R., Mimmack, M. L., Barbosa, A. D., Haider, A., Isaac, I., Ouberai, M. M., ... Savage, D. B. (2016). Conserved amphipathic helices mediate lipid droplet targeting of perilipins 1-3. *Journal of Biological Chemistry*, *291*(13), 6664–6678. doi:10.1074/jbc.M115.691048
- Salo, V. T., Belevich, I., Li, S., Karhinen, L., Vihinen, H., Vigouroux, C., ... Ikonen, E. (2016). Seipin regulates ER-lipid droplet contacts and cargo delivery. *The EMBO Journal*, *35*(24), e201695170. doi:10.15252/embj.201695170
- Salo, V. T., Belevich, I., Li, S., Karhinen, L., Vihinen, H., Vigouroux, C., ... Ikonen, E. (2016). Seipin regulates ER–lipid droplet contacts and cargo delivery. *The EMBO Journal*. doi:10.15252/embj.201695170
- Sandager, L., Gustavsson, M. H., Ståhl, U., Dahlqvist, A., Wiberg, E., Banas, A., ... Stymne, S. (2002). Storage lipid synthesis is non-essential in yeast. *Journal of Biological Chemistry*, *277*(8), 6478–6482. doi:10.1074/jbc.M109109200
- Schrader, M. (2001). Tubulo-reticular clusters of peroxisomes in living COS-7 cells: Dynamic behavior and association with lipid droplets. *The Journal of Histochemistry and Cytochemistry*, *49*(11), 1421–1429. doi:10.1177/002215540104901110
- Schrul, B., & Kopito, R. R. (2016). Peroxin-dependent targeting of a lipid-droplet-destined membrane protein to ER subdomains. *Nature Cell Biology*, *18*(7), 740–751. doi:10.1038/ncb3373
- Shibata, Y., Shemesh, T., Prinz, W. A., Palazzo, A. F., Kozlov, M. M., & Rapoport, T. A. (2010). Mechanisms determining the morphology of the peripheral ER. *Cell*, *143*(5), 774–788. doi:10.1016/j.cell.2010.11.007
- Shibata, Y., Voss, C., Rist, J. M., Hu, J., Rapoport, T. A., Prinz, W. A., & Voeltz, G. K. (2008). The reticulon and Dp1/Yop1p proteins form immobile oligomers in the tubular endoplasmic reticulum. *Journal of Biological Chemistry*, *283*(27), 18892–18904. doi:10.1074/jbc.M800986200
- Shin, O. H., Hau, W., Wang, Y., & Südhof, T. C. (2005). Evolutionarily conserved multiple C2 domain proteins with two transmembrane regions (MCTPs) and unusual Ca²⁺ binding properties. *Journal of Biological Chemistry*, *280*(2), 1641–1651. doi:10.1074/jbc.M407305200

- Shockey, J. M. (2006). Tung tree DGAT1 and DGAT2 have nonredundant functions in triacylglycerol biosynthesis and are localized to different subdomains of the endoplasmic reticulum. *The Plant Cell*, *18*(9), 2294–2313. doi:10.1105/tpc.106.043695
- Sim, M. F. M., Dennis, R. J., Aubry, E. M., Ramanathan, N., Sembongi, H., Saudek, V., ... Rochford, J. J. (2013). The human lipodystrophy protein seipin is an ER membrane adaptor for the adipogenic PA phosphatase lipin 1. *Molecular Metabolism*, *2*(1), 38–46. doi:10.1016/j.molmet.2012.11.002
- Sim, M. F. M., Talukder, M. M. U., Dennis, R. J., O’Rahilly, S., Edwardson, J. M., & Rochford, J. J. (2013). Analysis of naturally occurring mutations in the human lipodystrophy protein seipin reveals multiple potential pathogenic mechanisms. *Diabetologia*, *56*(11), 2498–2506. doi:10.1007/s00125-013-3029-3
- Smith, J. J., & Aitchison, J. D. (2013). Peroxisomes take shape. *Nature Reviews Molecular Cell Biology*, *14*(12), 803–817. doi:10.1038/nrm3700
- Sorger, D. (2002). Synthesis of triacylglycerols by the acyl-coenzyme A: Diacyl-glycerol acyltransferase Dga1p in lipid particles of the yeast *Saccharomyces cerevisiae*. *Journal of Bacteriology*, *184*(2), 519–524. doi:10.1128/JB.184.2.519
- Stevanovic, A., & Thiele, C. (2013). Monotopic topology is required for lipid droplet targeting of ancient ubiquitous protein 1. *Journal of Lipid Research*, *54*, 503–513. doi:10.1194/jlr.M033852
- Stone, S. J., Levin, M. C., Zhou, P., Han, J., Walther, T. C., & Farese, R. V. (2009). The endoplasmic reticulum enzyme DGAT2 is found in mitochondria-associated membranes and has a mitochondrial targeting signal that promotes its association with mitochondria. *Journal of Biological Chemistry*, *284*(8), 5352–5361. doi:10.1074/jbc.M805768200
- Stone, S. J., Myers, H. M., Watkins, S. M., Brown, B. E., Feingold, K. R., Elias, P. M., & Farese, R. V. (2004). Lipopenia and skin barrier abnormalities in DGAT2-deficient mice. *Journal of Biological Chemistry*, *279*(12), 11767–11776. doi:10.1074/jbc.M311000200
- Sui, X., Artl, H., Brook, K. P., Lai, Z. W., DiMaio, F., Marks, D. S., ... Walther, T. C. (2018). Cryo-electron microscopy structure of the lipid droplet-formation protein seipin. *Journal of Cell Biology*. doi:10.1101/418236
- Sula, A., Cole, A. R., Yeats, C., Orengo, C., & Keep, N. H. (2014). Crystal structures of the human Dysferlin inner DysF domain. *BMC Structural Biology*, *14*(1), 1–9. doi:10.1186/1472-6807-14-3

- Sztalryd, C., & Brasaemle, D. L. (2017). The perilipin family of lipid droplet proteins: Gatekeepers of intracellular lipolysis. *BBA - Molecular and Cell Biology of Lipids*, *1862*(10), 1221–1232. doi:10.1016/j.bbalip.2017.07.009
- Szymanski, K. M., Binns, D., Bartz, R., Grishin, N. V, Li, W.-P., Agarwal, A. K., ... Goodman, J. M. (2007). The lipodystrophy protein seipin is found at endoplasmic reticulum lipid droplet junctions and is important for droplet morphology. *Proceedings of the National Academy of Sciences of the United States of America*, *104*(52), 20890–20895. doi:10.1073/pnas.0704154104
- Talukder, M. M. U., Sim, M. F. M., O'Rahilly, S., Edwardson, J. M., & Rochford, J. J. (2015). Seipin oligomers can interact directly with AGPAT2 and lipin 1, physically scaffolding critical regulators of adipogenesis. *Molecular Metabolism*, *4*(3), 199–209. doi:10.1016/j.molmet.2014.12.013
- Tam, Y. Y. C., Rachubinski, R. A., & Gene, P. E. X. (2002). Yarrowia lipolytica Cells Mutant for the PEX24 Gene Encoding a Peroxisomal Membrane Peroxin Mislocalize Peroxisomal Proteins and Accumulate Membrane Structures Containing Both Peroxisomal Matrix and Membrane Proteins, *13*(August), 2681–2691. doi:10.1091/mbc.E02
- Tang, T., Abbott, M. J., Ahmadian, M., Lopes, A. B., Wang, Y., & Sul, H. S. (2013). Desnutrin/ATGL activates PPAR δ to promote mitochondrial function for insulin secretion in islet β cells. *Cell Metabolism*, *18*(6), 883–895. doi:10.1016/j.cmet.2013.10.012
- Tauchi-Sato, K., Ozeki, S., Houjou, T., Taguchi, R., & Fujimoto, T. (2002). The surface of lipid droplets is a phospholipid monolayer with a unique fatty acid composition. *Journal of Biological Chemistry*, *277*(46), 44507–44512. doi:10.1074/jbc.M207712200
- Therrien, C., Fulvio, S. Di, Pickles, S., & Sinnreich, M. (2009). Characterization of lipid binding specificities of dysferlin C2 domains reveals novel interactions with phosphoinositides. *Biochemistry*, *48*(11), 2377–2384. doi:10.1021/bi802242r
- Thiam, A. R., Farese Jr, R. V, & Walther, T. C. (2013). The Biophysics and cell biology of lipid droplets. *Nature Reviews Molecular Cell Biology*, *14*(12), 775–786. doi:10.1002/aur.1474.Replication
- Thiam, A. R., & Forêt, L. (2016). The physics of lipid droplet nucleation, growth and budding. *Biochimica et Biophysica Acta - Molecular and Cell Biology of Lipids*, *1861*(8), 715–722. doi:10.1016/j.bbalip.2016.04.018
- Thiele, C., & Spandl, J. (2008). Cell biology of lipid droplets, 378–385.

doi:10.1016/j.ceb.2008.05.009

- Tian, Y., Bi, J., Shui, G., Liu, Z., Xiang, Y., Liu, Y., ... Huang, X. (2011). Tissue-autonomous function of drosophila seipin in preventing ectopic lipid droplet formation. *PLoS Genetics*, *7*(4), e1001364. doi:10.1371/journal.pgen.1001364
- Vizeacoumar, F. J., Torres-Guzman, J. C., Bouard, D., Aitchison, J. D., & Rachubinski, R. A. (2004). Pex30p, Pex31p, and Pex32p Form a Family of Peroxisomal Integral Membrane Proteins Regulating Peroxisome Size and Number in *Saccharomyces cerevisiae*. *Molecular Biology*, *15*(February), 665–677. doi:10.1091/mbc.E03
- Vizeacoumar, F. J., Torres-guzman, J. C., Tam, Y. Y. C., Aitchison, J. D., & Rachubinski, R. A. (2003). YHR150w and YDR479c encode peroxisomal integral membrane proteins involved in the regulation of peroxisome number, size, and distribution in *Saccharomyces cerevisiae*. *The Journal of Cell Biology*, *161*(2), 321–332. doi:10.1083/jcb.200210130
- Vizeacoumar, F. J., Vreden, W. N., Aitchison, J. D., & Rachubinski, R. A. (2006). Pex19p Binds Pex30p and Pex32p at Regions Required for Their Peroxisomal Localization but Separate from Their Peroxisomal Targeting Signals *, *281*(21), 14805–14812. doi:10.1074/jbc.M601808200
- Voeltz, G. K., Prinz, W. A., Shibata, Y., Rist, J. M., & Rapoport, T. A. (2006a). A class of membrane proteins shaping the tubular endoplasmic reticulum. *Cell*, *124*(3), 573–586. doi:10.1016/j.cell.2005.11.047
- Voeltz, G. K., Prinz, W. A., Shibata, Y., Rist, J. M., & Rapoport, T. A. (2006b). A Class of Membrane Proteins Shaping the Tubular Endoplasmic Reticulum (Erratum). *Cell*, *124*, 573–586. doi:10.1016/j.cell.2007.08.004
- Wältermann, M., Hinz, A., Robenek, H., Troyer, D., Reichelt, R., Malkus, U., ... Steinbüchel, A. (2005). Mechanism of lipid-body formation in prokaryotes: How bacteria fatten up. *Molecular Microbiology*, *55*(3), 750–763. doi:10.1111/j.1365-2958.2004.04441.x
- Walther, T. C., & Farese Jr, R. V. (2012). Lipid droplets and cellular lipid metabolism. *Annual Review of Biochemistry*, *81*, 687–714. doi:10.1146/annurev-biochem-061009-102430
- Wang, C.-W., Miao, Y.-H., & Chang, Y.-S. (2014). Control of lipid droplet size in budding yeast requires the collaboration between Fld1 and Ldb16. *Journal of Cell Science*, *127*(Pt 6), 1214–1228. doi:10.1242/jcs.137737
- Wang, H., Becuwe, M., Housden, B. E., Chitraju, C., Porras, A. J., Graham, M. M., ... Farese Jr, R. V. (2016). Seipin is required for converting nascent to mature lipid droplets. *ELife*, *5*, e16582.

doi:10.7554/eLife.16582

- Wang, S., Idrissi, F.-Z., Hermansson, M., Grippa, A., Ejsing, C. S., & Carvalho, P. (2018). Seipin and the membrane shaping protein Pex30 cooperate in organelle budding from the endoplasmic reticulum. *Nature Communications*.
- Waterhouse, A., Bertoni, M., Bienert, S., Studer, G., Tauriello, G., Gumienny, R., ... Schwede, T. (2018). SWISS-MODEL: Homology modelling of protein structures and complexes. *Nucleic Acids Research*, *46*(W1), W296–W303. doi:10.1093/nar/gky427
- Wee, K., Yang, W., Sugii, S., & Han, W. (2014). Towards a mechanistic understanding of lipodystrophy and seipin functions. *Bioscience Reports*, *34*(5), 583–591. doi:10.1042/BSR20140114
- Welte, M. A. (2015). Expanding roles for lipid droplets. *Current Biology*, *25*(11), R470–R481. doi:10.1016/j.cub.2015.04.004
- Welte, M. A., & Gould, A. P. (2017). Lipid droplet functions beyond energy storage. *BBA - Molecular and Cell Biology of Lipids*, *1862*(May), 1260–1272. doi:10.1016/j.bbalip.2017.07.006
- Wenyan Jiang, David Bikard, David Cox, Feng Zhang, L. A. M. (2013). CRISPR-assisted editing of bacterial genomes. *Nat Biotechnol*, *31*(3), 233–239. doi:10.1038/nbt.2508.CRISPR-assisted
- Wilfling, F., Wang, H., Haas, J. T., Krahmer, N., Gould, T. J., Uchida, A., ... Walther, T. C. (2013). Triacylglycerol synthesis enzymes mediate lipid droplet growth by relocalizing from the ER to lipid droplets. *Developmental Cell*, *24*(4), 384–399. doi:10.1016/j.devcel.2013.01.013
- Wolinski, H., Hofbauer, H. F., Hellauer, K., Cristobal-Sarramian, A., Kolb, D., Radulovic, M., ... Kohlwein, S. D. (2015). Seipin is involved in the regulation of phosphatidic acid metabolism at a subdomain of the nuclear envelope in yeast. *Biochimica et Biophysica Acta - Molecular and Cell Biology of Lipids*, *1851*(11), 1450–1464. doi:10.1016/j.bbalip.2015.08.003
- Wolinski, H., Kolb, D., Hermann, S., Koning, R. I., & Kohlwein, S. D. (2011). A role for seipin in lipid droplet dynamics and inheritance in yeast. *Journal of Cell Science*, *124*(22), 3894–3904. doi:10.1242/jcs.091454
- Wolinski, H., Kolb, D., Hermann, S., Koning, R. I., & Kohlwein, S. D. (2011). A role for seipin in lipid droplet dynamics and inheritance in yeast. *Journal of Cell Science*, *124*(22), 3894–3904. doi:10.1242/jcs.091454
- Xu, S., Benoff, B., Liou, H.-L., Lobel, E., & Stock, A. M. (2007). Lysosomal Protein Deficient in Niemann-Pick Type C2. *J Biol Chem*, *282*(32), 23525–23531.

doi:10.1074/jbc.M703848200.STRUCTURAL

- Xu, S., Zhang, X., & Liu, P. (2017). Lipid droplet proteins and metabolic diseases. *Biochimica et Biophysica Acta - Molecular Basis of Disease*, 1864(5 Pt B), 1968–1983. doi:10.1016/j.bbadis.2017.07.019
- Yan, M., Rachubinski, D. A., Joshi, S., Rachubinski, R. A., & Subramani, S. (2008). Dysferlin domain-containing proteins, Pex30p and Pex31p, localized to two compartments, control the number and size of oleate-induced peroxisomes in *Pichia pastoris*. *Molecular Biology of the Cell*, 19(March), 885–898. doi:10.1091/mbc.E07
- Yan, R., Shi, Q., Hu, X., & Zhou, X. (2006). Reticulon proteins: Emerging players in neurodegenerative diseases. *Cellular and Molecular Life Sciences*, 63(7–8), 877–889. doi:10.1007/s00018-005-5338-2
- Yang, L., Ding, Y., Chen, Y., Zhang, S., Huo, C., Wang, Y., ... Liu, P. (2012). The proteomics of lipid droplets: Structure, dynamics, and functions of the organelle conserved from bacteria to humans. *Journal of Lipid Research*, 53(7), 1245–1253. doi:10.1194/jlr.R024117
- Yen, C.-L. E., Stone, S. J., Koliwad, S., Harris, C., & Farese, R. V. (2008). DGAT enzymes and triacylglycerol biosynthesis. *Journal of Lipid Research*, 49(11), 2283–2301. doi:10.1194/jlr.R800018-JLR200
- Zehmer, J. K., Bartz, R., Bisel, B., Liu, P., Seemann, J., & Anderson, R. G. W. (2009). Targeting sequences of UBXD8 and AAM-B reveal that the ER has a direct role in the emergence and regression of lipid droplets. *Journal of Cell Science*, 122(Pt 20), 3694–702. doi:10.1242/jcs.054700
- Zweytick, D., Leitner, E., Kohlwein, S. D., Yu, C., Rothblatt, J., & Daum, È. (2000). Contribution of Are1p and Are2p to sterol ester synthesis in the yeast *Saccharomyces cerevisiae*. *European Journal of Biochemistry*, 1082(4), 1075–1082.

6. Supplemental material

Table S1. Yeast strains used in this study.

Strain	Genotype	Origin
yPC1505	Mat a <i>ura3Δ0 his3Δ1 leu2Δ0 met15Δ0</i>	BY4741
yPC8808	Mat a <i>ura3Δ0 his3Δ1 leu2Δ0 met15Δ0 pex30::KANR</i>	Carvalho's lab
yPC8849	Mat a <i>ura3Δ0 his3Δ1 leu2Δ0 met15Δ0 pex30::KANR fld1::NAT</i>	Carvalho's lab
yPC8851	Mat a <i>ura3Δ0 his3Δ1 leu2Δ0 met15Δ0 pex30::KANR ldb16::HYGB</i>	Carvalho's lab
yPC10657	Mat a <i>ura3Δ0 his3Δ1 leu2Δ0 met15Δ0 Pex30-mNG-HIS</i>	Wang et al, 2018
yPC10676	Mat ? <i>ura3Δ0 his3Δ1 leu2Δ0 met15Δ0 Pex30-mNG-HIS fld1::NAT</i>	Wang et al, 2018
yPC10678	Mat ? <i>ura3Δ0 his3Δ1 leu2Δ0 met15Δ0 Pex30-mNG-HIS ldb16::HYGB</i>	Wang et al, 2018
yPC10782	Mat a <i>ura3Δ0 his3Δ1 leu2Δ0 met15Δ0 Pex30-tdTomato-HIS</i>	Wang et al, 2018
yPC10783	Mat a <i>ura3Δ0 his3Δ1 leu2Δ0 met15Δ0 Pex30-tdTomato-HIS fld1::KANR</i>	Wang et al, 2018
yPC10784	Mat a <i>ura3Δ0 his3Δ1 leu2Δ0 met15Δ0 Pex30-tdTomato-HIS ldb16::KANR</i>	Wang et al, 2018
yPC11183	Mat x <i>ura3Δ0 his3Δ1 leu2Δ0 met15Δ0 Pex30-mNG-HIS pex29::KAN</i>	Carvalho's lab
yPC11184	Mat x <i>ura3Δ0 his3Δ1 leu2Δ0 met15Δ0 Pex30-mNG-HIS pex31::KAN</i>	Carvalho's lab
yPC11185	Mat x <i>ura3Δ0 his3Δ1 leu2Δ0 met15Δ0 Pex30-mNG-HIS pex32::KAN</i>	Carvalho's lab
yPC11211	Mat ? <i>ura3Δ0 his3Δ1 leu2Δ0 met15Δ0 Pex30-mNG-HIS pex28::KAN</i>	Carvalho's lab
yPC11212	Mat ? <i>ura3Δ0 his3Δ1 leu2Δ0 met15Δ0 Pex30-mNG-HIS fld1::NAT pex29::KAN</i>	Carvalho's lab
yPC11213	Mat ? <i>ura3Δ0 his3Δ1 leu2Δ0 met15Δ0 Pex30-mNG-HIS fld1::NAT pex31::KAN</i>	Carvalho's lab
yPC11214	Mat ? <i>ura3Δ0 his3Δ1 leu2Δ0 met15Δ0 Pex30-mNG-HIS fld1::NAT pex32::KAN</i>	Carvalho's lab
yPC11311	Mat a <i>ura3Δ0 his3Δ1 leu2Δ0 met15Δ0 Pex30(Δ60-523)-mNG-KANR</i>	This study
yPC11312	Mat a <i>ura3Δ0 his3Δ1 leu2Δ0 met15Δ0 Pex30(Δ284-523)-mNG-KANR</i>	This study
yPC11313	Mat a <i>ura3Δ0 his3Δ1 leu2Δ0 met15Δ0 Pex30(Δ235-523)-mNG-KANR</i>	This study
yPC11314	Mat a <i>ura3Δ0 his3Δ1 leu2Δ0 met15Δ0 Pex30(Δ410-523)-mNG-KANR</i>	This study
yPC11315	Mat a <i>ura3Δ0 his3Δ1 leu2Δ0 met15Δ0 Pex30(Δ351-523)-mNG-KANR</i>	This study
yPC11316	Mat ? <i>ura3Δ0 his3Δ1 leu2Δ0 met15Δ0 Pex30(Δ60-523)-mNG-KANR fld1::NAT ldb16::HYGB</i>	This study
yPC11317	Mat ? <i>ura3Δ0 his3Δ1 leu2Δ0 met15Δ0 Pex30(Δ60-523)-mNG-KANR fld1::NAT</i>	This study
yPC11318	Mat ? <i>ura3Δ0 his3Δ1 leu2Δ0 met15Δ0 Pex30(Δ60-523)-mNG-KANR ldb16::HYGB</i>	This study
yPC11319	Mat ? <i>ura3Δ0 his3Δ1 leu2Δ0 met15Δ0 Pex30(Δ284-523)-mNG-KANR fld1::NAT ldb16::HYGB</i>	This study
yPC11320	Mat ? <i>ura3Δ0 his3Δ1 leu2Δ0 met15Δ0 Pex30(Δ284-523)-mNG-KANR fld1::NAT</i>	This study
yPC11321	Mat ? <i>ura3Δ0 his3Δ1 leu2Δ0 met15Δ0 Pex30(Δ284-523)-mNG-KANR ldb16::HYGB</i>	This study

yPC11322	Mat ?	<i>ura3Δ0 his3Δ1 leu2Δ0 met15Δ0 Pex30(Δ235-523)-mNG-KANR fld1::NAT ldb16::HYGB</i>	This study
yPC11323	Mat ?	<i>ura3Δ0 his3Δ1 leu2Δ0 met15Δ0 Pex30(Δ235-523)-mNG-KANR fld1::NAT</i>	This study
yPC11324	Mat ?	<i>ura3Δ0 his3Δ1 leu2Δ0 met15Δ0 Pex30(Δ235-523)-mNG-KANR ldb16::HYGB</i>	This study
yPC11325	Mat ?	<i>ura3Δ0 his3Δ1 leu2Δ0 met15Δ0 Pex30(Δ410-523)-mNG-KANR fld1::NAT ldb16::HYGB</i>	This study
yPC11326	Mat ?	<i>ura3Δ0 his3Δ1 leu2Δ0 met15Δ0 Pex30(Δ410-523)-mNG-KANR fld1::NAT</i>	This study
yPC11327	Mat ?	<i>ura3Δ0 his3Δ1 leu2Δ0 met15Δ0 Pex30(Δ410-523)-mNG-KANR ldb16::HYGB</i>	This study
yPC11328	Mat a	<i>ura3Δ0 his3Δ1 leu2Δ0 met15Δ0 Pex30(Δ351-523)-mNG-KANR fld1::</i>	This study
yPC11329	Mat a	<i>ura3Δ0 his3Δ1 leu2Δ0 met15Δ0 Pex30(Δ351-523)-mNG-KANR ldb16::</i>	This study
yPC11330	Mat a	<i>ura3Δ0 his3Δ1 leu2Δ0 met15Δ0 Pex30(Δ351-523)-mNG-KANR fld1:: ldb16::</i>	This study
yPC11331	Mat a	<i>ura3Δ0 his3Δ1 leu2Δ0 met15Δ0 Pex28-tdTomato-HIS</i>	This study
yPC11332	Mat a	<i>ura3Δ0 his3Δ1 leu2Δ0 met15Δ0 Pex29-tdTomato-HIS</i>	This study
yPC11333	Mat a	<i>ura3Δ0 his3Δ1 leu2Δ0 met15Δ0 Pex31-tdTomato-HIS</i>	This study
yPC11334	Mat a	<i>ura3Δ0 his3Δ1 leu2Δ0 met15Δ0 Pex32-tdTomato-HIS</i>	This study
yPC11335	Mat a	<i>ura3Δ0 his3Δ1 leu2Δ0 met15Δ0 Pex28(Δ461-580)-tdTomato-HIS</i>	This study
yPC11336	Mat a	<i>ura3Δ0 his3Δ1 leu2Δ0 met15Δ0 Pex29(Δ346-555)-tdTomato-HIS</i>	This study
yPC11337	Mat a	<i>ura3Δ0 his3Δ1 leu2Δ0 met15Δ0 Pex30(Δ278-523)-tdTomato-HIS</i>	This study
yPC11338	Mat a	<i>ura3Δ0 his3Δ1 leu2Δ0 met15Δ0 Pex31(Δ279-463)-tdTomato-HIS</i>	This study
yPC11339	Mat a	<i>ura3Δ0 his3Δ1 leu2Δ0 met15Δ0 Pex32(Δ301-414)-tdTomato-HIS</i>	This study
yPC11340	Mat a	<i>ura3Δ0 his3Δ1 leu2Δ0 met15Δ0 Pex28-tdTomato-HIS fld1::</i>	This study
yPC11341	Mat a	<i>ura3Δ0 his3Δ1 leu2Δ0 met15Δ0 Pex29-tdTomato-HIS fld1::</i>	This study
yPC11342	Mat a	<i>ura3Δ0 his3Δ1 leu2Δ0 met15Δ0 Pex30-tdTomato-HIS fld1::</i>	This study
yPC11343	Mat a	<i>ura3Δ0 his3Δ1 leu2Δ0 met15Δ0 Pex31-tdTomato-HIS fld1::</i>	This study
yPC11344	Mat a	<i>ura3Δ0 his3Δ1 leu2Δ0 met15Δ0 Pex32-tdTomato-HIS fld1::</i>	This study
yPC11345	Mat a	<i>ura3Δ0 his3Δ1 leu2Δ0 met15Δ0 Pex28(Δ461-580)-tdTomato-HIS fld1::</i>	This study
yPC11346	Mat a	<i>ura3Δ0 his3Δ1 leu2Δ0 met15Δ0 Pex29(Δ346-555)-tdTomato-HIS fld1::</i>	This study
yPC11347	Mat a	<i>ura3Δ0 his3Δ1 leu2Δ0 met15Δ0 Pex30(Δ278-523)-tdTomato-HIS fld1::</i>	This study
yPC11348	Mat a	<i>ura3Δ0 his3Δ1 leu2Δ0 met15Δ0 Pex31(Δ279-463)-tdTomato-HIS fld1::</i>	This study
yPC11349	Mat a	<i>ura3Δ0 his3Δ1 leu2Δ0 met15Δ0 Pex32(Δ301-414)-tdTomato-HIS fld1::</i>	This study
yPC11350	Mat a	<i>ura3Δ0 his3Δ1 leu2Δ0 met15Δ0 Pex28-tdTomato-HIS ldb16::</i>	This study
yPC11351	Mat a	<i>ura3Δ0 his3Δ1 leu2Δ0 met15Δ0 Pex29-tdTomato-HIS ldb16::</i>	This study
yPC11352	Mat a	<i>ura3Δ0 his3Δ1 leu2Δ0 met15Δ0 Pex30-tdTomato-HIS ldb16::</i>	This study
yPC11353	Mat a	<i>ura3Δ0 his3Δ1 leu2Δ0 met15Δ0 Pex31-tdTomato-HIS ldb16::</i>	This study
yPC11354	Mat a	<i>ura3Δ0 his3Δ1 leu2Δ0 met15Δ0 Pex32-tdTomato-HIS ldb16::</i>	This study
yPC11355	Mat a	<i>ura3Δ0 his3Δ1 leu2Δ0 met15Δ0 Pex28(Δ461-580)-tdTomato-HIS ldb16::</i>	This study
yPC11356	Mat a	<i>ura3Δ0 his3Δ1 leu2Δ0 met15Δ0 Pex29(Δ346-555)-tdTomato-HIS ldb16::</i>	This study
yPC11357	Mat a	<i>ura3Δ0 his3Δ1 leu2Δ0 met15Δ0 Pex30(Δ278-523)-tdTomato-HIS ldb16::</i>	This study

yPC11358	Mat a	<i>ura3Δ0 his3Δ1 leu2Δ0 met15Δ0</i> Pex31(Δ279-463)-tdTomato-HIS <i>ldb16::</i>	This study
yPC11359	Mat a	<i>ura3Δ0 his3Δ1 leu2Δ0 met15Δ0</i> Pex32(Δ301-414)-tdTomato-HIS <i>ldb16::</i>	This study
yPC11363	Mat a	<i>ura3Δ0 his3Δ1 leu2Δ0 met15Δ0</i> Pex30(Δ248-408::)-tdTomato-HIS	This study
yPC11364	Mat a	<i>ura3Δ0 his3Δ1 leu2Δ0 met15Δ0</i> Pex30(Δ248-408::)-tdTomato-HIS <i>fld1::KANR</i>	This study
yPC11365	Mat a	<i>ura3Δ0 his3Δ1 leu2Δ0 met15Δ0</i> Pex30(Δ248-408::)-tdTomato-HIS <i>ldb16::KANR</i>	This study
yPC11366	Mat a	<i>ura3Δ0 his3Δ1 leu2Δ0 met15Δ0</i> Pex30(Δ248-408 + Pex28 467-573)-tdTomato-HIS <i>fld1::KANR</i>	This study
yPC11367	Mat a	<i>ura3Δ0 his3Δ1 leu2Δ0 met15Δ0</i> Pex30(Δ248-408 + Pex29 351-470)-tdTomato-HIS <i>ldb16::KANR</i>	This study
yPC11368	Mat a	<i>ura3Δ0 his3Δ1 leu2Δ0 met15Δ0</i> Pex30(Δ248-408 + Pex31 284-408)-tdTomato-HIS <i>fld1::KANR</i>	This study
yPC11369	Mat a	<i>ura3Δ0 his3Δ1 leu2Δ0 met15Δ0</i> Pex30(Δ248-408 + Pex32 307-413)-tdTomato-HIS <i>ldb16::KANR</i>	This study
yPC11370	Mat a	<i>ura3Δ0 his3Δ1 leu2Δ0 met15Δ0</i> Pex30(Δ248-408 + Pex28 467-573)-tdTomato-HIS <i>fld1::KANR</i>	This study
yPC11371	Mat a	<i>ura3Δ0 his3Δ1 leu2Δ0 met15Δ0</i> Pex30(Δ248-408 + Pex28 467-573)-tdTomato-HIS <i>ldb16::KANR</i>	This study
yPC11372	Mat a	<i>ura3Δ0 his3Δ1 leu2Δ0 met15Δ0</i> Pex30(Δ248-408 + Pex29 351-470)-tdTomato-HIS <i>fld1::KANR</i>	This study
yPC11373	Mat a	<i>ura3Δ0 his3Δ1 leu2Δ0 met15Δ0</i> Pex30(Δ248-408 + Pex29 351-470)-tdTomato-HIS <i>ldb16::KANR</i>	This study
yPC11374	Mat a	<i>ura3Δ0 his3Δ1 leu2Δ0 met15Δ0</i> Pex30(Δ248-408 + Pex31 284-408)-tdTomato-HIS <i>fld1::KANR</i>	This study
yPC11375	Mat a	<i>ura3Δ0 his3Δ1 leu2Δ0 met15Δ0</i> Pex30(Δ248-408 + Pex31 284-408)-tdTomato-HIS <i>ldb16::KANR</i>	This study
yPC11376	Mat a	<i>ura3Δ0 his3Δ1 leu2Δ0 met15Δ0</i> Pex30(Δ248-408 + Pex32 307-413)-tdTomato-HIS <i>fld1::KANR</i>	This study
yPC11377	Mat a	<i>ura3Δ0 his3Δ1 leu2Δ0 met15Δ0</i> Pex30(Δ248-408 + Pex32 307-413)-tdTomato-HIS <i>ldb16::KANR</i>	This study
yPC11390	Mat a	<i>ura3Δ0 his3Δ1 leu2Δ0 met15Δ0</i> Pex30(Δ86-219::)-tdTomato-HIS	This study
yPC11391	Mat a	<i>ura3Δ0 his3Δ1 leu2Δ0 met15Δ0</i> Pex30(Δ86-219::)-tdTomato-HIS <i>fld1::KANR</i>	This study
yPC11392	Mat a	<i>ura3Δ0 his3Δ1 leu2Δ0 met15Δ0</i> Pex30(Δ86-219::)-tdTomato-HIS <i>ldb16::KANR</i>	This study
yPC11393	Mat a	<i>ura3Δ0 his3Δ1 leu2Δ0 met15Δ0</i> Pex30(W94C)-tdTomato-HIS	This study
yPC11394	Mat a	<i>ura3Δ0 his3Δ1 leu2Δ0 met15Δ0</i> Pex30(W94C)-tdTomato-HIS <i>fld1::KANR</i>	This study
yPC11395	Mat a	<i>ura3Δ0 his3Δ1 leu2Δ0 met15Δ0</i> Pex30(W94C)-tdTomato-HIS <i>ldb16::KANR</i>	This study
yPC11396	Mat a	<i>ura3Δ0 his3Δ1 leu2Δ0 met15Δ0</i> Pex30(W401C)-tdTomato-HIS	This study
yPC11397	Mat a	<i>ura3Δ0 his3Δ1 leu2Δ0 met15Δ0</i> Pex30(W401C)-tdTomato-HIS <i>fld1::KANR</i>	This study
yPC11398	Mat a	<i>ura3Δ0 his3Δ1 leu2Δ0 met15Δ0</i> Pex30(W401C)-tdTomato-HIS <i>ldb16::KANR</i>	This study

yPC11419	Mat a	<i>ura3Δ0 his3Δ1 leu2Δ0 met15Δ0</i> NAT-GPDpr-3HA-Pex28 <i>pex30::KANR</i>	This study
yPC11420	Mat a	<i>ura3Δ0 his3Δ1 leu2Δ0 met15Δ0</i> NAT-GPDpr-3HA-Pex29 <i>pex30::KANR</i>	This study
yPC11421	Mat a	<i>ura3Δ0 his3Δ1 leu2Δ0 met15Δ0</i> NAT-GPDpr-3HA-Pex31 <i>pex30::KANR</i>	This study
yPC11422	Mat a	<i>ura3Δ0 his3Δ1 leu2Δ0 met15Δ0</i> NAT-GPDpr-3HA-Pex32 <i>pex30::KANR</i>	This study
yPC11423	Mat ?	<i>ura3Δ0 his3Δ1 leu2Δ0 met15Δ0</i> NAT-GPDpr-3HA-Pex28	This study
yPC11424	Mat ?	<i>ura3Δ0 his3Δ1 leu2Δ0 met15Δ0</i> NAT-GPDpr-3HA-Pex28 <i>fld1::HIS</i>	This study
yPC11425	Mat ?	<i>ura3Δ0 his3Δ1 leu2Δ0 met15Δ0</i> NAT-GPDpr-3HA-Pex28 <i>ldb16::HYGB</i>	This study
yPC11427	Mat ?	<i>ura3Δ0 his3Δ1 leu2Δ0 met15Δ0</i> NAT-GPDpr-3HA-Pex28 <i>pex30::KANR fld1::HIS</i>	This study
yPC11428	Mat ?	<i>ura3Δ0 his3Δ1 leu2Δ0 met15Δ0</i> NAT-GPDpr-3HA-Pex28 <i>pex30::KANR</i> <i>ldb16::HYGB</i>	This study
yPC11429	Mat ?	<i>ura3Δ0 his3Δ1 leu2Δ0 met15Δ0</i> NAT-GPDpr-3HA-Pex28 <i>pex30::KANR fld1::HIS</i> <i>ldb16::HYGB</i>	This study
yPC11430	Mat ?	<i>ura3Δ0 his3Δ1 leu2Δ0 met15Δ0</i> NAT-GPDpr-3HA-Pex29	This study
yPC11431	Mat ?	<i>ura3Δ0 his3Δ1 leu2Δ0 met15Δ0</i> NAT-GPDpr-3HA-Pex29 <i>fld1::HIS</i>	This study
yPC11432	Mat ?	<i>ura3Δ0 his3Δ1 leu2Δ0 met15Δ0</i> NAT-GPDpr-3HA-Pex29 <i>ldb16::HYGB</i>	This study
yPC11433	Mat ?	<i>ura3Δ0 his3Δ1 leu2Δ0 met15Δ0</i> NAT-GPDpr-3HA-Pex29 <i>pex30::KANR fld1::HIS</i>	This study
yPC11434	Mat ?	<i>ura3Δ0 his3Δ1 leu2Δ0 met15Δ0</i> NAT-GPDpr-3HA-Pex29 <i>pex30::KANR</i> <i>ldb16::HYGB</i>	This study
yPC11435	Mat ?	<i>ura3Δ0 his3Δ1 leu2Δ0 met15Δ0</i> NAT-GPDpr-3HA-Pex29 <i>pex30::KANR fld1::HIS</i> <i>ldb16::HYGB</i>	This study
yPC11436	Mat a	<i>ura3Δ0 his3Δ1 leu2Δ0 met15Δ0</i> NAT-GPDpr-3HA-Pex31	This study
yPC11440	Mat a	<i>ura3Δ0 his3Δ1 leu2Δ0 met15Δ0</i> NAT-GPDpr-3HA-Pex31 <i>pex30::KANR fld1::</i>	This study
yPC11441	Mat a	<i>ura3Δ0 his3Δ1 leu2Δ0 met15Δ0</i> NAT-GPDpr-3HA-Pex31 <i>pex30::KANR ldb16::</i>	This study
yPC11447	Mat a	<i>ura3Δ0 his3Δ1 leu2Δ0 met15Δ0</i> NAT-GPDpr-3HA-Pex32 <i>pex30::KANR fld1::</i>	This study
yPC11448	Mat a	<i>ura3Δ0 his3Δ1 leu2Δ0 met15Δ0</i> NAT-GPDpr-3HA-Pex32 <i>pex30::KANR ldb16::</i>	This study
yPC11450	Mat a	<i>ura3Δ0 his3Δ1 leu2Δ0 met15Δ0</i> NAT-GPDpr-3HA-Pex30	This study
yPC11451	Mat a	<i>ura3Δ0 his3Δ1 leu2Δ0 met15Δ0</i> NAT-GPDpr-3HA-Pex30 <i>fld1::</i>	This study
yPC11452	Mat a	<i>ura3Δ0 his3Δ1 leu2Δ0 met15Δ0</i> NAT-GPDpr-3HA-Pex30 <i>ldb16::</i>	This study
yPC11453	Mat a	<i>ura3Δ0 his3Δ1 leu2Δ0 met15Δ0</i> Pex30($\Delta 86-219$ + MCTP2 660-849)-tdTomato- HIS	This study
yPC11454	Mat a	<i>ura3Δ0 his3Δ1 leu2Δ0 met15Δ0</i> Pex30($\Delta 86-219$ + MCTP2 660-849)-tdTomato- HIS <i>fld1::KANR</i>	This study
yPC11455	Mat a	<i>ura3Δ0 his3Δ1 leu2Δ0 met15Δ0</i> Pex30($\Delta 86-219$ + MCTP2 660-849)-tdTomato- HIS <i>ldb16::KANR</i>	This study
yPC11456	Mat a	<i>ura3Δ0 his3Δ1 leu2Δ0 met15Δ0</i> Pex30($\Delta 248-408$ + MCTP2 191-321)-tdTomato- HIS	This study
yPC11457	Mat a	<i>ura3Δ0 his3Δ1 leu2Δ0 met15Δ0</i> Pex30($\Delta 248-408$ + MCTP2 191-321)-tdTomato- HIS <i>fld1::KANR</i>	This study

yPC11458	Mat a	<i>ura3Δ0 his3Δ1 leu2Δ0 met15Δ0</i> Pex30(Δ248-408 + MCTP2 191-321)-tdTomato-HIS <i>ldb16::KANR</i>	This study
yPC11459	Mat a	<i>ura3Δ0 his3Δ1 leu2Δ0 met15Δ0</i> Pex30(Δ248-408 + MCTP2 191-634)-tdTomato-HIS	This study
yPC11460	Mat a	<i>ura3Δ0 his3Δ1 leu2Δ0 met15Δ0</i> Pex30(Δ248-408 + MCTP2 191-634)-tdTomato-HIS <i>fld1::KANR</i>	This study
yPC11461	Mat a	<i>ura3Δ0 his3Δ1 leu2Δ0 met15Δ0</i> Pex30(Δ248-408 + MCTP2 191-634)-tdTomato-HIS <i>ldb16::KANR</i>	This study
yPC11468	Mat a	<i>ura3Δ0 his3Δ1 leu2Δ0 met15Δ0</i> Pex30(Δ248-408 + Rtn1 18-160)-tdTomato-HIS	This study
yPC11469	Mat a	<i>ura3Δ0 his3Δ1 leu2Δ0 met15Δ0</i> Pex30(Δ248-408 + Rtn1 18-160)-tdTomato-HIS <i>fld1::KANR</i>	This study
yPC11470	Mat a	<i>ura3Δ0 his3Δ1 leu2Δ0 met15Δ0</i> Pex30(Δ248-408 + Rtn1 18-160)-tdTomato-HIS <i>ldb16::KANR</i>	This study
yPC11471	Mat ?	<i>ura3Δ0 his3Δ1 leu2Δ0 met15Δ0</i> NAT-GPDpr-3HA-Pex29 <i>Pex30-tdTomato</i>	This study
yPC11472	Mat ?	<i>ura3Δ0 his3Δ1 leu2Δ0 met15Δ0</i> NAT-GPDpr-3HA-Pex29 <i>Pex30-tdTomato fld1::</i>	This study
yPC11473	Mat ?	<i>ura3Δ0 his3Δ1 leu2Δ0 met15Δ0</i> NAT-GPDpr-3HA-Pex29 <i>Pex30-tdTomato ldb16::</i>	This study
yPC11480	Mat a	<i>ura3Δ0 his3Δ1 leu2Δ0 met15Δ0</i> Pex28-3HA-KANR <i>fld1::</i>	This study
yPC11481	Mat a	<i>ura3Δ0 his3Δ1 leu2Δ0 met15Δ0</i> Pex29-3HA-KANR <i>fld1::</i>	This study
yPC11482	Mat a	<i>ura3Δ0 his3Δ1 leu2Δ0 met15Δ0</i> Pex30-3HA-KANR <i>fld1::</i>	This study
yPC11484	Mat a	<i>ura3Δ0 his3Δ1 leu2Δ0 met15Δ0</i> Pex32-3HA-KANR <i>fld1::</i>	This study
yPC11485	Mat a	<i>ura3Δ0 his3Δ1 leu2Δ0 met15Δ0</i> Pex28-3HA-KANR <i>ldb16::</i>	This study
yPC11486	Mat a	<i>ura3Δ0 his3Δ1 leu2Δ0 met15Δ0</i> Pex29-3HA-KANR <i>ldb16::</i>	This study
yPC11487	Mat a	<i>ura3Δ0 his3Δ1 leu2Δ0 met15Δ0</i> Pex30-3HA-KANR <i>ldb16::</i>	This study
yPC11489	Mat a	<i>ura3Δ0 his3Δ1 leu2Δ0 met15Δ0</i> Pex32-3HA-KANR <i>ldb16::</i>	This study
yPC11490	Mat a	<i>ura3Δ0 his3Δ1 leu2Δ0 met15Δ0</i> Pex28-3HA-KANR	This study
yPC11491	Mat a	<i>ura3Δ0 his3Δ1 leu2Δ0 met15Δ0</i> Pex29-3HA-KANR	This study
yPC11492	Mat a	<i>ura3Δ0 his3Δ1 leu2Δ0 met15Δ0</i> Pex30-3HA-KANR	This study
yPC11494	Mat a	<i>ura3Δ0 his3Δ1 leu2Δ0 met15Δ0</i> Pex32-3HA-KANR	This study
yPC11539	Mat ?	<i>ura3Δ0 his3Δ1 leu2Δ0 met15Δ0</i> Pex30-mNG-HIS <i>pex28::KAN fld1::NAT</i>	This study
yPC11540	Mat ?	<i>ura3Δ0 his3Δ1 leu2Δ0 met15Δ0</i> Pex30-mNG-HIS <i>pex28::KAN ldb16::HYGB</i>	This study
yPC11541	Mat ?	<i>ura3Δ0 his3Δ1 leu2Δ0 met15Δ0</i> Pex30-mNG-HIS <i>pex29::KAN ldb16::HYGB</i>	This study
yPC11542	Mat ?	<i>ura3Δ0 his3Δ1 leu2Δ0 met15Δ0</i> Pex30-mNG-HIS <i>pex31::KAN ldb16::HYGB</i>	This study
yPC11543	Mat ?	<i>ura3Δ0 his3Δ1 leu2Δ0 met15Δ0</i> Pex30-mNG-HIS <i>pex32::KAN ldb16::HYGB</i>	This study

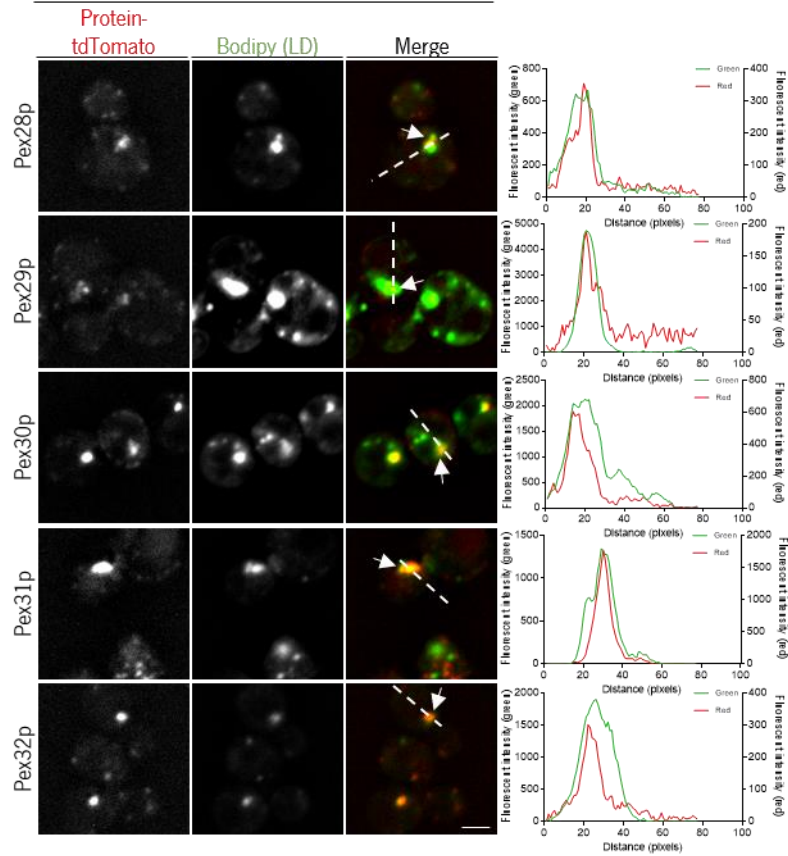


Figure S1. Dysferlin domain-containing peroxins concentrate at lipid droplets in absence of the Seipin complex. Localisation of endogenous Pex28p, Pex29p, Pex30p, pex31p and Pex32p tagged with tdTomato (Protein-tdTomato) in *ldb16Δ* cells. Graphs to right show signal intensity of green and red fluorescence on white line. LDs were stained with the neutral lipid dye Bodipy. White arrows show where the peroxin-tdTomato is located proximal to lipid droplets (LD). Bar 2 μ m.

Project developed at:

